University of the Pacific
Scholarly Commons

University of the Pacific Theses and Dissertations

Graduate School

1968

Measurement Of Fluorescence Lifetimes Of Biologically Significant Compounds

Irene Adele Petz
University of the Pacific

Follow this and additional works at: https://scholarlycommons.pacific.edu/uop_etds

 Part of the Chemistry Commons

Recommended Citation

Petz, Irene Adele. (1968). *Measurement Of Fluorescence Lifetimes Of Biologically Significant Compounds*. University of the Pacific, Dissertation. https://scholarlycommons.pacific.edu/uop_etds/2913

This Dissertation is brought to you for free and open access by the Graduate School at Scholarly Commons. It has been accepted for inclusion in University of the Pacific Theses and Dissertations by an authorized administrator of Scholarly Commons. For more information, please contact mgibney@pacific.edu.

MEASUREMENT OF FLUORESCENCE LIFETIMES OF BIOLOGICALLY SIGNIFICANT COMPOUNDS

A Dissertation

Presented to

The Faculty of the Graduate School

University of the Pacific

In Partial Fulfillment

of the Requirements for the Degree

Doctor of Philosophy

by

Irene Adele Petz

April 1968

This dissertation, written and submitted by

IRENE A. PETZ ,

is approved for recommendation to the

Graduate Council, University of the Pacific.

Department Chairman or Dean:

Emerson P. Cobb

Dissertation Committee:

Richard P. Dodge

Donald K. Wedegaertner

Calvin Potts

Merschel Long

Floyd E. Kelton

Dated January 20, 1968

MEASUREMENT OF FLUORESCENCE LIFETIMES

OF

BIOLOGICALLY SIGNIFICANT COMPOUNDS

Abstract of Dissertation

The purpose of this research was to measure fluorescence decay-times of several biologically significant compounds. Although various equations are available which permit one to calculate fluorescence lifetimes from spectral data, ample evidence exists which indicates such calculations are at considerable variance with experimental results.

As fluorescence lifetimes involved become shorter and/or the intensity of fluorescence decreases the experimental difficulties in their measurement increase. Since an instrument to measure fluorescence lifetimes in the nano second region was at the time commercially unavailable, a large part of the research was directed toward the construction of a suitable instrument. The circuit used was essentially that originated by R. G. Bennett and modified by W. R. Ware.

The performance of the instrument was checked against three standards: quinine bisulfate, anthracene, and acridine. Theoretical calculations were compared with experimentally obtained lifetimes and were found to be significantly longer. Quenching studies of riboflavin with iodide indicated the system obeys the Stern-Volmer equation.

A change in the time-base from a linear to an exponential function is suggested in order to improve the read-out system of the instrument.

ACKNOWLEDGMENTS

I express my gratitude and thanks to Dr. W. Ware of San Diego State College without whose advice and guidance the construction of the fluorescene lifetime apparatus would not have been possible. To Dr. Emerson Cobb of the University of the Pacific I express my appreciation for his encouragement and advice during my graduate years at the University of the Pacific. I thank Dr. R. Dodge, the Chairman of my Dissertation Committee, for his support and acceptance of my research project under his directorship; and the entire committee for its interest and advice in the area of my research.

I further thank Mr. Inman of the University of the Pacific for his instruction in electronics and use of shop equipment which was of considerable value; and Mr. George Austin of Palomar College for graphing the diphenylanthracene and methyl anthranilate graphs.

I express my gratitude to the Board of Governors and the Administration of Palomar College who by granting me Sabbatical Leave made this research and the educational benefit derived therefrom possible. The Engineering Department and Physics Department of the University of the Pacific are remembered by me for the use of their equipment and facilities; I thank Dr. Matusak and the Pharmacy Department of the University of the Pacific for their generous supply of pure chemicals.

Dated this 12th day of November, 1967.

Irene A. Petz

TABLE OF CONTENTS

LIST OF DIAGRAMS

LIST OF ABSORBANCE CURVES

FIGURE PAGE

LIST OF FLUORESCENCE DECAY CURVES

SEMILOGARITHMIC PLOTS OF FLUORESCENCE DECAY

LIST OF GRAPHS AND TABLES

CHAPTER I

INTRODUCTION

The purpose of this research was to measure fluorescence decay-times of several biologically significant molecules. Although various equations (1) are available which permit one to calculate lifetimes from spectral data, ample evidence exists which indicates such calculations are at considerable variance with experimental results (2, 3).

Since an instrument to measure fluorescence lifetime was at the time commercially unavailable, a suitable instrument had to be constructed. The circuit was essentially that originated by R. G. Bennett (4) and modified by R. W. Ware (2).

As fluorescence lifetimes involved become shorter and/or the intensity of fluorescence decreases, the experimental difficulties in their measurement increase. Because of this, a large part of the research work was directed toward the construction of suitable instrumentation and the development of appropriate techniques.

The performance of the instrument was checked against three standards: Quinine bisulfate, anthracene, and acridine. Theoretical calculations were compared with experimentally obtained lifetimes and were found to be significantly longer.

Historical Development

One of the first measurements of luminescence decay-time was made by Wood (5) in 1905. He placed a phosphor on the rim of a wheel which was rapidly rotated. The phosphor was excited at some point along the wheel and the luminescence was followed as the wheel rotated. Wood developed another technique (6) in 1921. In the place of a wheel, he used a jet of scintillating solution, and excited it along a small area. He was unable to observe fluorescence along the jet path beyond the point of excitation, and concluded that fluorescence decay-time was less than 0.5 nsec. In 1923 Abraham and Lamoine (7) used a spark to excite a solution and then used the double refractive property of a Kerr cell to measure the time delay of fluorescence. In the same year Gottling (8) used this technique to establish the fluorescence decay-time of Rhodamine as 21 nsec.

In 1926 Gariola (9) built an apparatus which used the phase-shift method developed by Abraham and Lamoine and was able to set the decay-time of Rhodamine B in water at 2.5 nsec. Thereafter, many researchers employed this technique, including Tumerman (10) in 1941 and Bailey and Rollefson in 1953.

Recently many techniques for the measurement of fluorescence decay-time have been developed. Phillips and Swank (12) first used a pulsed X-ray to excite their phosphors, and later modified their original technique to a

pulsed beam of 75 Kev electrons. In 1960, R. G. Bennett (4) developed the stroboscopic method, which is described in this paper.

CHAPTER II

THEORY

By absorption of electromagnetic radiation a molecule is raised to a higher energy electronic state and becomes excited. There are several paths open to the excited molecule formed in the above primary process:

1. It may re-emit a quantum of either the same or different frequency. This emission is called fluorescence or phosphorescence depending on its multiplicity.
2. It may collide with other molecules and pass on to them some or all of its excitation energy. This energy can cause reaction in the other molecule or can be gradually degraded into heat.
3. It may collide with another molecule and react with it.
4. It may spontaneously decompose if its excitation energy reaches a bond that can be broken (predissociation).

As indicated in the Jablonski diagram (Figure 1, page 39) a transition to a higher electronic state often leaves the molecule in one of the higher vibrational states of the new electronic state. In solution molecular collisions are very effective in removing the excess energy

which goes into the thermal or perhaps the vibrational energy of the molecules of the solvent, and is not detected as emitted radiation. Approximately 10^{-10} second is the time required for the dissipation of excess vibrational energy. A typical vibrational period is 10^{-13} second. This means that it would take about 1,000 vibrations before this energy is lost (13).

The way in which the potential energy of a diatomic molecule might vary, as a function of internuclear distance for the two different electronic states is shown in Figure 2, page 40. The electronic transition, because of the small electronic mass takes place within an interval of approximately 10^{-15} second (13), which is short compared to the change in the distance of the nuclei of the atoms which vibrate at a frequency of about 10^{13} sec^{-1} (13) at room temperature. Also, the vibration of a molecule at a given level is very similar to simple harmonic motion with the result that the molecule spends most of the time at the limits of the level, and the transition will most likely occur at these points or at the middle of the J = 0 level. These characteristics of electronic and nuclear motion lead to the Franck-Condon principle which states that the electronic transition in a molecule takes place so rapidly compared to the vibrational motion of the nuclei that the internuclear distance can be regarded as fixed during the transition until after the electronic transition is completed.

The temperature is generally near room temperature in absorption experiments and the j = 0 level is most populated. A progression of absorption lines in the electronic absorption band can be expected with j = 0 and j^1 varying from 0 to rather large numbers (Figure 2, page 40).

In polyatomic molecules many potential energy surfaces exist which correspond to different electronic states of the molecule. The result is that the potential energy surfaces cross one another and thus provide a path for the molecule to return to ground state without radiating. Such a process is known as "internal conversion." This is represented in Figure 3, page 41, where the curves represent surfaces.

If molecules do not have crossing potential surfaces, or if the efficiency of internal conversion is not too high, emission of radiation can take place. Although the absorbed energy may place a molecule in one of the higher vibrational levels of the excited state, the vibrational deactivation is so rapid that fluorescence generally occurs from the lowest vibrational level of the excited state, j = 0, Figure 2.

The lifetime of fluorescence that spontaneously emits after exciting radiation is turned off can be calculated as a half-life.

1. $\frac{dN_u}{dt} = -k N_u$; $\frac{dN_u}{N_u} = -k\, dt$

where N_u = the number of molecules in the excited state. k is a constant characteristic of the substance, and is related to the Einstein

coefficient of spontaneous emission.

2. $\frac{dN_u}{N_u} = -k\,dt$

3. $\ln \frac{1/2\ N_u}{N_u} = -k\ t_{1/2}$

4. $t_{1/2} = \frac{\ln 2}{k}$ Let τ = fluorescence lifetime

Since $k = \frac{1}{\tau}$, the above equation yields:

5. $t_{1/2} = \ln 2\,\tau$

6. τ (ave.) $= \frac{t_{1/2}}{0.693}$

The above equations are true if decay-time is exponential.

The fluorescence lifetimes were determined by means of a stroboscopic fluorescence lifetime apparatus described in this paper. The recorder read-out gives the decay curve directly. Several points from each curve were plotted on semilogarithmic paper which yielded a straight line. The half-life was determined and τ, the fluorescence lifetime, was calculated by means of equation 6.

Fluorescence lifetimes can also be calculated from absorption spectra and the following equations:

$$7.\quad A_{u \rightarrow g} = \frac{8\pi(1000)\, c\, (\bar{\nu}_{gu})^2}{N} \int \epsilon(\bar{\nu})d\bar{\nu}$$

where: $\bar{\nu}$ = the wave number of maximum absorption.

N = Avogadro's number, 6.022×10^{23}

c = speed of light, 3×10^{10} cm sec^{-1}.

$$8.\quad \tau_o = \frac{1}{A_{u \rightarrow g}} = \text{the inherent fluorescence lifetime}$$

The integral, $\int \epsilon(\bar{\nu})d\bar{\nu}$ is determined by means of a planimeter and converted to proper units.

The values thus obtained are compared with experimentally determined using the following equation:

$$9.\quad \tau_o = \frac{\tau}{\Phi_o} \qquad \text{where } \Phi = \text{absolute quantum yield}$$

Both τ and Φ_o are determined experimentally. However, Φ_o has been determined for relatively few compounds, and therefore this report contains τ_o values for only methyl anthranilate and 9,10-diphenylanthracene.

Quenching studies were made on riboflavin using I^- ion as a quenching agent, and the quenching constant k_q was determined from the data.

If the above system is time independent (I) the fate of the excited molecule can be described adequately by the following equations:

10. $A + h_\nu \longrightarrow A^*$ (absorption)

11. $A^* \xrightarrow{k_1} A + h_\nu$ (fluorescence)

12. $A^* \xrightarrow{k_2} A + \text{heat}$ (radiationless process)

If a quencher molecule Q is present, there is another path available to the excited molecule.

13. $A^* + Q \xrightarrow{kq} A + Q + \text{heat}$ (quenching)

The concentration of A* reaches a constant value under conditions of steady state illumination and no irreversible photochemical reactions. Based on this steady state assumption and the four equations above, the following can be written:

14. $$-\frac{d[A^*]}{dt} = k_1[A^*]$$

15. $$-\frac{d[A^*]}{dt} = k_2[A^*]$$

16. $$-\frac{d[A^*]}{dt} = kq[A^*][Q]$$

17. $$\frac{d[A^*]}{dt} = I_a - k_1[A^*] - k_2[A^*] - kq[A^*][Q]$$

where I_a = intensity of absorbed light. After steady state conditions are established $\frac{d[A^*]}{dt} = 0$ and:

18. $Ia = k_1[A^*] + k_2[A^*] + kq[A^*][Q]$.

Let ϕ_o = the quantum yield in absence of Q_1, then

19. $$\Phi_o = \frac{k_1[A^*]}{I_a} = \frac{k_1}{k_1 + k_2}$$

Let Φ_q = the quantum yield in the presence of Q, then

20. $$\Phi_q = \frac{k_1[A^*]}{I_a} = \frac{k_1}{k_1 + k_2 + k_q[Q]}$$

$$21.\quad \frac{\Phi_o}{\Phi_q} = \frac{k_1 + k_2 + k_q[\,Q\,]}{k_1 + k_2} = 1 + \frac{k_q[\,Q\,]}{k_1 + k_2}$$

Let $\tau' = \frac{k_1}{k_1 + k_2}$ = fluorescence lifetime when $[\,Q\,] = 0$

$$22.\quad \frac{\Phi_o}{\Phi_q} = 1 + k_q\,[Q]\tau'$$

$$23.\quad k_q\tau' = \left[\frac{\Phi_o}{\Phi_q} - 1\right]\frac{1}{[Q]} = Ksv.$$

The constant Ksv is usually determined by means of the Stern-Volmer apparatus. Since this instrument was not available, $k_q\tau'$ was determined with the stroboscopic lifetime apparatus.

By determining the fluorescence lifetime of riboflavin in deaerated and temperature-controlled samples containing increasing concentrations of iodide ions, a series of results were obtained showing a constant decrease in fluorescence lifetimes. The reciprocal of lifetimes so obtained plotted versus concentration of iodide ion yielded a straight line. The slope of the line multiplied by should yield the Stern-Volmer constant, Ksv. (See equation 23.) The straight line indicates that the above mechanism (equations 10 through 13) is operating (13).

CHAPTER III

INSTRUMENTATION

A block diagram, and the detailed circuit for the instrument are given below, Figures 4 through 8, pages 42 through 46. One can best grasp the general operative principles of the instrument by examining the block diagram. (See Figure 4.)

The blocking oscillator produces a voltage pulse at approximately 5 kc, which is divided between two systems. In the first, the lamp system, the voltage pulse fires a thyratron which in turn fires the lamp. In the second, the photomultiplier system, the pulse is delayed by a variable delay line. This delayed pulse is shaped, inverted, and then used to pulse the photomultiplier. Advantage is taken of the fact that the photomultiplier tube is reactive to light only when proper voltages are applied to the cathode and dynodes. By applying these voltages the tube is made to function as a light shutter. The fluorescence decay is then detected by periodically gating on the photomultiplier for a time interval short compared to the fluorescence decay time at some time after the excitation pulse, and electronically integrating the signals obtained over a relatively long period of time. The time variation of fluorescence radiation is observed by increasing the delay time between the photomultiplier gate (by means of the variable delay line)

and the excitation pulse which are triggered synchronously. The integrated signal is actually a time stretched recording of the actual fluorescence decay. The current from the photomultiplier is amplified by means of a Hewlett-Packard micro-micro-ammeter and the result displayed on a recorder as a function of delay time.

The function of the various components of the instrument, (Figures 5 through 8, pages 43 through 46) are described below:

1. The blocking oscillator (Figure 5A) is a free-running type producing a continuous series of pulses at the output. The transformer provides a coupling between plate and grid circuits. As the current through the transformer windings is increased, the resulting magnetic field induces a voltage in the secondary winding. Since the plate current is increasing, the voltage in the secondary winding and the grid is positive with respect to the cathode. A positive increase in grid voltage further increases plate current and thus regenerative feedback results. The plate current increases until the saturation point of the tube is reached, at which time the current becomes constant. Since the plate current is no longer changing, no voltage is induced in the secondary windings of the transformer. At this

point, it might be expected that the grid voltage would drop to zero and the tube should start conducting again. This does not happen in a blocking oscillator, because capacitor C_1 charges up to the positive voltage of the secondary winding during the positive cycle of the tube. When the grid-current drops to zero and the transformer secondary winding voltage becomes zero, the tube is biased below cut-off by the capacitor's voltage. The capacitor, C_1, begins to discharge through R_1 because the grid to cathode circuit is now an open circuit. The cut-off period will depend upon the R_1C_1 time constant.

As the capacitor discharges through the resistor, the grid voltage increases until after a period of time the cut-off value is reached. At this time the tube starts to conduct again.

2. The 1258 Tungsol thyratron (Figure 5B, page 43) is triggered by the blocking oscillator at a repititious frequency of 5 kc. The capacitor C_2 is charged to the full value of the supply voltage and no current is flowing. A positive pulse on the grid fires the thyratron and C_2 will discharge through it and the series resistor R_2; a short and a very large output can be taken across

R_2. If the plate resistor is greater than approximately 20 K, it does not pass enough current to keep the thyratron conducting, and it goes out. The capacitor C_2 charges up again through the plate resistor and after a few time constants is ready to deliver another pulse of essentially the same size. (The resistor R_2 is necessary to prevent the tube from carrying too much current and damaging itself.)

3. The Helidel delay line (Figure 6A, page 44) is a continuously variable, distributed constant, electromagnetic delay line that permits precise selection of extremely short times with linearity and exceptionally fine resolution. Its construction can be compared to a coaxial cable wound in a tight helix. This arrangement permits an electrical contact with the inner conductor; this contact can be readily moved along the delay line by a shaft input. The electrical output will lag the input proportional to the mechanical shaft angle.

4. The lamp delay line (Figure 6B) is also a Helidel variable delay line. However, it is set at a fixed value. This allows the photomultiplier to be gated synchronously with the lamp.

5. The lamp (Figure 8B, page 46) was constructed

following the design of Malmberg (15) and modified by Ware (2), except that the 2 D 21 thyratron was replaced by a 7191 A. Tungsol thyratron.

The lamp is filled with dry air approximately at 300 mm. pressure. The electrodes are platinum and set 0.5 mm. apart. The lamp envelope is made of pyrex glass and the window of quartz. The lamp yields a high intensity between 3000 ^{o}A - 4000 ^{o}A with a decay of 2.0 nanoseconds and almost no tail.

In the photomultiplier system (Figure 7, page 45) the variable delay line makes it possible to examine different sections of the decay curve by varying the gating time of the photomultiplier. A 7191 A Tungsol thyratron (Figure 7A) with its 6 feet of RG - 62/U cable generates a fast rising positive pulse which is applied to the grid of a 5687 Tungsol tube (Figure 7B). In this way the thyratron serves as a switch. A grid bias (67.5 battery) of the 5687 vacuum tube (2 sections in parallel) is used to control the amplitude and the leading edge slope of the negative pulse which is applied to the photomultiplier transmission cable.

The photomultiplier tube (Figure 8A) consists of a photoemissive cathode and a chain of

secondary emissive dynodes. The cathode material (C_s - Sb) determines the quantum efficiency of the tube and the wave length regions in which the photomultiplier will be useful. This efficiency is defined as the ratio of the number of photoelectrons ejected to the number of light quanta incident on the cathode. When suitable voltages are applied to the successive dynodes electron multiplication results at each dynode. The amplification of the tube depends upon the number of dynodes and the secondary emission coefficient of each dynode.

The electrons from the last dynode are collected at the anode which is at ground potential.

Ideally the response of the tube is linear with respect to light intensity, but actually it depends upon the characteristics of the circuit supplying the required inter-electrode operating voltages. The type of voltage divider commonly used is a string of resistors in series, which divides the applied voltage equally or unequally among the various stages as required by the electrostatic focusing system of the tube.

The photomultiplier tube has many sources of noise, the principle ones at ordinary signal levels, are the fluctuation of the dark current and the random fluctuations in the number of electrons emitted from the various dynodes.

Variation of thermal emission of electrons from the cathode is responsible for the fluctuation of the dark current. This can be reduced by lowering the temperature of the photocathode (16).

Although the chain of resistors are used most frequently as voltage dividers between the dynodes, in the present instrument approximately 16" of R.G. 62/U cable was used between the dynode stages (4). By careful sequential trimming of the interdynode transmission line, it was possible to achieve very short gating times of approximately 1×10^{-9} sec. A low voltage pulse (about 200 volts) is propagated along a tapped delay line cable connected to the photomultiplier dynodes. By proper selection of cable, the pulse waveform is made to travel at the same average speed as the electrons between the dynodes; thus cutting down one source of noise and defocussing effects in the tube. The optical system is arranged as in Figure 9, page 47, and entirely sealed from light sources. The lenses are pyrex and the sample holder is liquid cooled.

CHAPTER IV

CALCULATIONS

Lifetimes

The Helidel Delay Line has 20 turns with a total delay of 200 nanoseconds (nsec). It is driven by a motor which makes 4 revolutions per minute. Therefore each turn of the delay line represents 10 nsec., and each minute represents 40 nsec. The recorder chart speed is 2" per minute; therefore each inch on the chart represents 20 nsec. There are 5 divisions per inch on the chart, which means that each division represents 4 nsec. Each major division on the graph also represents 4 nsec.

Semilogarithmic plots are made by taking readings at intervals of 2 nsec. from each decay curve. The half-lives are determined from each semilogarithmic curve and $t_{\frac{1}{2}}$ is determined. The lifetime τ is then calculated for the compound using the equation:

$$\tau\,(\text{ave}) = \frac{t_{\frac{1}{2}}\,(\text{ave})}{0.693}$$

See Figure 68, page 106, and Table II, page 30.

Calculation of Fluorescence Lifetimes from Absorption Curves (19)

1. Methyl Anthranilate

$$A_{u \rightarrow g} = \frac{8\pi^2 (\ 1000\ )\ c\ (\bar{\nu}_{gu})^2}{N} \int \epsilon\,(\bar{\nu})\,d\bar{\nu}.$$

where $\bar{\nu}_{gu}$ = the mean frequency for the absorption band.

$A_{u \longrightarrow g}$ = the probability coefficient of absorption (related to the Einstein absorption coefficient).

N = Avogadro's number = 6.02×10^{23}

c = speed of light = 3.0×10^{10} cm. $sec.^{-1}$

$\int \epsilon(\bar{\nu})d\bar{\nu}$ = area under the absorption curve determined by means of a planimeter.

From Figure 54, page 92 , the following values were assigned to the above variables:

$$\bar{\nu}_{gu} = 2.92 \times 10^{4} \text{ cm.}^{-1}$$

$$\int \epsilon(\bar{\nu})d\bar{\nu} = 145.25 \text{ cm.}^{2}$$

Absorbance coordinate (ϵ) = 4.00×10^{2}

Wave number Coordinate ($\bar{\nu}$) = 4.00×10^{2}

Therefore, $\int \epsilon(\bar{\nu})d\bar{\nu} = 145.25 \times 4.00 \times 10^{2} \times 4.00 \times 10^{2} = 2.32 \times 10^{7}$.

$$A_{u \longrightarrow g} = \frac{8 \times 3.14 \times 2.3 \times 3 \times 10^{10} \times 1000 \times (2.92 \times 10^{4})^{2} \times 2.32 \times 10^{7}}{6.02 \times 10^{23}}$$

$$A_{u \longrightarrow g} = 5.714 \times 10^{7} \text{ sec.}^{-1}$$

$$\tau_{o} = \frac{1}{A_{u \longrightarrow g}} = \frac{1}{5.714 \times 10^{7}} \text{ sec.} = 1.750 \times 10^{-8} \text{ sec.}$$

$$\tau_{o} = 17.50 \text{ nsec.}$$

From experiment (Figure 58, page 96) τ = 15.37 nsec. = 1.537×10^{-8} sec. The absolute quantum yield (Φ_{o}) for methyl anthranilate has been determined as 0.685 (17).

Since $\tau_o = \frac{\tau\,(ave.)}{\Phi_o}$

where Φ_o = absolute quantum yield

$$\tau_o = \frac{1.537 \times 10^{-8}}{0.685} \text{ sec.} = 2.243 \times 10^{-8} \text{ sec.}$$

$$\tau_o = 22.43 \text{ nsec.}$$

This value is significantly different from 17.50 nsec., the calculated value.

2. 9,10-Diphenylanthracene (Figure 55, page 93)

$$\int \epsilon(\bar{\nu})d\bar{\nu} = 74.92 \text{ cm.}^2$$

$$\bar{\nu}_{gu} = 2.59 \times 10^4 \text{ cm.}^{-1}$$

Absorbance coordinate = 8×10^2 per cm.

Wave number coordinate = 8×10^2 ($\bar{\nu}$) per cm.

$$\int \epsilon(\bar{\nu})d\bar{\nu} = 74.92 \times 8.00 \times 10^2 \times 8.00 \times 10^2 = 4.79 \times 10^7$$

$$A_{u \rightarrow g} = \frac{8 \times 3.14 \times 2.3 \times 3.0 \times 10^{10} \times 10^3 \times (2.59 \times 10^4)^2 \times 4.79 \times 10^7}{6.02 \times 10^{23}}$$

$$A_{u \rightarrow g} = 9.149 \times 10^7 \text{ sec.}^{-1}$$

$$\tau_o = \frac{1}{A_{u \rightarrow g}} = 1.093 \times 10^{-8} \text{ sec.}$$

$$\tau_o = 10.93 \text{ nsec.}$$

The absolute quantum yield for 9,10-Diphenylanthracene (Φ_o) = 0.81 (17).

$$\tau_o = \frac{\tau\,(exp)}{\Phi_o} = \frac{9.63 \times 10^{-9}}{0.81} = 1.19 \times 10^{-8}$$

Here the difference between calculated and experimental τ_o is approximately 1 nsec.

Calculation on the Quenching of Fluorescence of Riboflavin (18)

[Riboflavin]	$[I^-] \times 10^3$	τ(ave)nsec.	$k \times 10^{-7} = \frac{1}{\tau}$ sec^{-1}
1×10^{-5}	0.0	12.8	7.8
1×10^{-5}	5.0	12.1	8.25
1×10^{-5}	10.0	11.5	8.68
1×10^{-5}	15.0	11.07	9.05
1×10^{-5}	17.5	10.62	9.40

The plot of kvs $[I^-]$ yields a straight line (Figure 69, page 10% The slope of the line yields:

$$k_q = \frac{(9.575 - 7.800) \times 10^7}{20 \times 10^{-3}} = 8.88 \times 10^8 \text{ l mole}^{-1} \text{ sec}^{-1}$$

$$k_o = 7.80 \times 10^7 \text{ sec}^{-1}$$

$$\tau' = \frac{1}{7.8 \times 10^7} = 12.8 \times 10^{-9} \text{sec} = 12.8 \text{ nsec}$$

$$Ksv = k_q \tau' = 8.88 \times 10^8 \times 12.8 \times 10^{-9} = 11.37$$

The Stern-Volmer constant can also be calculated from the following equation (19):

$$Ksv = \frac{k_q \tau'}{[I-F(x)]} + \frac{F(x)}{[Q]\,[I-F(x)]}$$

$$F(x) = xe^{x}\,[\mathrm{erfc}\,(x)]$$

$$x = \frac{k^1 \tau'\,[Q]}{I + k_q \tau'\,[Q]}$$

$$k^1 = 4\sqrt{R_o^2\,\frac{N}{1000}}\,\sqrt{\frac{D}{10}}$$

where:

k_q = the quenching constant observed from fluorescence lifetime measurement. (1 $mole^{-1} sec^{-1}$)

$[Q]$ = Concentration of quencher in moles l^{-1}

τ' = fluorescence lifetime when $[Q] = 0$ (sec.)

R_a = radius of molecule in cm.

R_b = radius of quencher in cm.

R_o = $R_a + R_b$ in cm.

D_a = diffusion constant for molecule in $cm.^2$ $sec.^{-1}$

D_b = diffusion constant for quencher in $cm.^2$ $sec.^{-1}$

$D = D_a + D_b$

$$\mathrm{erf}(x) = \frac{2}{\sqrt{\pi}} \int e^{-y^2} dy$$

$\mathrm{erfc}(x) = I - \mathrm{erf}(x)$.

Calculation of Errors in Measurement

1. Average Lifetime = τ (ave.) $\frac{1}{n} \sum_{i=1}^{n} \tau_i$

n = number of measurements.

2. Range (w) = τ (max.) - τ (min.)

3. Relative Range % = $\frac{w}{\tau(\text{ave.})} \times 100$

4. Deviation from the average (d) = $\tau - \tau(\text{ave.})$

5. Standard Deviation (s) = $\sqrt{\frac{d_1^2 + d_2^2 + \cdots d_n^2}{n-1}}$

6. Relative Deviation = $\frac{s}{\tau(\text{ave.})}$

TABLE I

ERROR TREATMENT OF QUANTITATIVE DATA

Compound	τ (nsec.)	τ (ave.)	Deviation from average	Range	Relative Range %
Methyl Anthranilate					
a.	15.60		+ 0.23		
b.	15.30	15.37	- 0.07	0.40	2.62
c.	15.20		- 0.17		
9,10-Diphenylanthracene					
a.	9.23		- 0.39		
b.	9.82	9.62	+ 0.20	0.59	6.14
c.	9.82		+ 0.20		
Acridine					
a.	15.0				
b.	15.6	15.4	- 0.40		
c.	15.6		+ 0.20	0.60	3.87
			+ 0.20		
Anthracene					
a.	6.35		+ 0.38		
b.	5.78	5.97	+ 0.38	0.57	9.6
c.	5.78		- 0.19		
Barbituric Acid					
a.	5.78				
b.	5.78	5.78	0	0	0
c.	5.78				

TABLE I (continued)

Compound	τ (nsec.)	τ (ave.)	Deviation from average	Range	Relative Range %
Glycine					
a.	4.85		+ 0.07		
b.	4.85	4.78	+ 0.07	0.22	4.60
c.	4.63		- 0.15		
Proflavin					
a.	4.05		- 0.03		
b.	4.05	4.08	- 0.03	0.08	1.96
c.	4.13		+ 0.05		
L-Ascorbic Acid					
a.	4.16		- 0.45		
b.	4.48	4.61	- 0.13	1.13	24.6
c.	5.19		+ 0.38		
Alloxazine (H_2O)					
Long-lived species					
a.	20.20		+ 0.80		
b.	19.10	19.40	- 0.30	1.10	5.67
c.	19.10		- 0.30		
Short-lived species					
a.	5.80				
b.	5.80	5.80	0	0	0
c.	5.80				
Alloxazine (9 M H_2SO_4)					
Long-lived species					
a.	22.50		+ 1.30		
b.	21.60	21.20	+ 0.40	1.30	6.13
c.	21.20		0		

TABLE I (continued)

Compound	τ (nsec.)	τ (ave.)	Deviation from average	Range	Relative Range %
Short-lived species					
a.	10.95		+ 0.75		
b.	9.83	10.20	+ 0.37	1.12	11.0
c.	9.83		+ 0.37		
Quinine bisulfate					
a.	20.8		+ 0.10		
b.	20.9	20.7	+ 0.20	0.40	1.93
c.	20.5		- 0.20		
2-Aminopyrimidine					
a.	4.71		+ 0.02		
b.	4.64	4.69	- 0.05	0.07	1.50
c.	4.71		+ 0.02		
1,6-Diphenyl-1,3,5-hexatriene					
a.	10.4				
b.	10.4	10.4	0	0	0
c.	10.4				
Quinidine Sulfate					
a.	12.7				
b.	12.7	12.7	0	0	0
c.	12.7				
Riboflavin					
a.	12.60		- 0.20		
b.	12.90	12.80	+ 0.10	0.30	2.34
c.	12.90		+ 0.10		

TABLE I (continued)

Compound	τ (nsec.)	τ (ave.)	Deviation from average	Range	Relative Range %
Riboflavin + $[I^-] = 5 \times 10^{-3}$					
a.	12.10				
b.	12.10	12.10	0	0	0
c.	12.10				
Riboflavin + $[I^-] = 10 \times 10^{-3}$					
a.	11.50				
b.	11.50	11.50	0	0	0
c.	11.50				
Riboflavin + $[I^-] = 15 \times 10^{-3}$					
a.	11.20				
b.	11.00	11.08	+ 0.12		
c.	11.05		- 0.08	0.20	1.81
			- 0.03		
Riboflavin + $[I^-] = 17.5 \times 10^{-3}$					
a.	10.62		0		
b.	10.70	10.62	+ 0.08	0.18	1.69
c.	10.52		- 0.10		
Indazole (0.01 N NaOH) Short-lived species					
a.	3.76		0		
b.	3.76	3.76	0	0	0
c.	3.76		0		

TABLE I (continued)

Compound	τ (nsec.)	τ (ave.)	Deviation from average	Range	Relative Range %
Long-lived species					
a.	11.60		- 0.5		
b.	12.70	12.10	+ 0.6	1.10	9.1
c.	12.10		0		
(Lamp)					
a.	2.31		+ 0.09		
b.	2.31	2.22	+ 0.09	0.26	11.7
c.	2.05		- 0.17		

TABLE I (continued)

Compound	Standard Deviation(s)	Relative(s)	Compound	Standard Deviation(s)	Relative(s)
Methyl Anthranilate	0.21	0.014	1,6-Diphenyl-1,3,5-hexatriene	0	0
9,10-Diphenylanthracene	0.34	0.035	Quonidine Sulfate	0	0
Acridine	0.49	0.022	Riboflavin	0.173	0.17
Anthracene	0.40	0.068	Riboflavin + $[I^-] = 5 \times 10^{-3}$	0	0
Barbituric Acid	0	0	Riboflavin + $[I^-] = 10 \times 10^{-3}$	0	0
Glycine	0.13	0.273	Riboflavin + $[I^-] = 15 \times 10^{-3}$	0.075	
Proflavin	0.13	0.010	Riboflavin + $[I^-] = 17.5 \times 10^{-3}$	0.128	0.09
L-Ascorbic Acid	0.42	0.091	Quinine bisulfate	0.21	0.010
Alloxazine (H_2O) Long-lived species	0.63	0.017	Indazole (0.01 N NaOH) Short-lived species	0	0
Short-lived species	0	0	Long-lived species	0.56	0.046
Alloxazine (9 M H_2SO_4) Long-lived species	0.94	0.044			
Short-lived species	0.65	0.064			
2-Aminopyrimidine	0.04	0.008			
(Lamp)	0.15	0.068			

TABLE II

FLUORESCENCE LIFETIMES

Compound	Concentration (M)	Solvent	τ (experimental) $\pm$s (nsec.)	τ (literature) (nsec.)
Quinine bisulfate	1×10^{-6} to 1×10^{-4}	1 N H_2SO_4 (H_2O)	20.7 $\pm$ 0.21	20.1
Acridine	Saturated	H_2O	15.4 $\pm$ 0.49	15.5
Anthracene	1×10^{-6}	Hexane	5.97 $\pm$ 0.40	5.7
9,10-Diphenyl-anthracene	1×10^{-6} to 1×10^{-4}	Abs. Ethanol	9.63 $\pm$ 0.34	----
Methyl Anthranilate	1×10^{-6} to 1×10^{-4}	Abs. Ethanol	15.37 $\pm$ 0.21	----
1,6-Diphenyl-1,3,5-hexatriene	1×10^{-6} 1×10^{-4}	Abs. Ethanol	10.40 $\pm$ 0.0	----
Indazole	1×10^{-4}	0.01 N NaOH (H_2O)		
Short-lived species			3.76 $\pm$ 0.0	----
Long-lived species			12.01 $\pm$ 0.56	----
2-Aminopyrimidine	1×10^{-4}	0.01 N N_2SO_4 (H_2O)	4.69 $\pm$ 0.41	----
Proflavin	1×10^{-6} to 1×10^{-4}	H_2O	4.08 $\pm$ 0.13	4.5
L-Ascorbic Acid		H_2O	4.61 $\pm$ 0.42	----
Glycine	1×10^{-3}	H_2O	4.78 $\pm$ 0.13	----

TABLE II (continued)

Compound	Concentration (M)	Solvent	τ (experimental) $\pm$ s (nsec.)	τ (literature) (nsec.)
Quinidine Sulfate	1×10^{-4}	H_2O	12.7 ± 0.0	----
Barbituric Acid	1×10^{-4}	0.01 N H_2SO_4 (H_2O)	5.8 ± 0.0	----
Alloxazine	Saturated	H_2O		
Short-lived species			5.8 ± 0.0	----
Long-lived species			19.4 ± 0.63	----
Alloxazine	1×10^{-5}	9 M H_2SO_4 (H_2O)		
Short-lived species			10.20 ± 0.65	----
Long-lived species			21.80 ± 0.94	----
Riboflavin	1×10^{-6} to 1×10^{-4}	H_2O	12.80 ± 0.17	4.2
Riboflavin	1×10^{-5}	$[I^-] = 5 \times 10^{-3}$ (H_2O)	12.10 ± 0.0	----
Riboflavin	1×10^{-5}	$[I^-] = 10 \times 10^{-3}$ (H_2O)	11.50 ± 0.0	----
Riboflavin	1×10^{-5}	$[I^-] = 15 \times 10^{-3}$ (H_2O)	11.08 ± 0.08	----
Riboflavin	1×10^{-5}	$[I^-] = 17.5 \times 10^{-3}$ (H_2O)	10.62 ± 0.13	----
(Lamp)			2.22 ± 0.07	1.8(2)

CHAPTER V

CONCLUSIONS

The fluorescence lifetimes of the standards, quinine bisulfate, acridine, and anthracene, are in good agreement with those obtained from the literature indicating the instrument is reliable at least within the range from 2.0 nsec to approximately 25 nsec. The performance of the instrument can also be checked by measuring the speed of light over distances of several meters.

The fluorescence lifetimes of 9,10-diphenylanthracene, 1,6-diphenyl-1,3,5-hexatriene, methyl anthranilate, proflavin, and riboflavin were concentration independent within the range 1×10^{-6} M to 1×10^{-4}M. Further investigations as to temperature and solvent effects together with studies in quenching would provide more insight into the structure of the excited state, as well as the mechanism of dissipation of excitation energy.

The fluorescence lifetime of riboflavin is not in agreement with the value obtained by Chen, Vurek, and Alexander (3). The value reported in this paper was obtained from a 1×10^{-5} M deaerated water solution of riboflavin, and the temperature was controlled at 25° C ± 2° C. Chen, et al., used a 0.01 tris Cl^- solution as a solvent at 23° C. The concentration of riboflavin was also 1×10^{-5} M, but the solution was not deaerated. Further studies must be made on

the effect of Cl^- on the fluorescence lifetime of riboflavin, and the effectiveness of air as a quenching agent, before any valid comparisons between the reported results can be made.

The results obtained from the quenching studies of riboflavin with I^- ion, indicate that a mechanism is operating in which there is competition between bimolecular quenching and a unimolecular process (emission) for the deactivation of A* (1) (13). This is expressed by equations 10 through 13. The k_q value can be checked by measuring the diffusion coefficients for riboflavin, for the I^- ion, and the radius of each, using equation 19. A more accurate check can be obtained by measuring the Stern-Volmer constant by means of a Stern-Volmer apparatus (18).

Although the quenching process as well as the relationship between the chemical nature of the quenching molecule and its quenching effectiveness is not completely understood. It is believed that the deactivation process is not a simple collisional one (19) (24). It is believed that an activated complex is formed between the fluorescent molecule and the quencher; and that a rearrangement of energy then takes place within the activated complex. Two types of quenching processes might occur (20):

1. Static Quenching

   In this type a complex may form with the fluorescent molecule before excitation.

$$Q + A = QA$$

where Q A is non-fluorescent.

2. Dynamic Quenching

The quencher interacts directly with fluorescent molecule after it has been excited, forming a complex that can return to ground state without emitting light.

$$h\nu + A \rightarrow A^* \rightarrow A + h\nu \quad \text{fluorescence}$$

$$A^* + Q \rightarrow A^*Q \rightarrow A + Q + \text{heat}$$

In order to determine which of the above processes is operating in the Riboflavin-iodide system, the following studies should be made:

1. Increase of solvent viscosity should increase fluorescence lifetime of Riboflavin* if dynamic quenching is taking place. No change should be noticed if static quenching is taking place.
2. Increase in temperature should decrease the lifetime of Riboflavin* in the case of dynamic quenching but should have no effect on static quenching.
3. Increase in concentration of I^- should decrease lifetime of Riboflavin* for dynamic quenching, and no effect should be noticeable for static quenching.

The non-exponential behavior of Alloxazine and

Indazole cannot be explained without additional information. Although compounds of highest purity commercially available were used, it is possible that both compounds contained fluorescent impurities.

The fluorescence lifetimes of Alloxazine increased significantly in a highly acidic solution. The fluorescence lifetimes in water were 5.8 and 19.7 nsec. for the short-lived and long-lived species respectively. In a 9M H_2SO_4 solution the lifetimes increased to 10.3 and 21.8 nsec. for the above species. Since the $\pi^* \rightarrow \pi$ transitions are short-lived compared to the $\pi^* \rightarrow n$ transitions (21), it is tempting to attribute the excited to ground state transitions in Alloxazine and Indazole to the $\pi^* - \pi$ transition. Since absorption spectra of $n \rightarrow \pi^*$ transition in polar solvents tend to shift toward shorter wavelengths and since the opposite is true for $\pi \rightarrow \pi^*$ transition, it would be informative to study absorption spectra and fluorescence lifetimes of both compounds in polar as well as non-polar solvents. It may be possible that the lower energy $n \rightarrow \pi^*$ transitions change to the higher $\pi - \pi^*$ transitions in polar solvents (22).

The 1×10^{-5} M solution of Alloxazine in 9 M H_2SO_4 had an intense yellow color, whereas the saturated water solution was colorless. This would indicate a shift toward absorption of longer wavelengths. However, the solubility

of Alloxazine in water is very low and a saturated water solution may be substantially lower in concentration than a 1 x 10^{-5} M solution of Alloxazine in 9 M H_2SO_4.

The fluorescence of anthracene, 9,10-diphenylanthracene and 1,6-diphenyl-1,3,5-hexatriene is probably due to $\pi^*-\pi$ transitions. This may also be true of glycine, and L-ascorbic acid (13) (21). No further conclusions regarding the structure of the excited states can be advanced on the basis of the data presented in this paper.

Although the maximum intensity of the lamp lies between 3000 ^{o}A and 4000 ^{o}A the entire emission spectrum was not measured. The intensity of the lamp may be low within the region 2500 ^{o}A to 4000 ^{o}A where glycine, indazole, and alloxazine show maximum absorption. The micro-microammeter indicated a current of 100 micro-microamperes output from the photomultiplier. This suggests a low fluorescence intensity. L-ascorbic acid also yielded an exceptionally low fluorescence intensity. The photo-current for this compound was approximately 30 micro-microamperes. The absolute quantum yield has not been measured for any of the above-mentioned compounds. All the other compounds yielded a relatively high fluorescence intensity. The photo-current indicated by the micro-microammeter was within the 1 to 30 milli-microampere range.

A chart-speed of two inches per minute was used for all the decay curves. A faster chart-speed would provide a

curve with greater spread and would make it possible to read more points with higher precision. This is particularly true for decay curves of five nanoseconds or less.

A further improvement in calculating the relationship of τ_o (exp) amd τ_o (theoretical) can be made by using the equation developed by Strickler and Berg (23), which attempts to correct for the fact that in molecular transitions one is not dealing with narrow band absorption nor with resonance fluorescence. Their equation is:

$$\frac{1}{\tau_o} = 2.880 \times 10^{-9} \times n^2 \left\langle \bar{\nu}_f^{-3} \right\rangle_{ave.}^{-1} \times \int e(\bar{\nu})\, d\ln\bar{\nu}$$

where $\left\langle \bar{\nu}_f^{-3} \right\rangle_{ave.}^{-1} = \int F(\bar{\nu})d\bar{\nu} \Big/ \int F(\bar{\nu})\bar{\nu}^{-3}d\bar{\nu}$.

$F(\bar{\nu})$ being the fluorescence intensity in units of relative number of quanta at each frequency, and n^2 is the square of the index of refraction of the solvent. For the above calculation it would be necessary to have the fluorescence spectrum of the compound in question. Since this was not available, the lifetime of fluorescence was calculated from absorption spectra.

An improvement of the instrument is possible by making changes in the readout system. Instead of using a linear time base, it would be possible to use an exponential time base by using an analog computer in conjunction with the lifetime apparatus. The exponential time base would then give a straight line for thefunction, thereby elimin-

ating the laborious process of plotting a semilogarithmic curve. (See Figure 70, page 108.) The above program was checked using the Donner Analog Computer Model 3500. The exponential decay of acridine was simulated and the output fed into the vertical axis of the plotter. The value for k (see Figure 70) was set at 2.96 and the value of I.C. was set at 100 V, and the output fed into the horizontal axis of the X-Y plotter. The result was a straight line.

JABLONSKI DIAGRAM

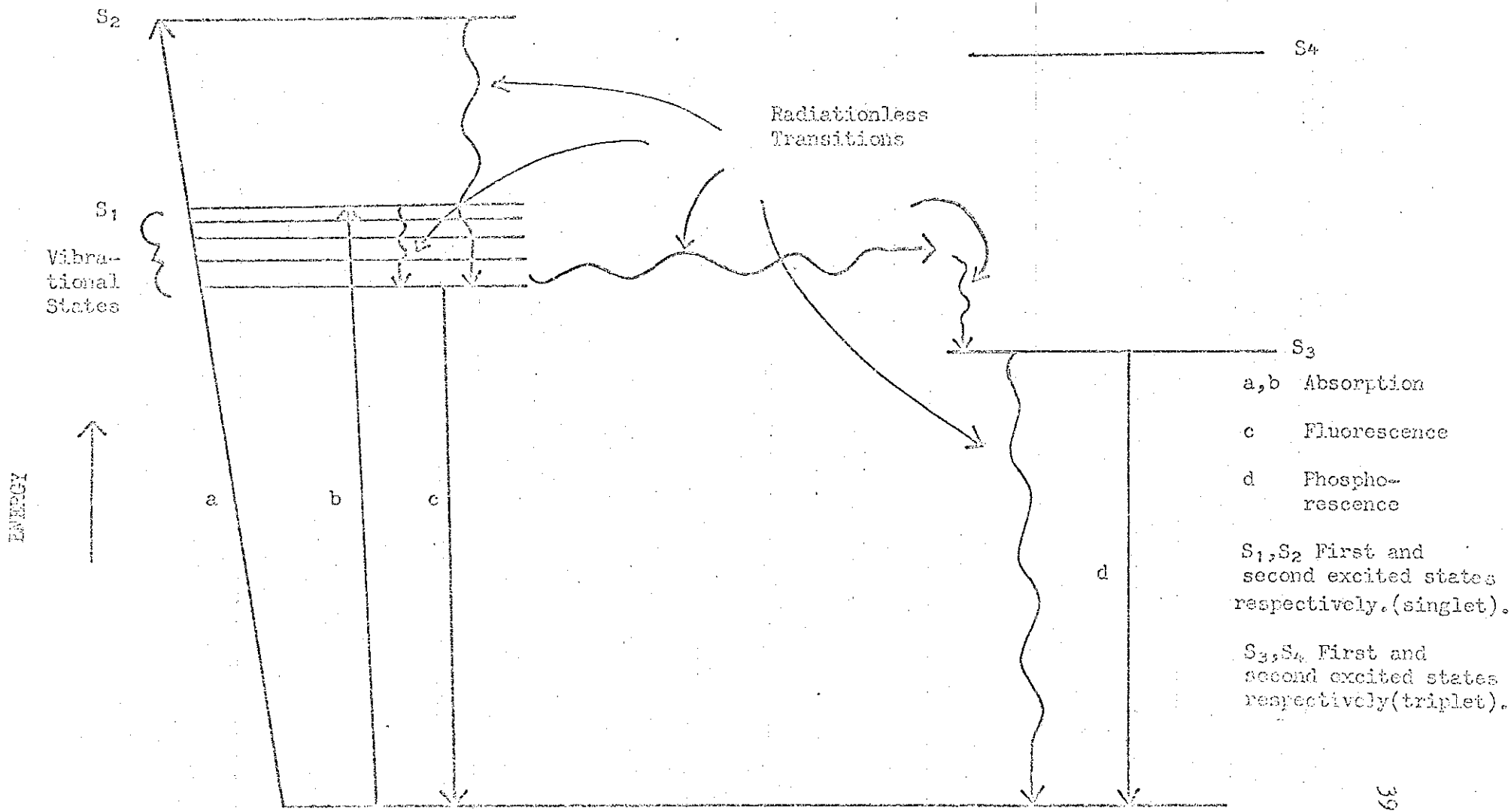

FIG.I

Typical Franck-Condon Emission

From Excited To Ground State (13)

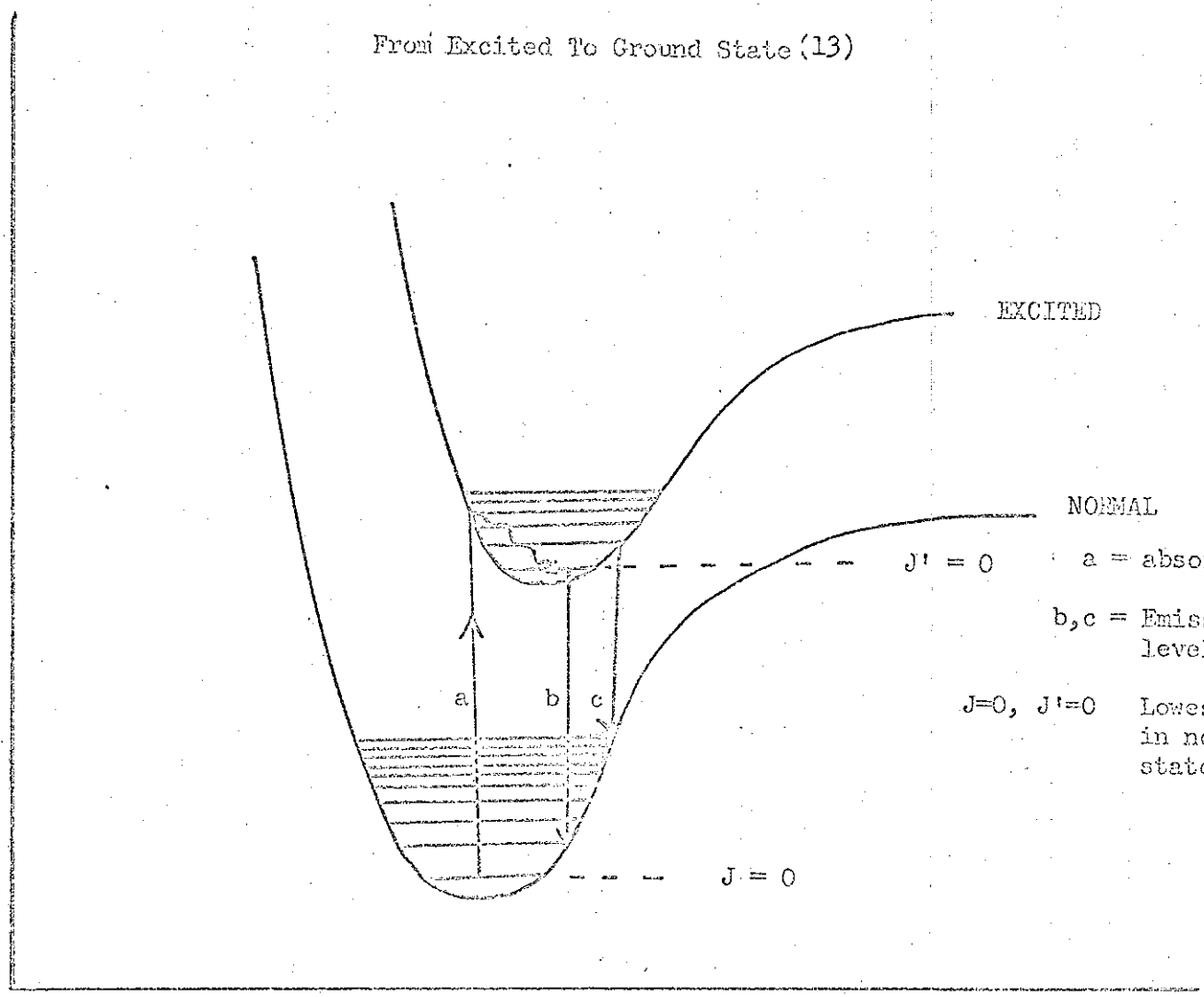

FIG. 2

Energy Dissipation By

Vibrational Deactivation (13)

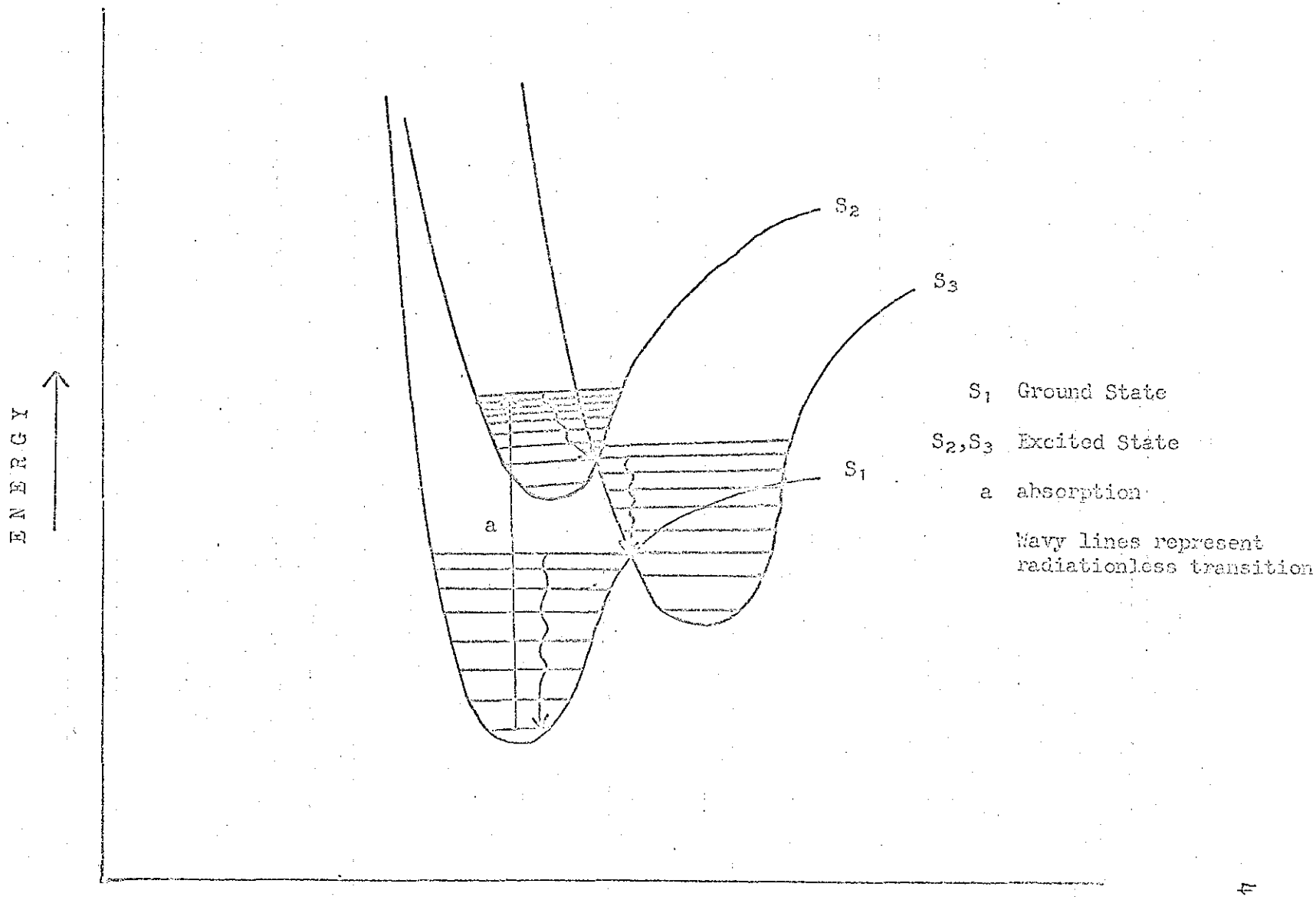

FIG. 3

BLOCK DIAGRAM

FOR

TIMING CIRCUIT

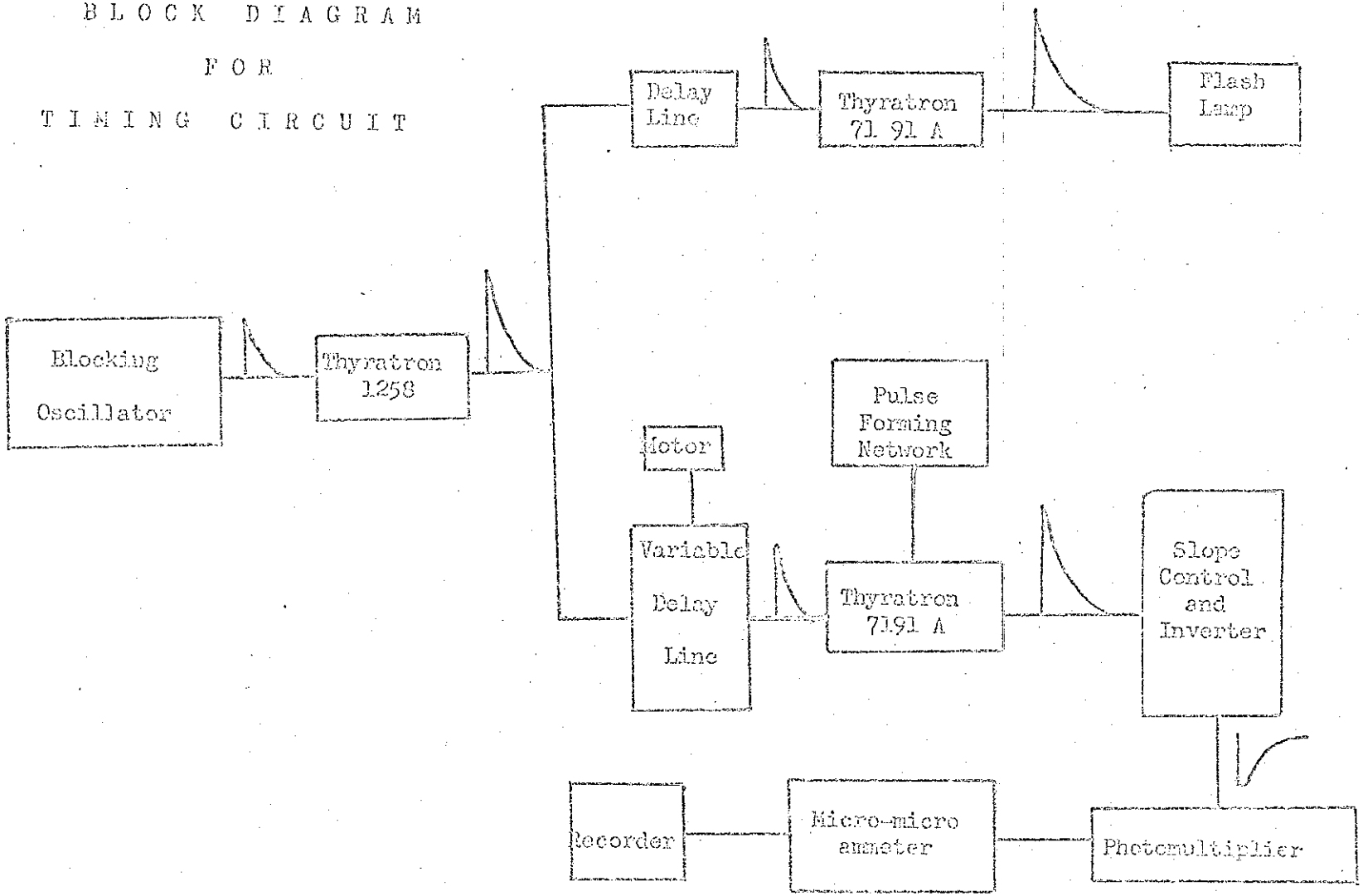

FIG. 4

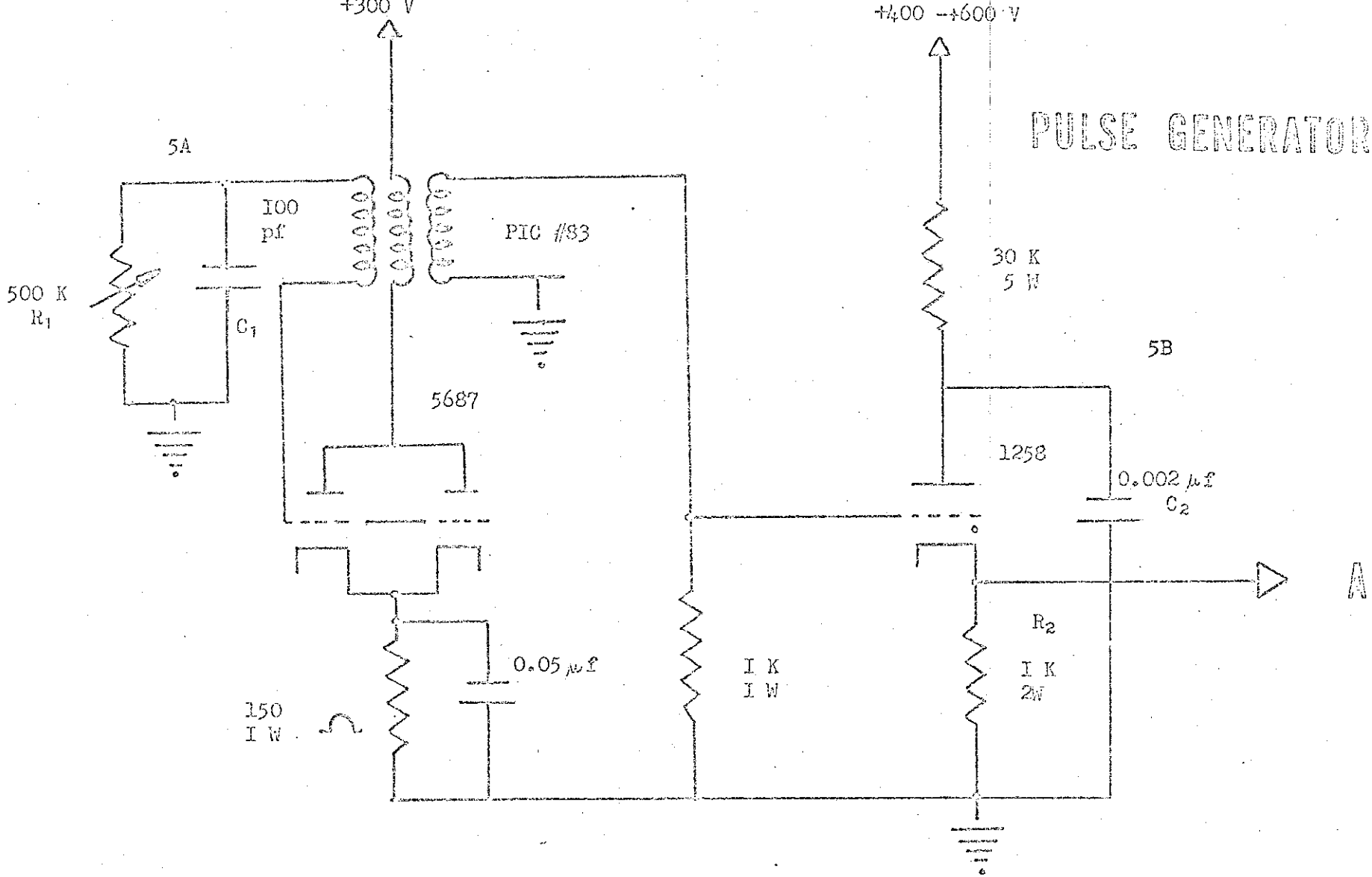
+300 V
+400 - +600 V
PULSE GENERATOR
5A
100
pf
PIC #83
500 K
R1
C1
5687
30 K
5 W
5B
1258
0.002 μf
C2
A
R2
I K
2W
0.05 μf
150
I W
I K
I W

FIG 5.

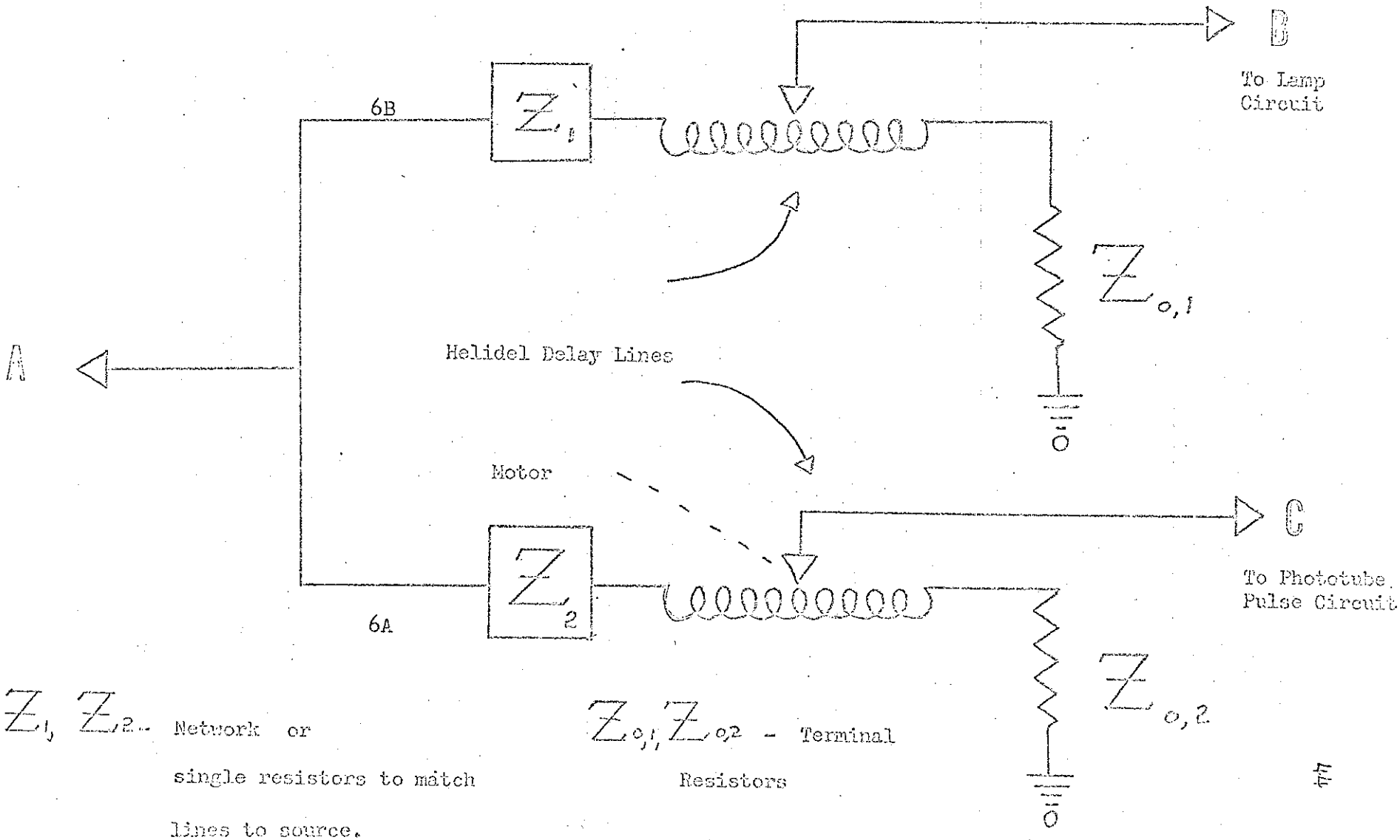

Z_1, Z_2 - Network or single resistors to match lines to source.

$Z_{o,1}$, Z_{o2} - Terminal Resistors

FIG. 6

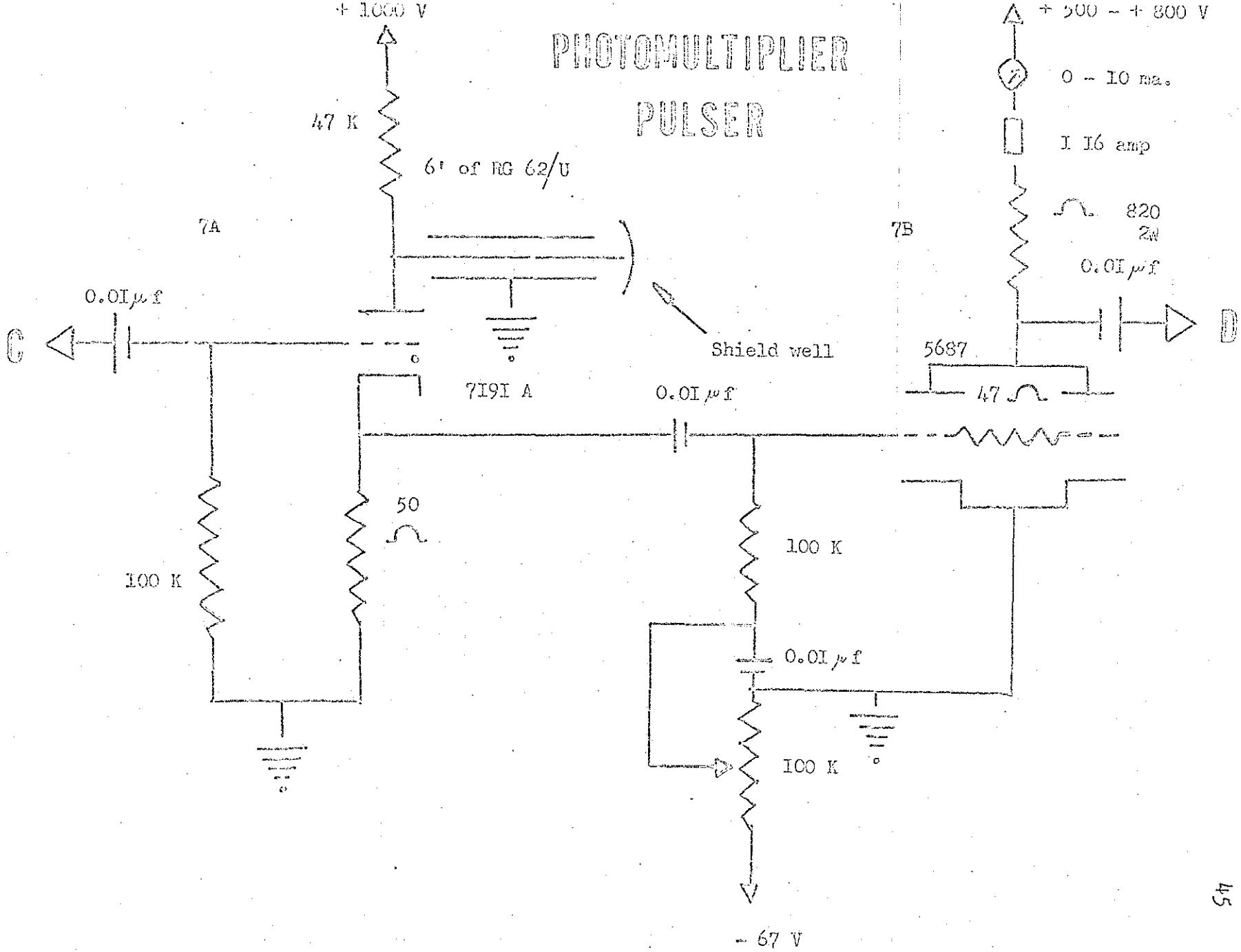
PHOTOMULTIPLIER
PULSER
+ 1000 V
47 K
6' of RG 62/U
7A
7B
0.01 μf
C
7191 A
Shield well
+ 500 ~ + 800 V
0 - 10 ma.
1 16 amp
820
2W
0.01 μf
D
5687
47
0.01 μf
50
100 K
100 K
0.01 μf
100 K
- 67 V

FIG. 7

PHOTOTUBE AND LAMP CIRCUIT

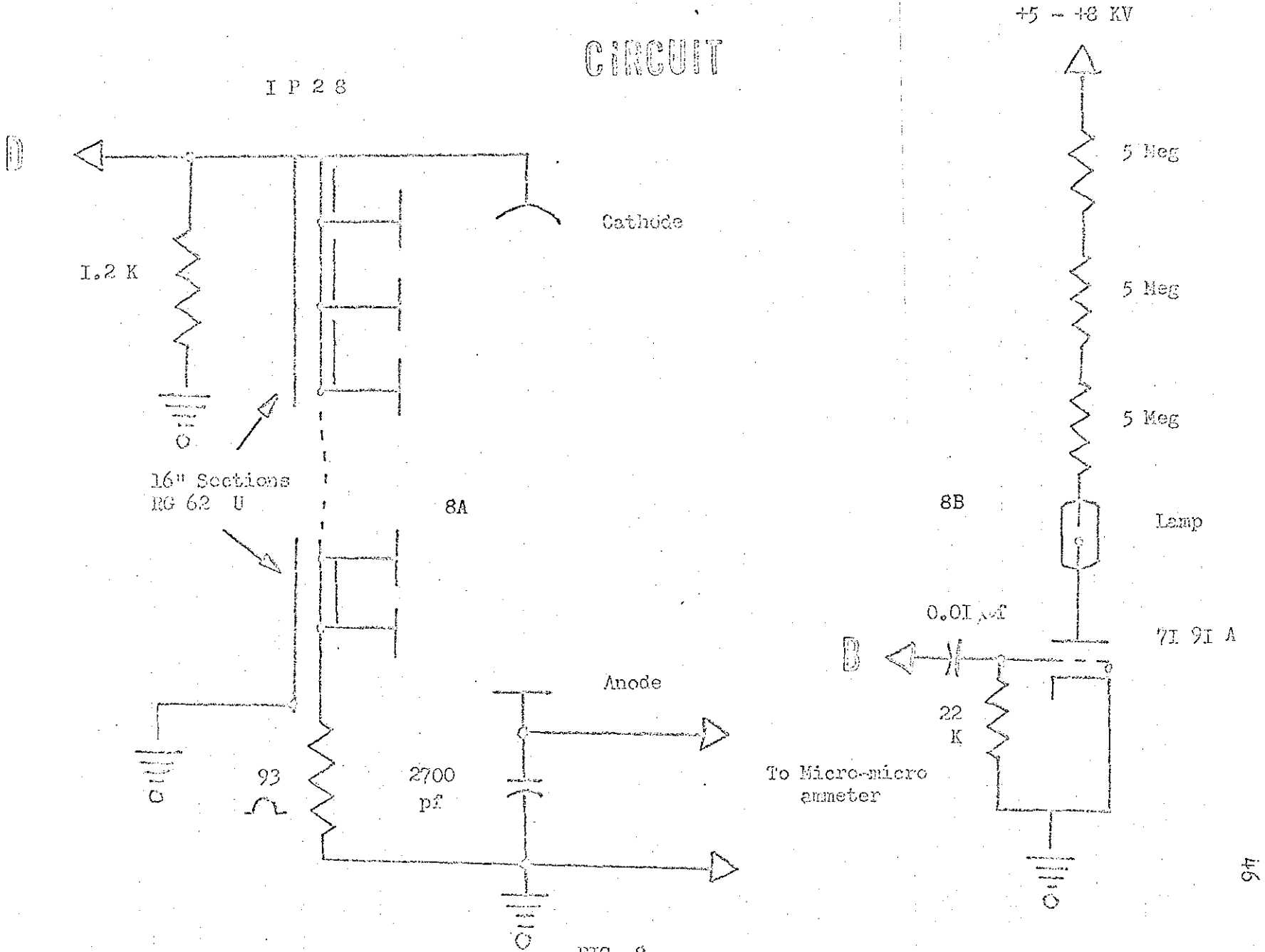

FIG. 8

Schematic

of

Lamp System

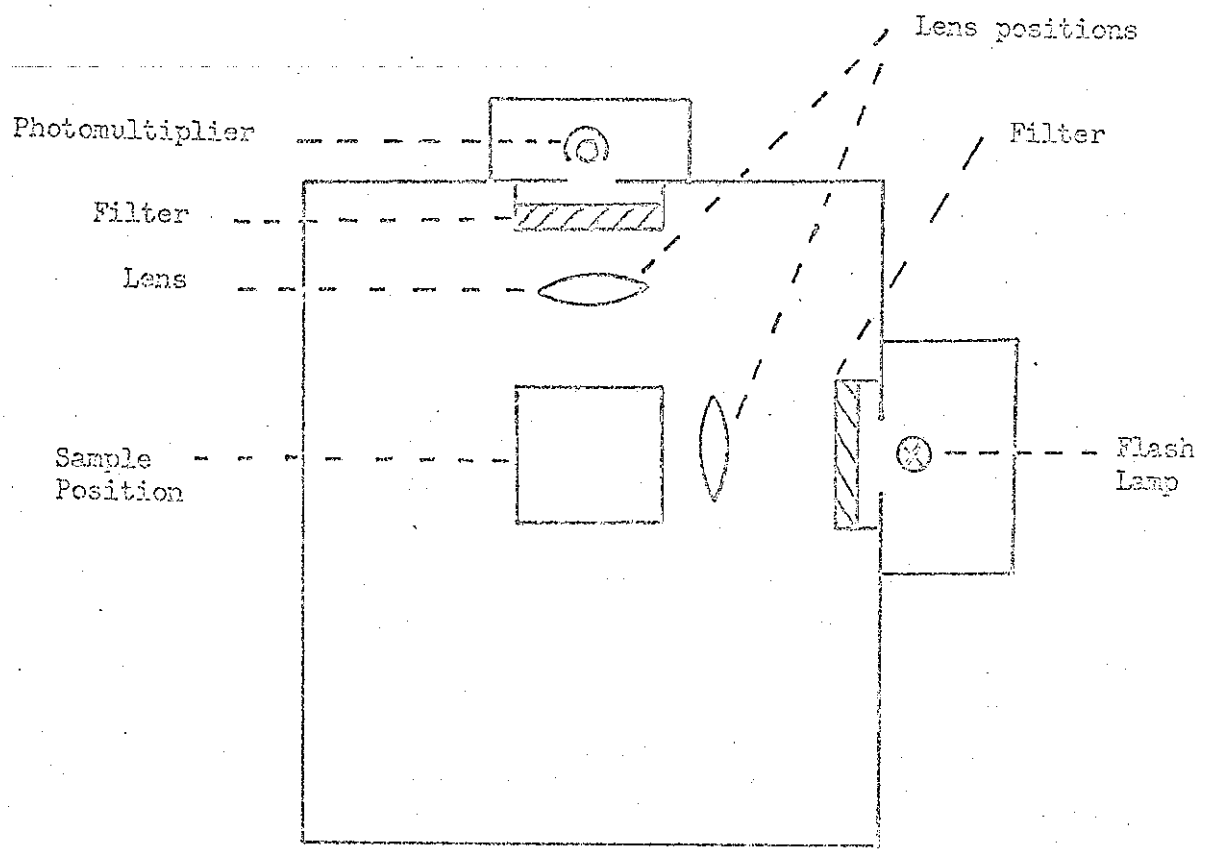

FIG. 9

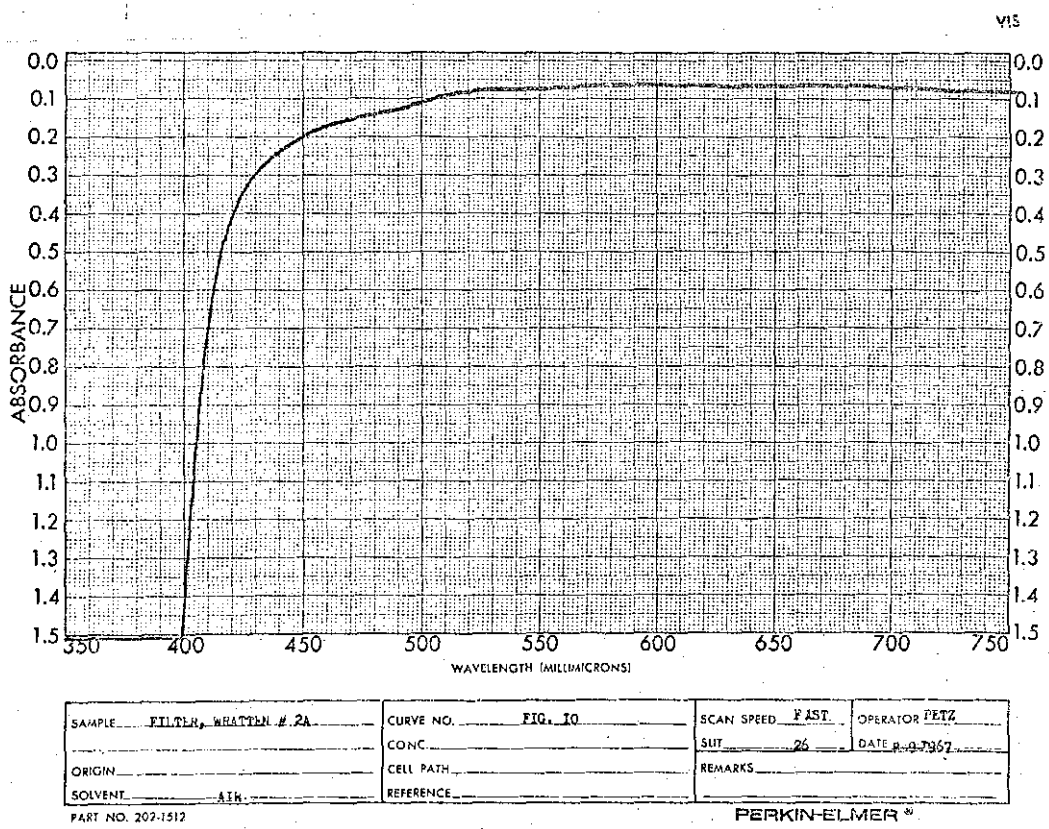
VIS
ABSORBANCE
0.0
0.1
0.2
0.3
0.4
0.5
0.6
0.7
0.8
0.9
1.0
1.1
1.2
1.3
1.4
1.5
350
400
450
500
550
600
650
700
750
WAVELENGTH (MILLIMICRONS)
SAMPLE FILTER, WHATTEN # 2A
CURVE NO. FIG. 10
SCAN SPEED FAST
OPERATOR PETZ
SLIT 26
DATE 8-9-1967
ORIGIN
CONC.
CELL PATH
REMARKS
SOLVENT AIR
REFERENCE
PART NO. 209-1512
PERKIN-ELMER

FIGURE 10

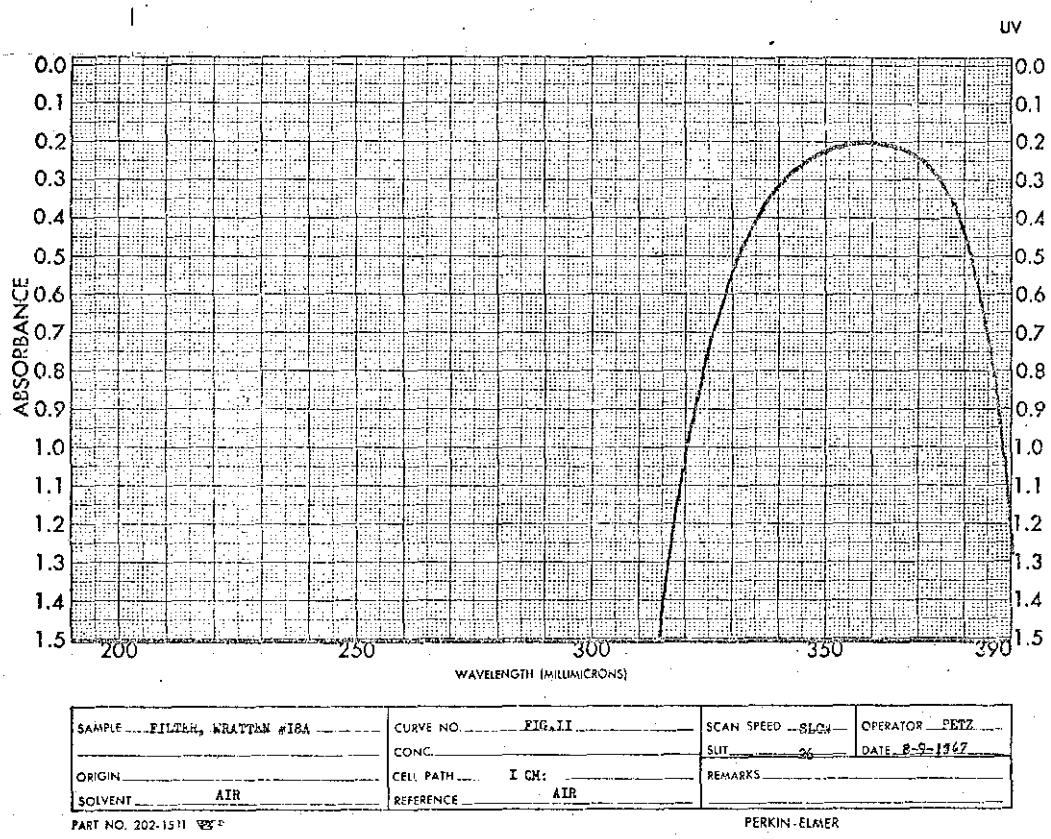
UV
ABSORBANCE
0.0
0.1
0.2
0.3
0.4
0.5
0.6
0.7
0.8
0.9
1.0
1.1
1.2
1.3
1.4
1.5
200
250
300
350
390
WAVELENGTH (MILLIMICRONS)
SAMPLE FILTER, WRATTEN #18A
CURVE NO. FIG.II
SCAN SPEED SLOW
OPERATOR PETZ
CONC.
SLIT 96
DATE 8-9-1967
ORIGIN
CELL PATH 1 CM:
REMARKS
SOLVENT AIR
REFERENCE AIR
PART NO. 202-1511
PERKIN-ELMER

FIGURE 11

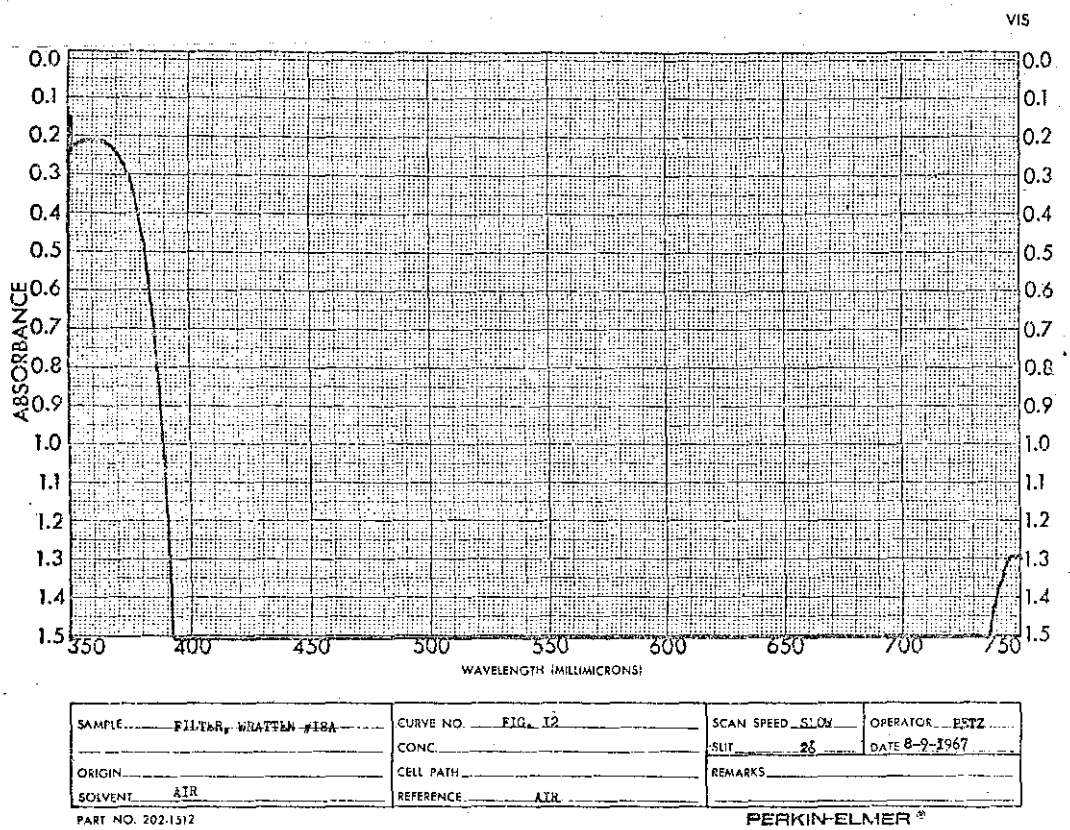
VIS
ABSORBANCE
0.0
0.1
0.2
0.3
0.4
0.5
0.6
0.7
0.8
0.9
1.0
1.1
1.2
1.3
1.4
1.5
350
400
450
500
550
600
650
700
750
WAVELENGTH (MILLIMICRONS)
SAMPLE FILTER, WRATTEN #18A
CURVE NO. FIG. 12
SCAN SPEED SLOW
OPERATOR PSTZ
SLIT 2S
DATE 8-9-1967
ORIGIN
CONC.
CELL PATH
REMARKS
SOLVENT AIR
REFERENCE AIR
PART NO. 202-1512
PERKIN-ELMER

FIGURE 12

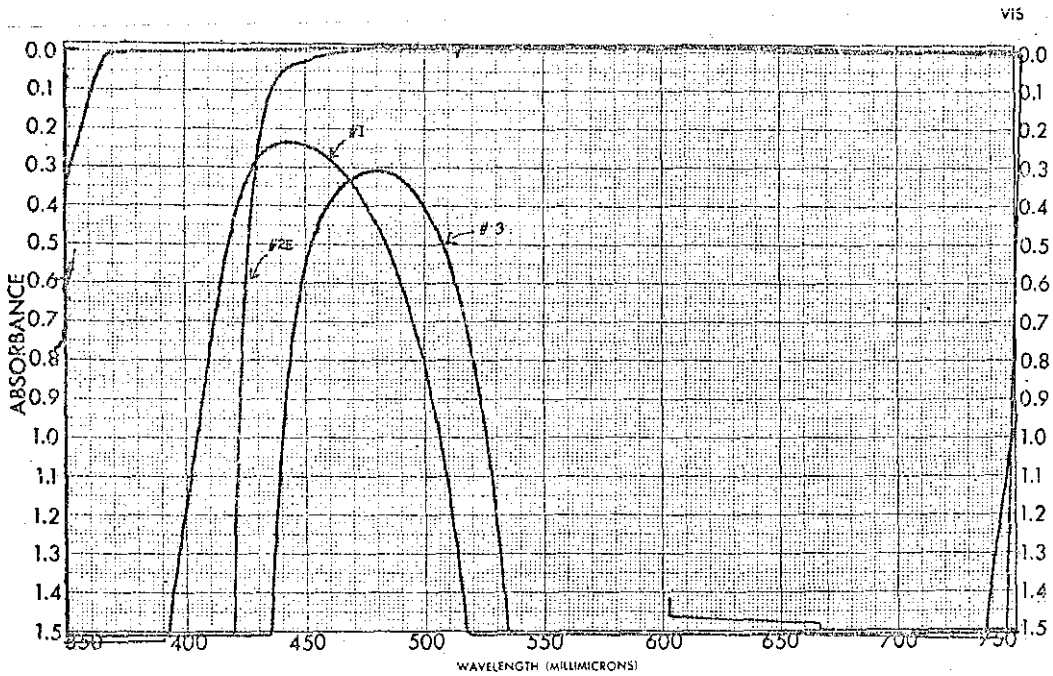

SAMPLE FILTERS: #I, WRATTEN # 47	CURVE NO. FIG.13	SCAN SPEED FAST	OPERATOR FETZ
#2, WRATTEN #2E #3, WRATTEN #45	CONC.	SLIT 26	DATE 8-9-1967
ORIGIN	CELL PATH	REMARKS	
SOLVENT SOLVENT: AIR	REFERENCE AIR		

FIGURE 13

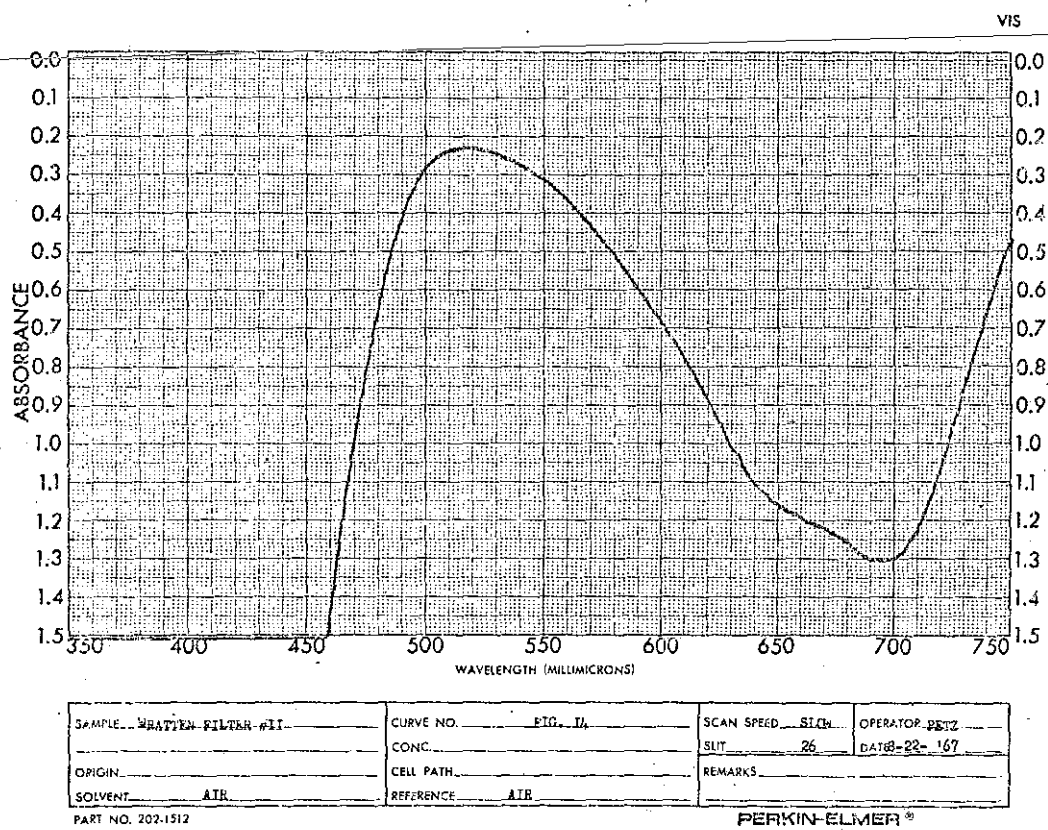
VIS
ABSORBANCE
0.0
0.1
0.2
0.3
0.4
0.5
0.6
0.7
0.8
0.9
1.0
1.1
1.2
1.3
1.4
1.5
350
400
450
500
550
600
650
700
750
WAVELENGTH (MILLIMICRONS)
SAMPLE WRATTEN FILTER #11
CURVE NO. FIG. 11A
SCAN SPEED SLOW
OPERATOR PETZ
SLIT 26
DATE 8-22-'67
ORIGIN
CONC.
CELL PATH
REMARKS
SOLVENT AIR
REFERENCE AIR
PART NO. 202-1512
PERKIN-ELMER

FIGURE 14

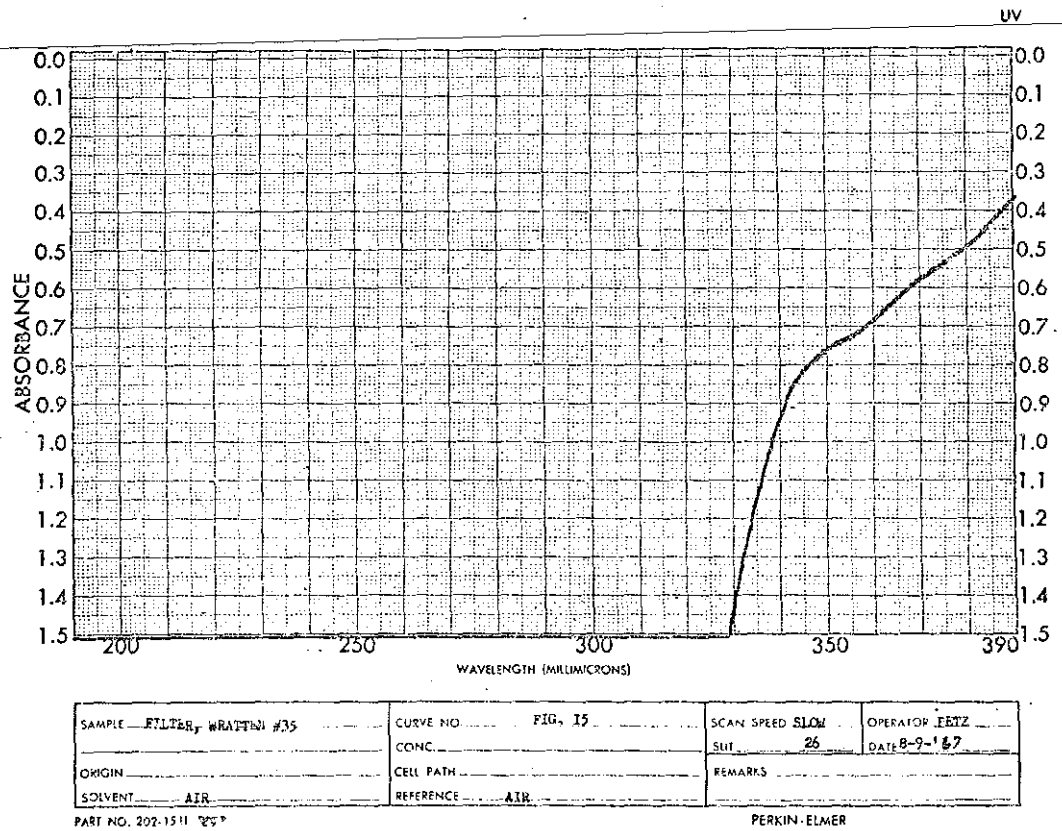
UV
ABSORBANCE
0.0
0.1
0.2
0.3
0.4
0.5
0.6
0.7
0.8
0.9
1.0
1.1
1.2
1.3
1.4
1.5
200
250
300
350
390
WAVELENGTH (MILLIMICRONS)
SAMPLE FILTER, WRATTEN #35
CURVE NO. FIG. 15
SCAN SPEED SLOW
SLIT 26
OPERATOR FETZ
DATE 8-9-67
ORIGIN
CONC.
CELL PATH
REMARKS
SOLVENT AIR
REFERENCE AIR
PART NO. 202-1511
PERKIN-ELMER

FIGURE 15

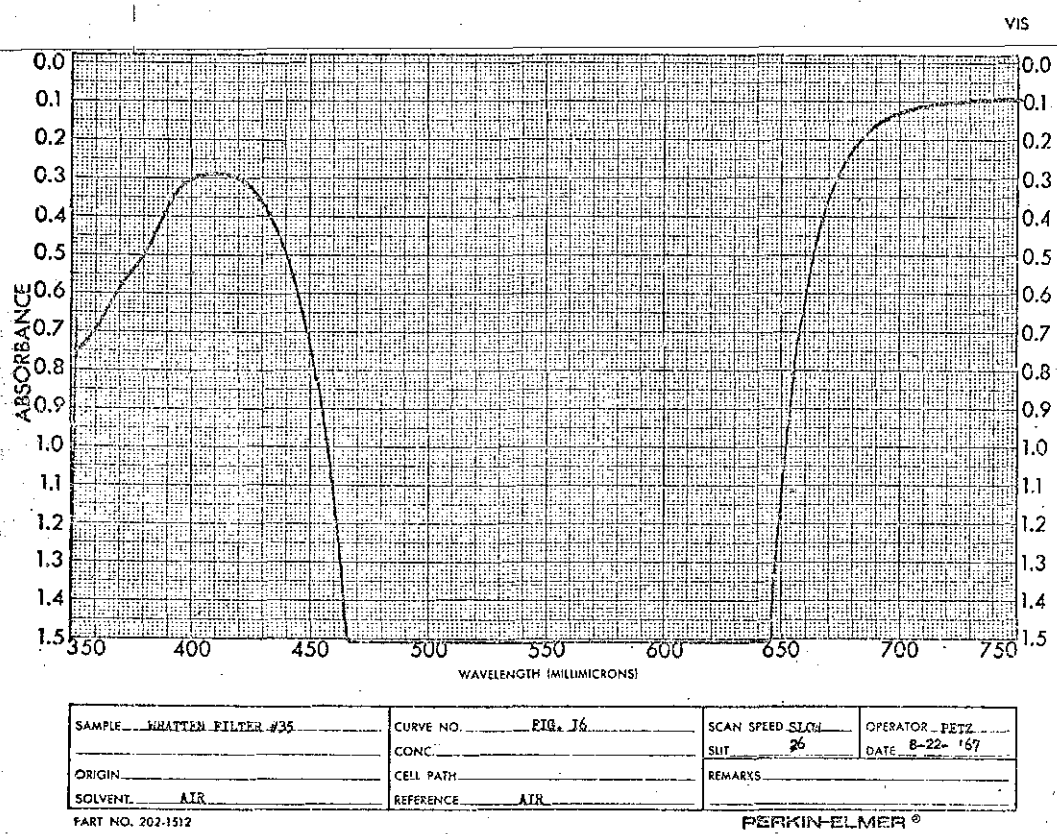
VIS
ABSORBANCE
0.0
0.1
0.2
0.3
0.4
0.5
0.6
0.7
0.8
0.9
1.0
1.1
1.2
1.3
1.4
1.5
350
400
450
500
550
600
650
700
750
WAVELENGTH (MILLIMICRONS)
SAMPLE KRATTEN FILTER #35
CURVE NO. FIG. J6
SCAN SPEED SLOW
OPERATOR PETZ
SLIT 26
DATE 8-22-'67
CONC.
ORIGIN
CELL PATH
REMARKS
SOLVENT AIR
REFERENCE AIR
PART NO. 202-1512
PERKIN-ELMER ®

FIGURE 16

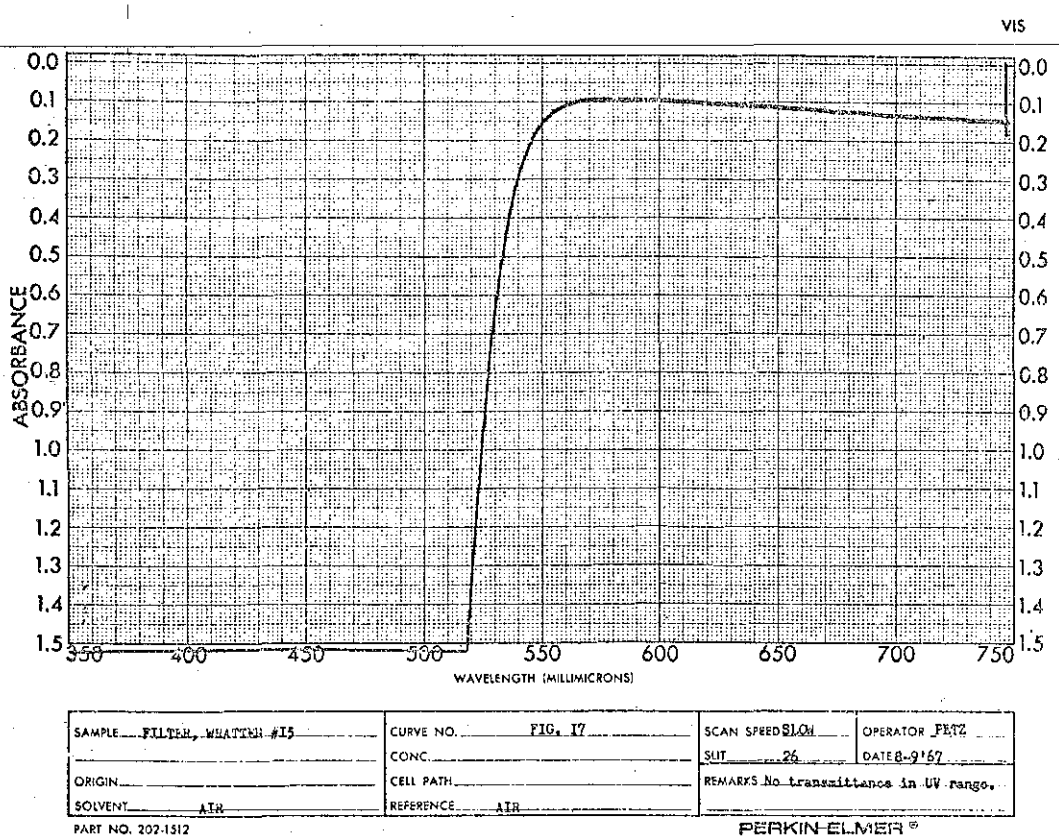
VIS
ABSORBANCE
0.0
0.1
0.2
0.3
0.4
0.5
0.6
0.7
0.8
0.9
1.0
1.1
1.2
1.3
1.4
1.5
350
400
450
500
550
600
650
700
750
WAVELENGTH (MILLIMICRONS)
SAMPLE FILTER, WHATTEN #15
CURVE NO. FIG. 17
SCAN SPEED SLOW
OPERATOR PETZ
CONC.
SLIT 26
DATE 8-9'67
ORIGIN
CELL PATH
REMARKS No transmittance in UV range.
SOLVENT AIR
REFERENCE AIR
PART NO. 202-1512
PERKIN-ELMER ©

FIGURE 17

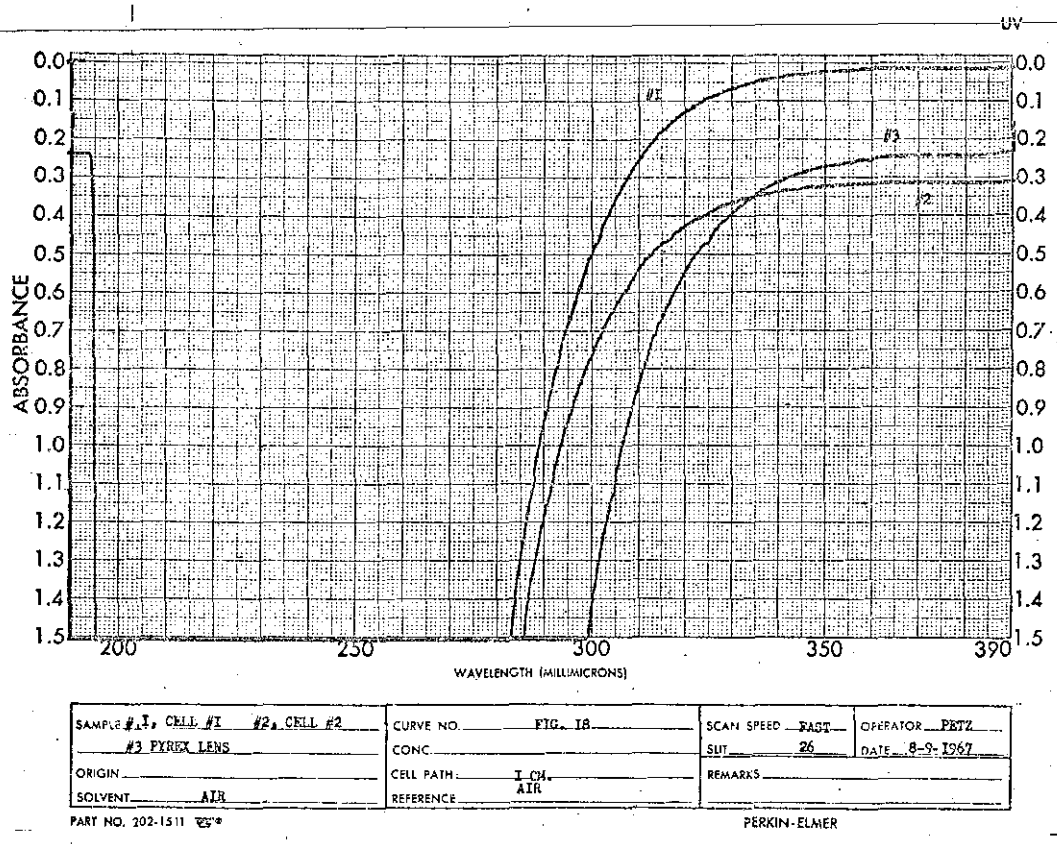
UV
ABSORBANCE
0.0
0.1
0.2
0.3
0.4
0.5
0.6
0.7
0.8
0.9
1.0
1.1
1.2
1.3
1.4
1.5
200
250
300
350
390
WAVELENGTH (MILLIMICRONS)
#1
#3
#2
SAMPLE #1, I, CELL #1 #2, CELL #2
#3 PYREX LENS
ORIGIN
SOLVENT AIR
CURVE NO. FIG. 18
CONC.
CELL PATH: 1 CM.
REFERENCE AIR
SCAN SPEED FAST
SLIT 26
OPERATOR PETZ
DATE 8-9-1967
REMARKS
PART NO. 202-1511
PERKIN-ELMER

FIGURE 18

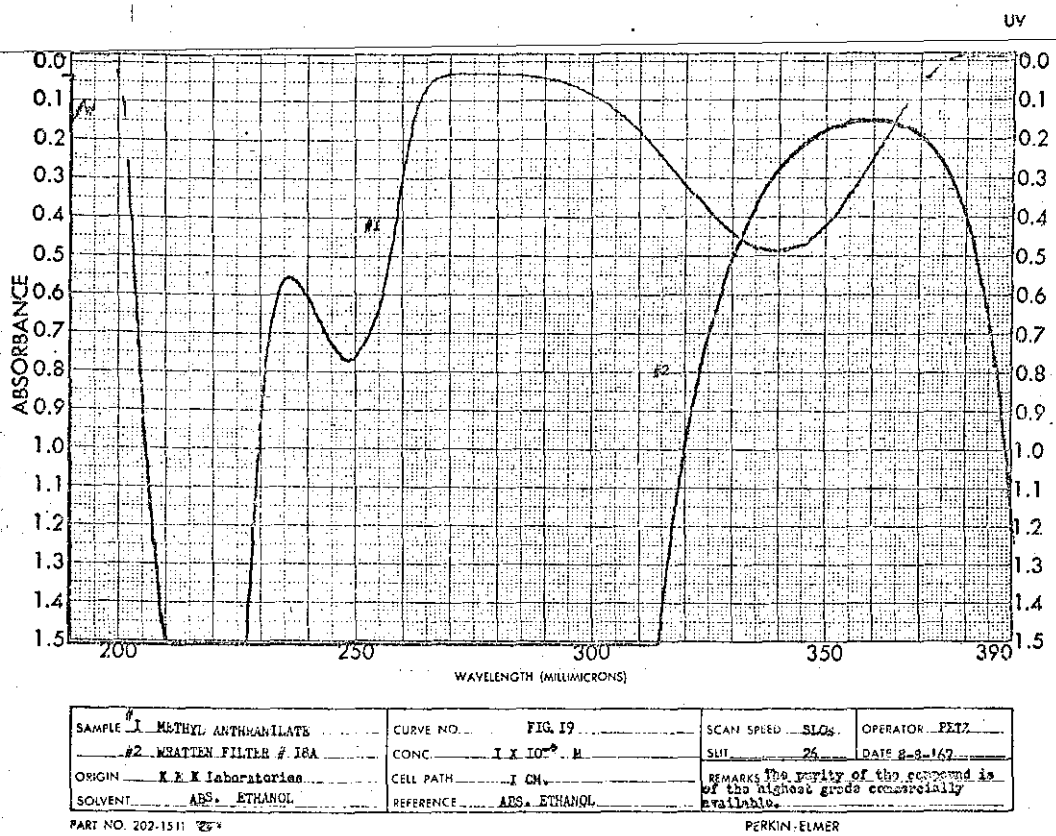
UV
ABSORBANCE
0.0
0.1
0.2
0.3
0.4
0.5
0.6
0.7
0.8
0.9
1.0
1.1
1.2
1.3
1.4
1.5
200
250
300
350
390
WAVELENGTH (MILLIMICRONS)
#1
#2
SAMPLE #1 METHYL ANTHRANILATE
#2 WRATTEN FILTER # 18A
ORIGIN K & K Laboratories
SOLVENT ABS. ETHANOL
CURVE NO. FIG. 19
CONC. 1 X 10⁻⁵ M
CELL PATH 1 CM.
REFERENCE ABS. ETHANOL
SCAN SPEED SLOW
SLIT 25
OPERATOR PETZ
DATE 8-8-67
REMARKS The purity of the compound is of the highest grade commercially available.
PART NO. 202-1511
PERKIN-ELMER

FIGURE 19

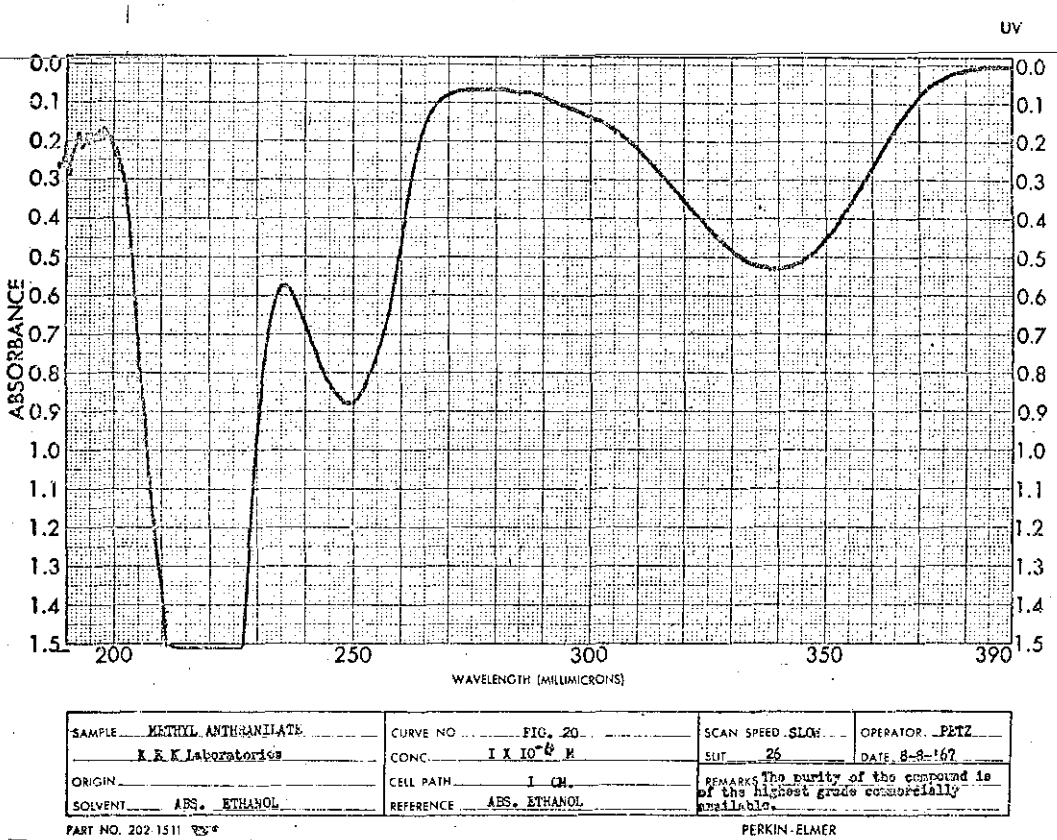
UV
ABSORBANCE
0.0
0.1
0.2
0.3
0.4
0.5
0.6
0.7
0.8
0.9
1.0
1.1
1.2
1.3
1.4
1.5
200
250
300
350
390
WAVELENGTH (MILLIMICRONS)
SAMPLE METHYL ANTHRANILATE
K & K Laboratories
ORIGIN
SOLVENT ABS. ETHANOL
CURVE NO FIG. 20
CONC. 1 X 10⁻⁴ M
CELL PATH 1 CM.
REFERENCE ABS. ETHANOL
SCAN SPEED SLOW
SLIT 26
OPERATOR PETZ
DATE 8-8-'67
REMARKS The purity of the compound is of the highest grade commercially available.
PART NO. 202-1511
PERKIN-ELMER

FIGURE 20

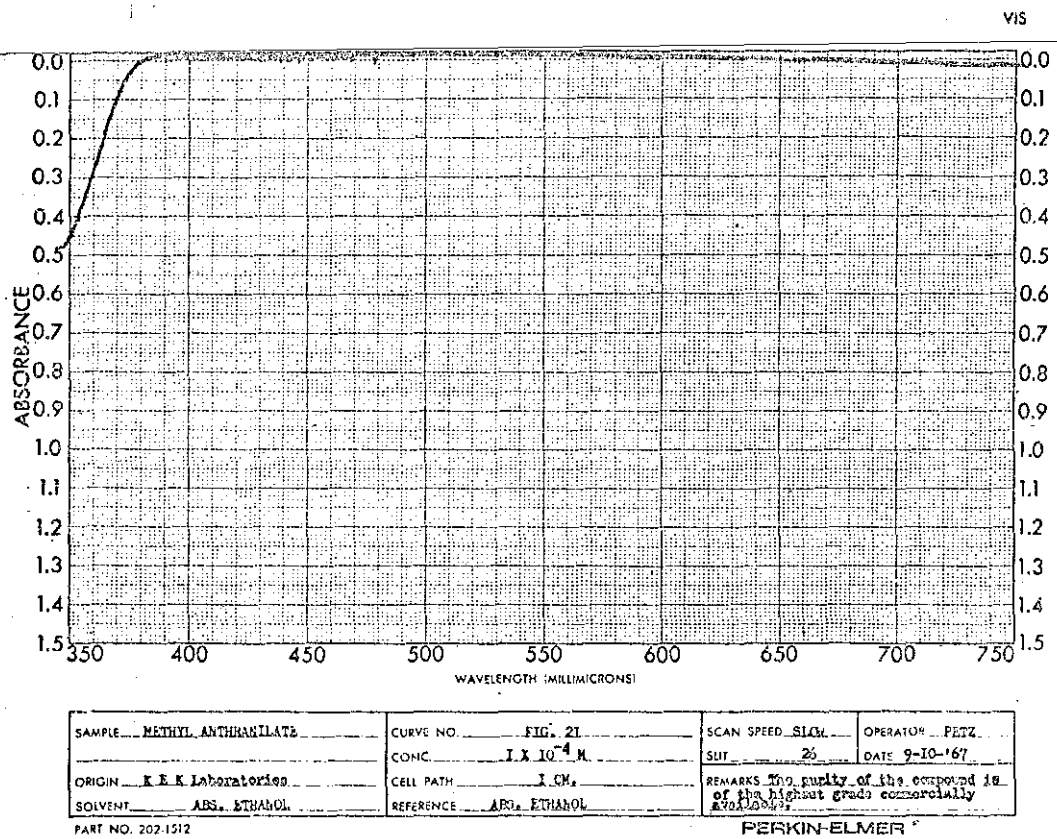
VIS
ABSORBANCE
0.0
0.1
0.2
0.3
0.4
0.5
0.6
0.7
0.8
0.9
1.0
1.1
1.2
1.3
1.4
1.5
350
400
450
500
550
600
650
700
750
WAVELENGTH (MILLIMICRONS)
SAMPLE METHYL ANTHRANILATE
CURVE NO. FIG. 21
SCAN SPEED SLOW
OPERATOR PETZ
CONC. 1 X 10⁻⁴ M.
SLIT 26
DATE 9-10-'67
ORIGIN K & K Laboratories
CELL PATH 1 CM.
REMARKS The purity of the compound is of the highest grade commercially available.
SOLVENT ABS. ETHANOL
REFERENCE ABS. ETHANOL
PART NO. 202-1512
PERKIN-ELMER

FIGURE 21

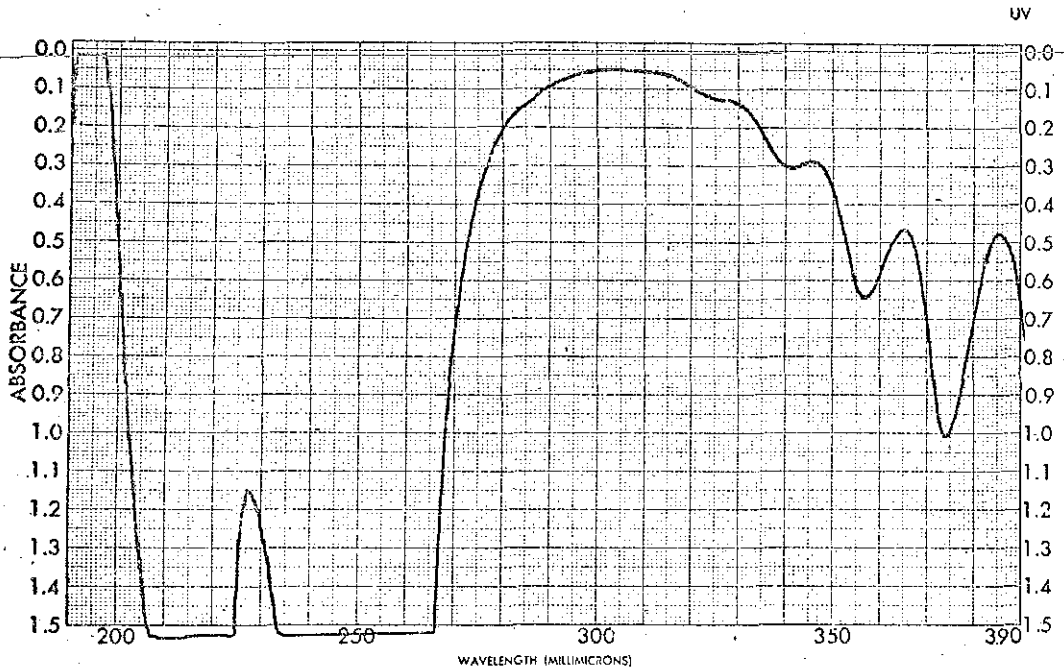

SAMPLE 9, 10-DIPHENYL ANTHRACENE	CURVE NO. FIG. 22	SCAN SPEED SLOW	OPERATOR PETZ
	CONC. 1×10^{-4} M	SLIT 26	DATE 8-8-'57
ORIGIN K.E.K laboratories	CELL PATH 1 CM.	REMARKS The purity of the compound is of the highest grade commercially available.	
SOLVENT ABS. ETHANOL	REFERENCE ABS. ETHANOL		

PART NO. 202-1511 "S" PERKIN-ELMER

FIGURE 22

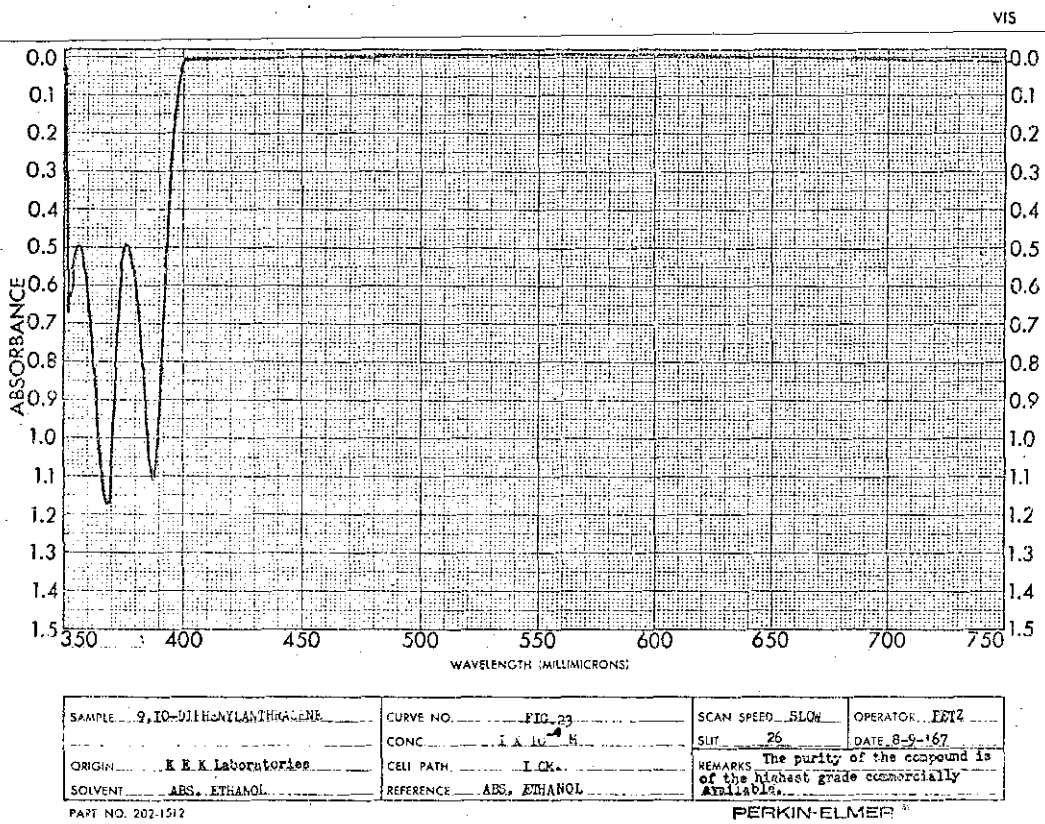
VIS
ABSORBANCE
0.0
0.1
0.2
0.3
0.4
0.5
0.6
0.7
0.8
0.9
1.0
1.1
1.2
1.3
1.4
1.5
350
400
450
500
550
600
650
700
750
WAVELENGTH (MILLIMICRONS)
SAMPLE 9,10-DIPHENYLANTHRACENE
CURVE NO. FIG 23
SCAN SPEED SLOW
OPERATOR FETZ
CONC 1 X 10⁻⁴ M
SLIT 26
DATE 8-9-'67
ORIGIN K & K Laboratories
CELL PATH 1 CM.
REMARKS The purity of the compound is of the highest grade commercially available.
SOLVENT ABS. ETHANOL
REFERENCE ABS. ETHANOL
PART NO. 202-1512
PERKIN-ELMER

FIGURE 23

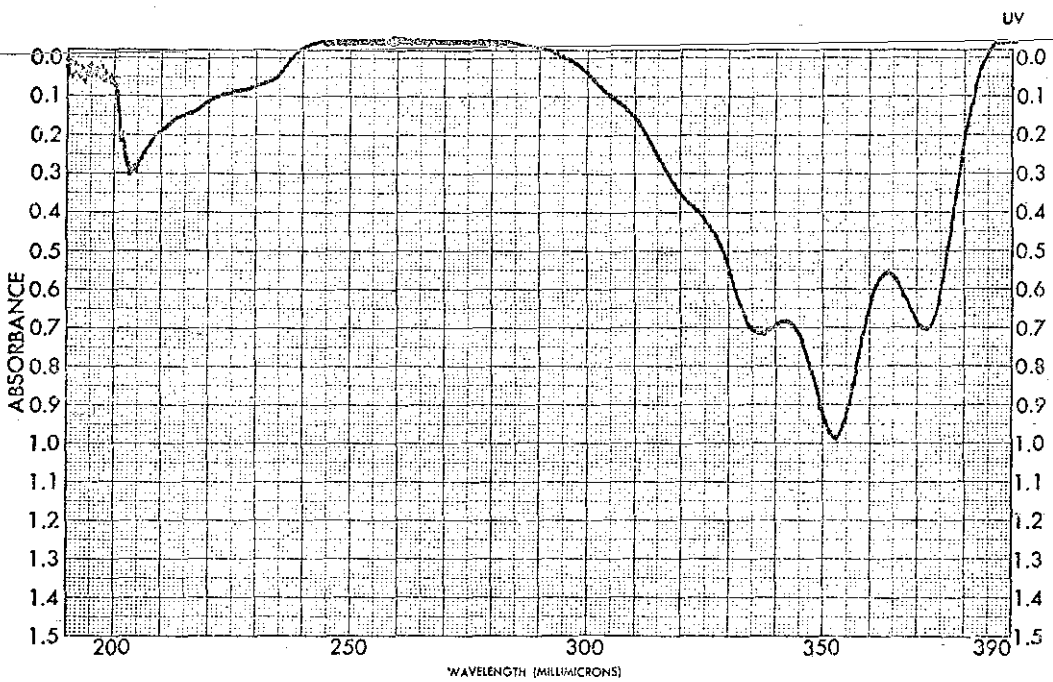

SAMPLE 1,6-DIPHENYL-1,3,5-HEXATRIENE	CURVE NO. FIG. 24	SCAN SPEED SLOW	OPERATOR PETZ
	CONC. 1×10^{-4} M	SLIT 26	DATE 8-8-'67
ORIGIN K & K Laboratories	CELL PATH 1 CM.	REMARKS The purity of the compound is of the highest grade commercially available	
SOLVENT ABS. ETHANOL	REFERENCE ABS. ETHANOL		

PART NO. 202-1511 "S"

PERKIN-ELMER

FIGURE 24

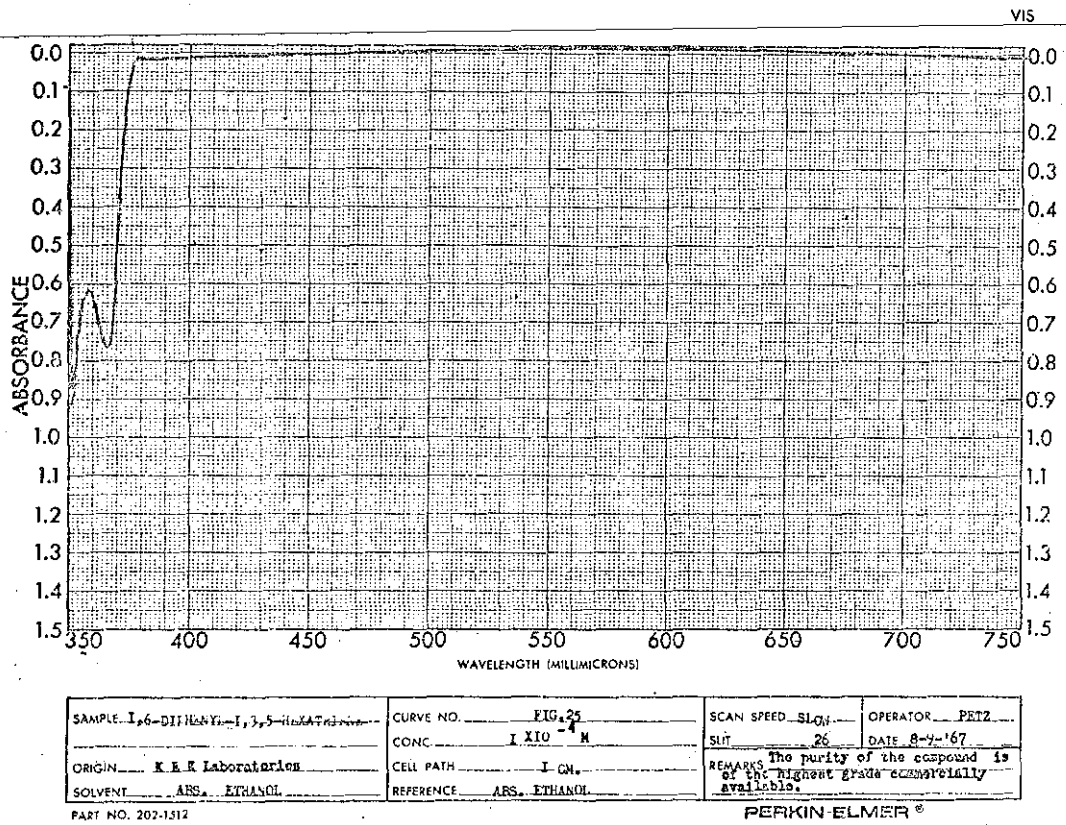
VIS
ABSORBANCE
0.0
0.1
0.2
0.3
0.4
0.5
0.6
0.7
0.8
0.9
1.0
1.1
1.2
1.3
1.4
1.5
350
400
450
500
550
600
650
700
750
WAVELENGTH (MILLIMICRONS)
SAMPLE 1,6-DIPHENYL-1,3,5-HEXATRIENE
ORIGIN K & R Laboratories
SOLVENT ABS. ETHANOL
CURVE NO. FIG. 25
CONC. 1 X10 -4 M
CELL PATH 1 CM.
REFERENCE ABS. ETHANOL
SCAN SPEED SLOW
SLIT 26
OPERATOR PETZ
DATE 8-4-'67
REMARKS The purity of the compound is of the highest grade commercially available.
PART NO. 202-1512
PERKIN-ELMER ®

FIGURE 25

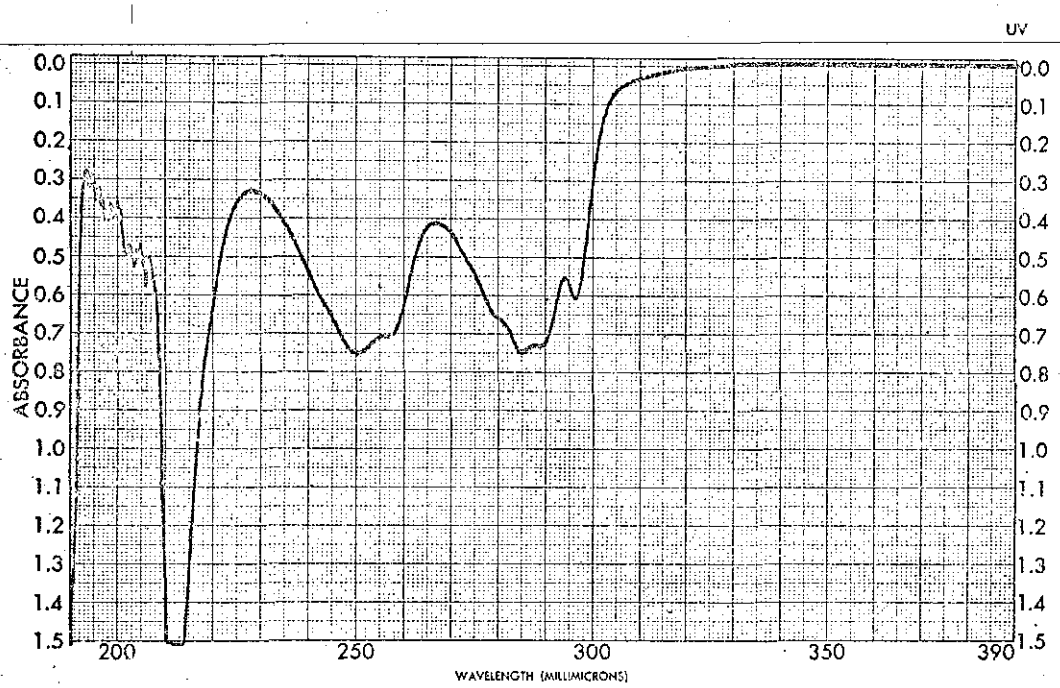
UV
ABSORBANCE
0.0
0.1
0.2
0.3
0.4
0.5
0.6
0.7
0.8
0.9
1.0
1.1
1.2
1.3
1.4
1.5
200
250
300
350
390
WAVELENGTH (MILLIMICRONS)
SAMPLE INDAZOLE
Merck & Co.
ORIGIN
SOLVENT 0.01 IN WATER (1 X 10⁻² M)
CURVE NO. FIG. 26
CONC. 1 X 10⁻⁴ M
CELL PATH 1 CM.
REFERENCE 0.01 M NaOH (WATER)
SCAN SPEED SLOW
SLIT 26
OPERATOR FETZ
DATE 8-18-'67
REMARKS The purity of the compound is of the highest grade commercially available.
PART NO. 202-1511
PERKIN-ELMER

FIGURE 26

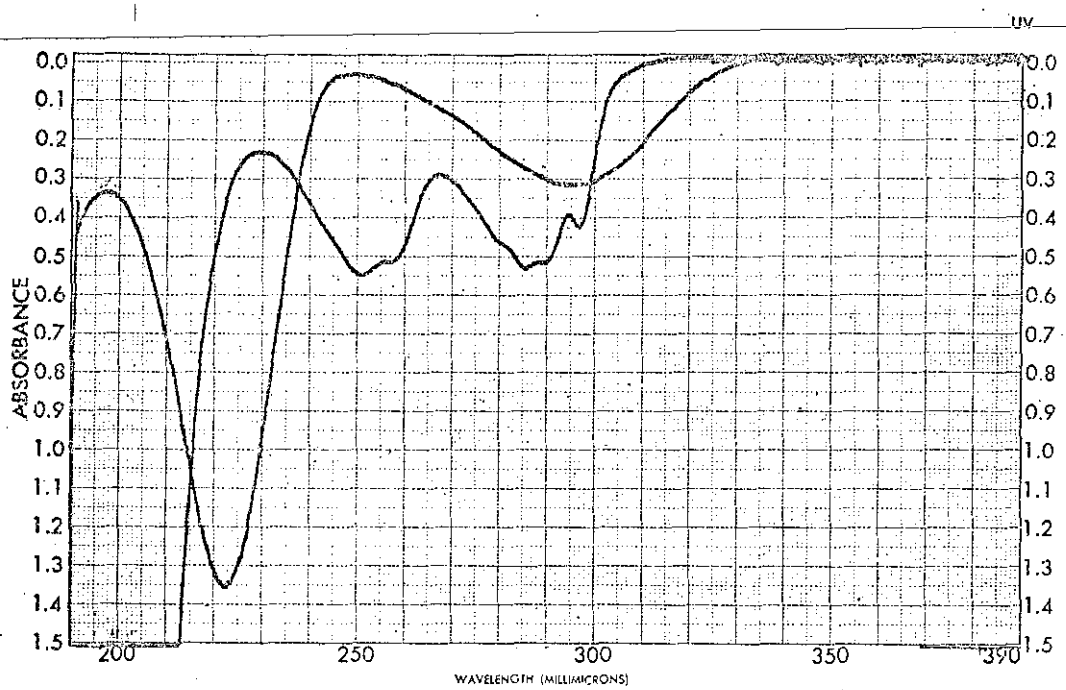
UV
ABSORBANCE
0.0
0.1
0.2
0.3
0.4
0.5
0.6
0.7
0.8
0.9
1.0
1.1
1.2
1.3
1.4
1.5
200
250
300
350
390
WAVELENGTH (MILLIMICRONS)
SAMPLE # 1 IMIDAZOLE # 2 2-AMINOPYRIMIDINE
CURVE NO. FIG. 27
CONC. 1.0 X 10⁻⁴
SCAN SPEED SLOW
SLIT 2%
OPERATOR PETZ
DATE 8-16-67
ORIGIN Merck & Co.
SOLVENT 0.01 N [illegible](H2O)
CELL PATH 1 cm.
REFERENCE 0.01 N H2SO4(H2O)
REMARKS The purity of the compound is of the highest grade commercially available.
PART NO. 202-1511
PERKIN-ELMER

FIGURE 27

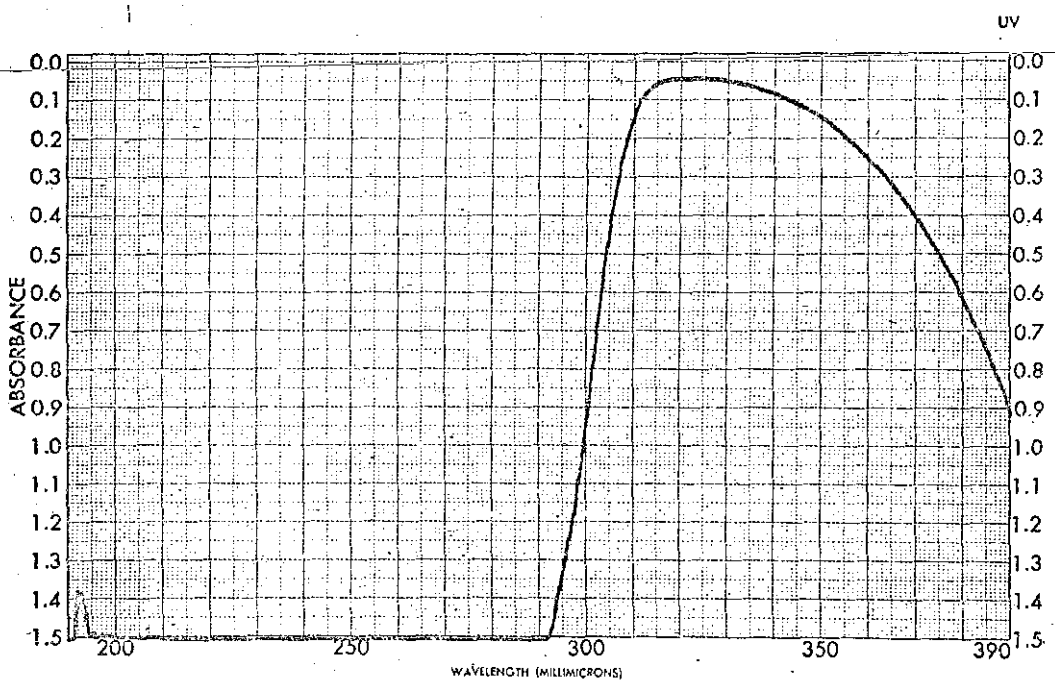
UV
ABSORBANCE
0.0
0.1
0.2
0.3
0.4
0.5
0.6
0.7
0.8
0.9
1.0
1.1
1.2
1.3
1.4
1.5
200
250
300
350
390
WAVELENGTH (MILLIMICRONS)
SAMPLE PROFLAVIN
CURVE NO. FIG. 28
SCAN SPEED SLOW
OPERATOR PETZ
CONC. 1 x 10⁻⁵ M
SLIT 26
DATE 22-167
ORIGIN K & K Laboratories
CELL PATH 1 CM.
REMARKS The purity of the compound is of the highest grade commercially available.
SOLVENT WATER
REFERENCE WATER
PART NO. 202-1511
PERKIN-ELMER

FIGURE 28

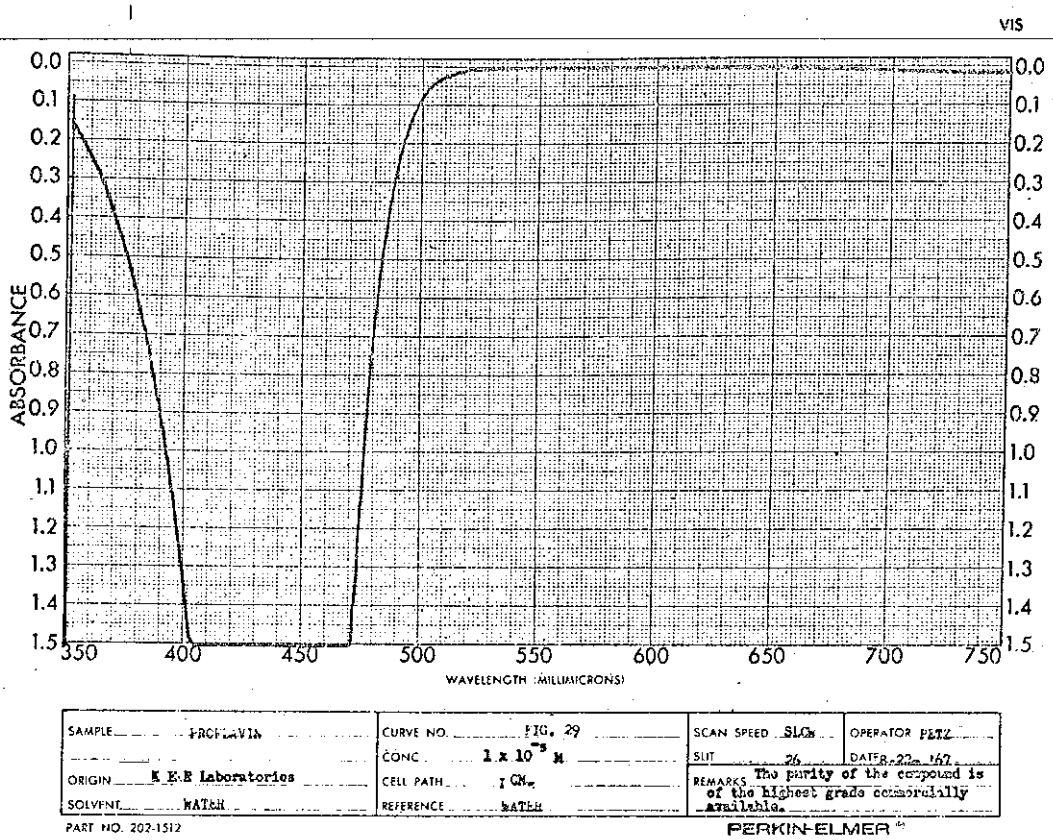
VIS
ABSORBANCE
0.0
0.1
0.2
0.3
0.4
0.5
0.6
0.7
0.8
0.9
1.0
1.1
1.2
1.3
1.4
1.5
350
400
450
500
550
600
650
700
750
WAVELENGTH (MILLIMICRONS)
SAMPLE PROFLAVIN
ORIGIN K & K Laboratories
SOLVENT WATER
CURVE NO. FIG. 29
CONC 1 x 10⁻⁵ M
CELL PATH 1 CM.
REFERENCE WATER
SCAN SPEED SLOW
SLIT 26
OPERATOR PETZ
DATE 8-22-67
REMARKS The purity of the compound is of the highest grade commercially available.
PART NO. 202-1512
PERKIN-ELMER

FIGURE 29

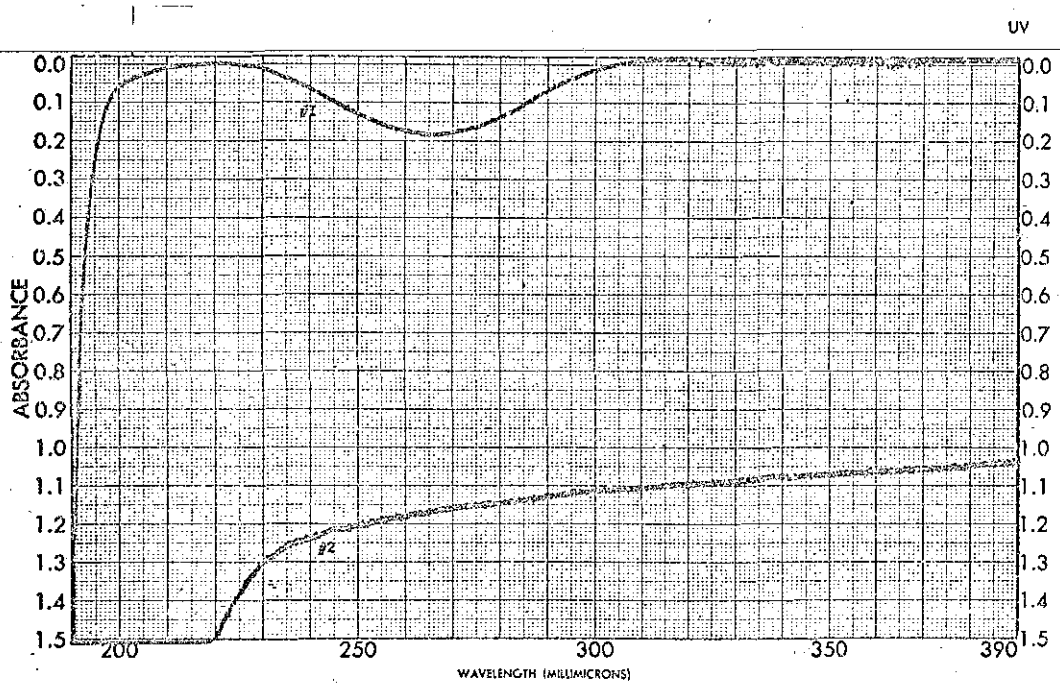
UV
ABSORBANCE
0.0
0.1
0.2
0.3
0.4
0.5
0.6
0.7
0.8
0.9
1.0
1.1
1.2
1.3
1.4
1.5
#1
#2
200
250
300
350
390
WAVELENGTH (MILLIMICRONS)
SAMPLE #1 GLYCINE
2 L-ASCORBIC ACID
ORIGIN Eastman Kodak Co.
SOLVENT WATER
CURVE NO. FIG. 30
CONC. #1 1 X 10⁻³ M
#2 1 X 10⁻⁴ M
CELL PATH 1 CM.
REFERENCE WATER
SCAN SPEED SLOW
SUI 25
OPERATOR FETZ
DATE 8-16-'67
REMARKS The purity of the compound is of the highest grade commercially available.
PART NO. 202-1511
PERKIN-ELMER

FIGURE 30

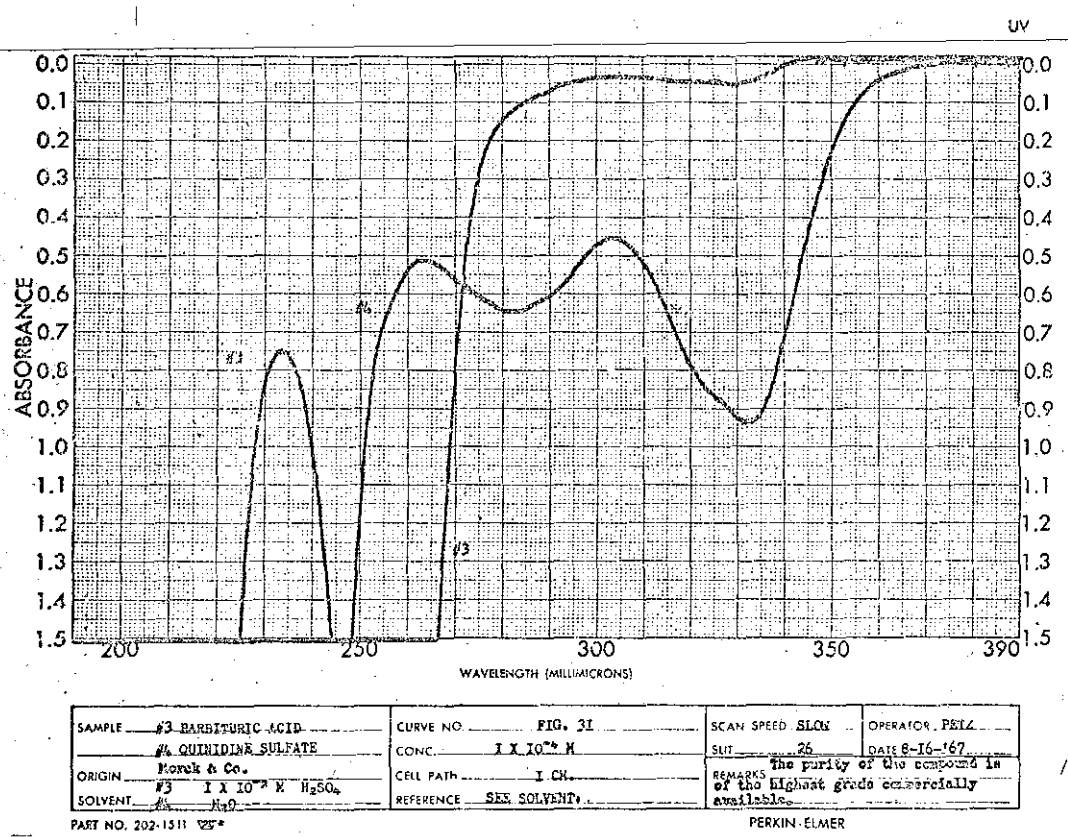
UV
ABSORBANCE
0.0
0.1
0.2
0.3
0.4
0.5
0.6
0.7
0.8
0.9
1.0
1.1
1.2
1.3
1.4
1.5
200
250
300
350
390
WAVELENGTH (MILLIMICRONS)
#1
#2
#3
SAMPLE #3 BARBITURIC ACID
#4 QUINIDINE SULFATE
ORIGIN Merck & Co.
SOLVENT #3 1 X 10⁻² M H₂SO₄
#4 H₂O
CURVE NO. FIG. 31
CONC. 1 X 10⁻⁴ M
CELL PATH 1 CM.
REFERENCE SEE SOLVENT
SCAN SPEED SLOW
SLIT 26
OPERATOR PETZ
DATE 8-16-'67
REMARKS The purity of the compound is of the highest grade commercially available.
PART NO. 202-1511
PERKIN-ELMER

FIGURE 31

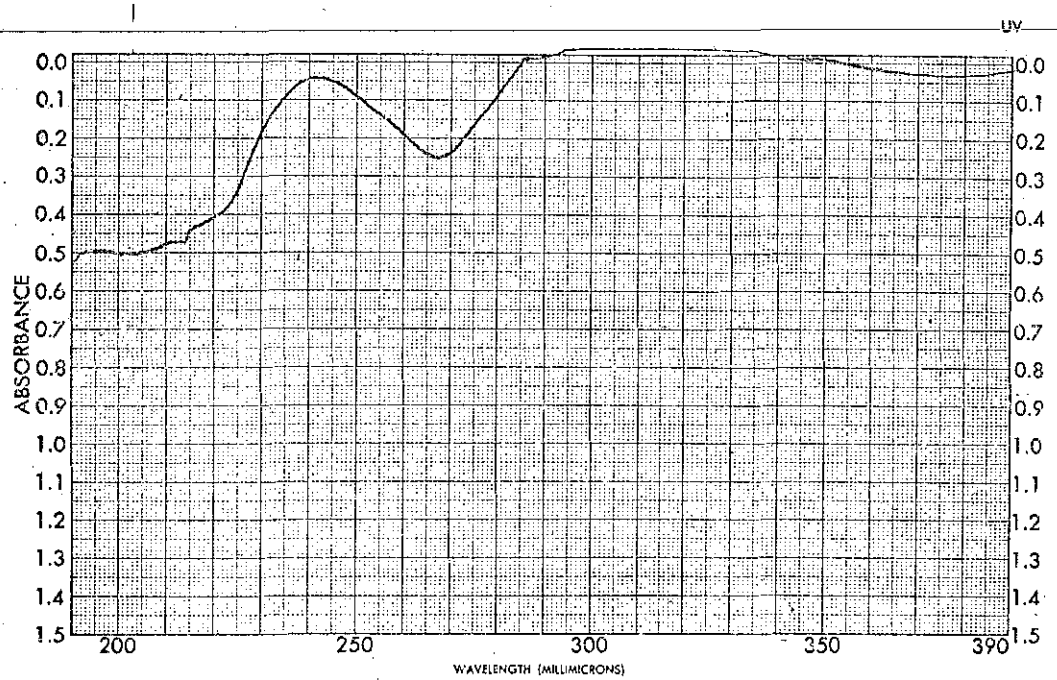

SAMPLE ALLOXAZINE	CURVE NO. FIG. 32	SCAN SPEED SLOW	OPERATOR PETZ
	CONC. 1.0×10^{-5} M	SLIT 26	DATE 8-9-'67
ORIGIN K & K Laboratories	CELL PATH 1 cm	REMARKS The purity of the compound is of the highest grade commercially available.	
SOLVENT 9 M H_2SO_4	REFERENCE 9 M. H_2SO_4		

PART NO. 202-1511

PERKIN-ELMER

FIGURE 32

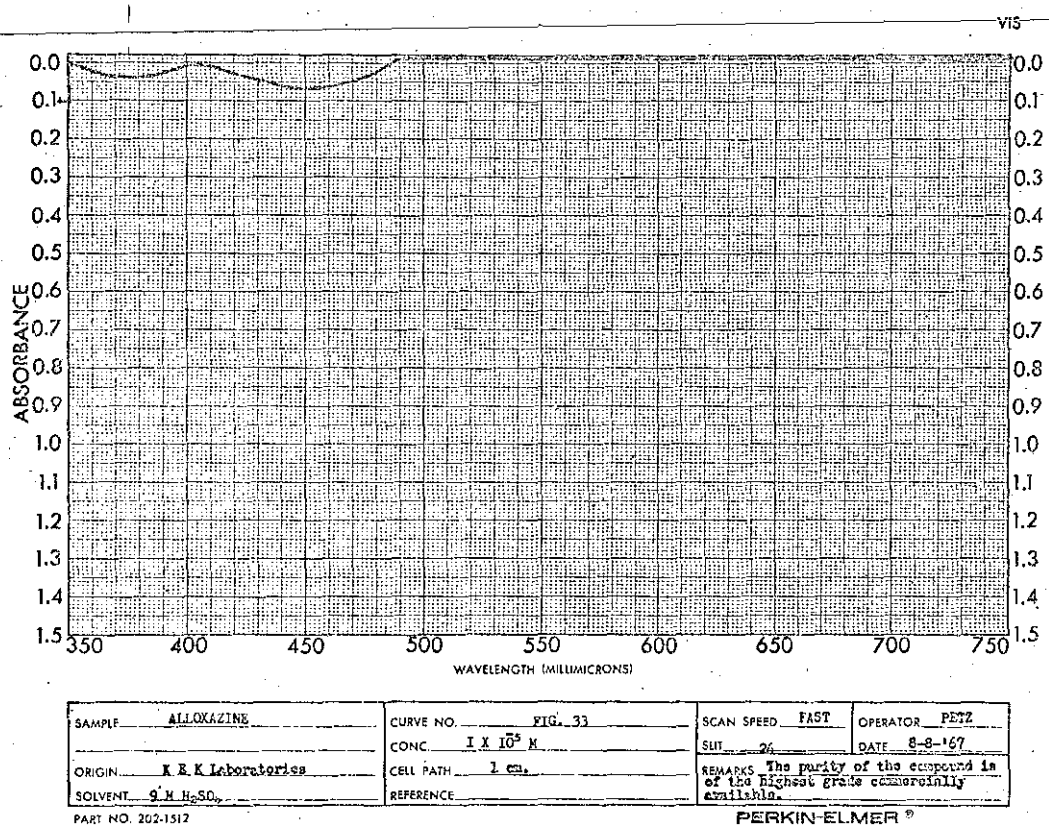
VIS
ABSORBANCE
0.0
0.1
0.2
0.3
0.4
0.5
0.6
0.7
0.8
0.9
1.0
1.1
1.2
1.3
1.4
1.5
350
400
450
500
550
600
650
700
750
WAVELENGTH (MILLIMICRONS)
SAMPLE ALLOXAZINE
ORIGIN K & K Laboratories
SOLVENT 9 M H2SO4
CURVE NO. FIG. 33
CONC. 1 X 10-5 M
CELL PATH 1 cm.
REFERENCE
SCAN SPEED FAST
SLIT 2
OPERATOR PETZ
DATE 8-8-'67
REMARKS The purity of the compound is of the highest grade commercially available.
PART NO. 202-1512
PERKIN-ELMER

FIGURE 33

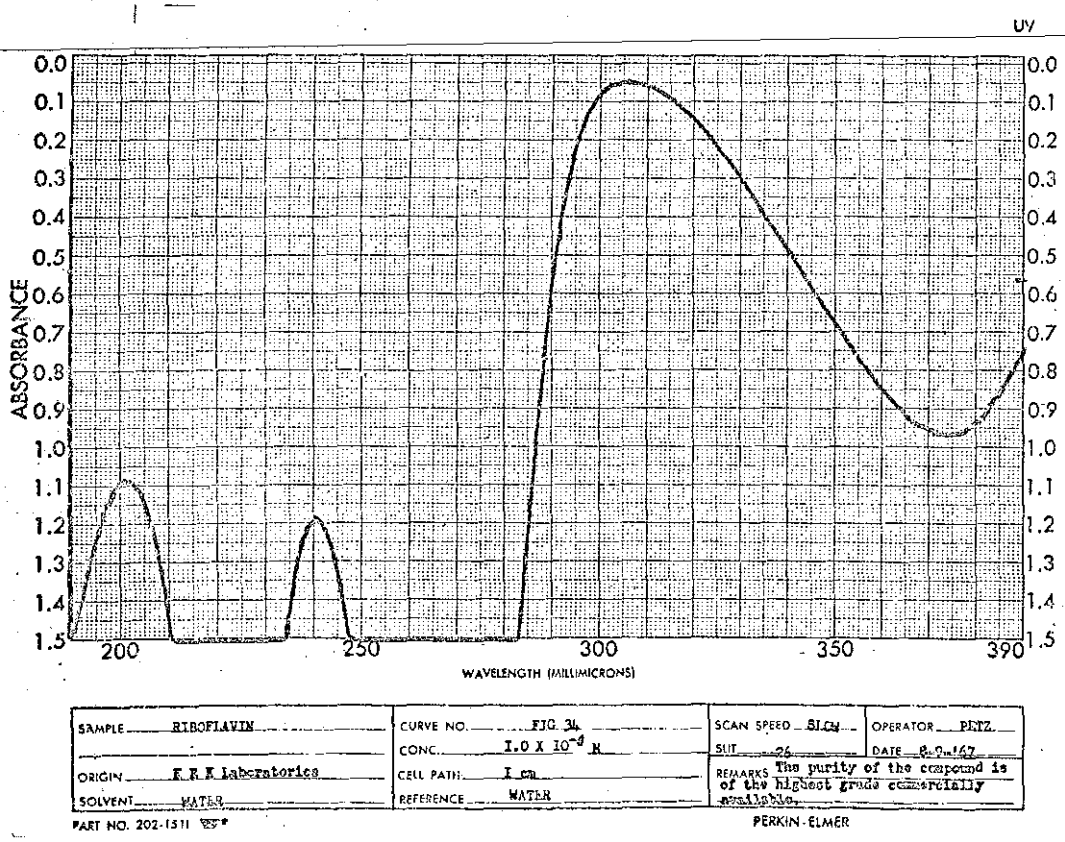
UV
ABSORBANCE
0.0
0.1
0.2
0.3
0.4
0.5
0.6
0.7
0.8
0.9
1.0
1.1
1.2
1.3
1.4
1.5
200
250
300
350
390
WAVELENGTH (MILLIMICRONS)
SAMPLE RIBOFLAVIN
ORIGIN E K K Laboratories
SOLVENT WATER
CURVE NO. FIG. 34
CONC. 1.0 X 10⁻⁴ M
CELL PATH 1 cm
REFERENCE WATER
SCAN SPEED SLOW
SLIT 26
OPERATOR PETZ
DATE 8-9-'47
REMARKS The purity of the compound is of the highest grade commercially available.
PART NO. 202-1511
PERKIN-ELMER

FIGURE 34

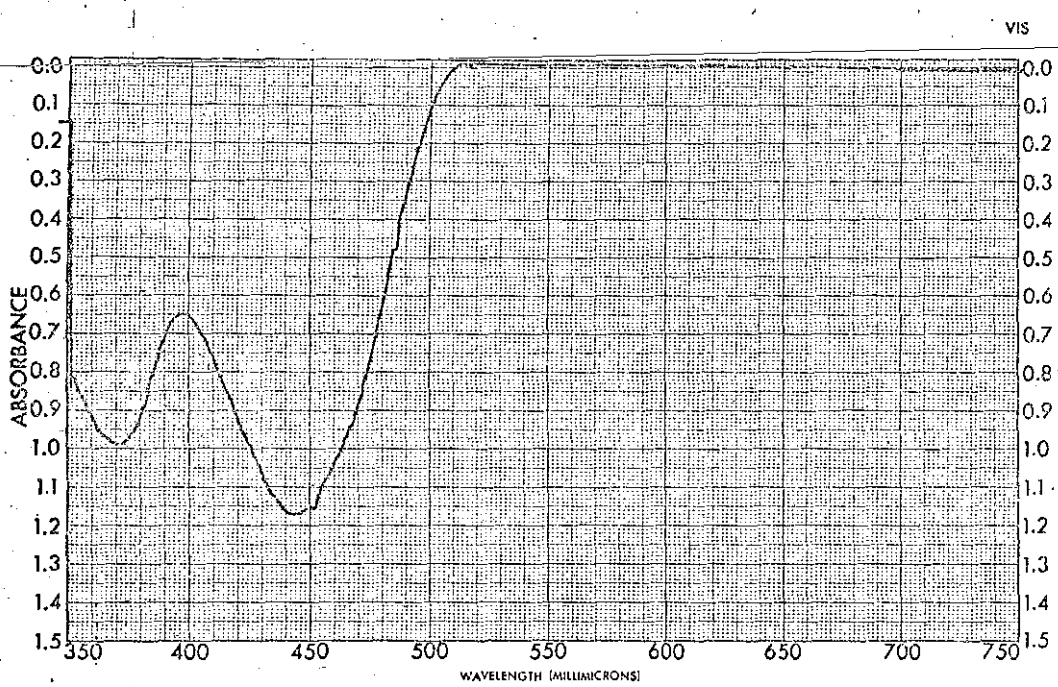
VIS
ABSORBANCE
0.0
0.1
0.2
0.3
0.4
0.5
0.6
0.7
0.8
0.9
1.0
1.1
1.2
1.3
1.4
1.5
350
400
450
500
550
600
650
700
750
WAVELENGTH (MILLIMICRONS)
SAMPLE RIBOFLAVIN
CURVE NO. FIG. 35
SCAN SPEED SLOW
OPERATOR PETZ
CONC. 1:0 X10⁻⁹ M
SLIT 26
DATE 8-22-'67
ORIGIN K E K laboratories
CELL PATH 1 CM.
REMARKS The purity of the compound is of the highest grade commercially available.
SOLVENT WATER
REFERENCE WATER
PART NO. 202-1512
PERKIN-ELMER

FIGURE 35

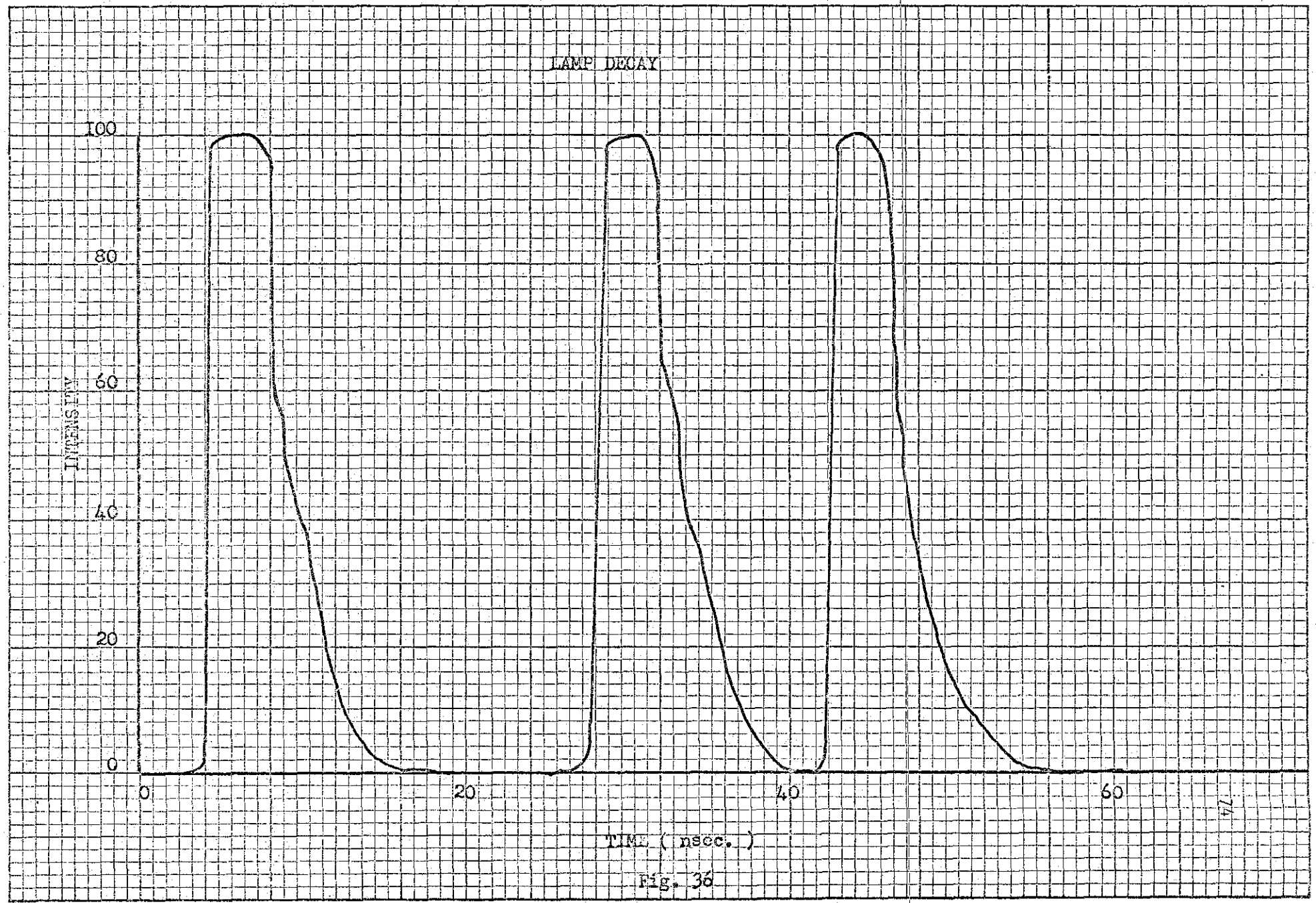

Fig. 36

REFERENCE STANDARD

QUININE BISULFATE

1×10^{-6} M

Solution: 1 N H_2SO_4 (H_2O)

Filters: Lamp, Wratten #18A

Sample, Wratten #2E

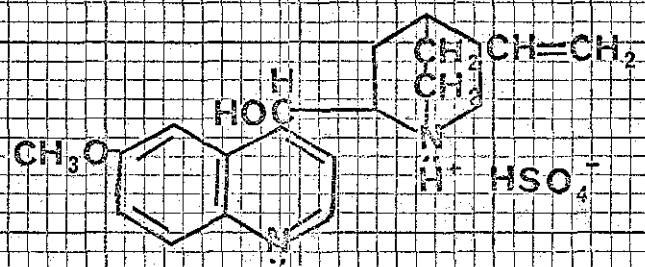

Fig. 37

REFERENCE STANDARDS

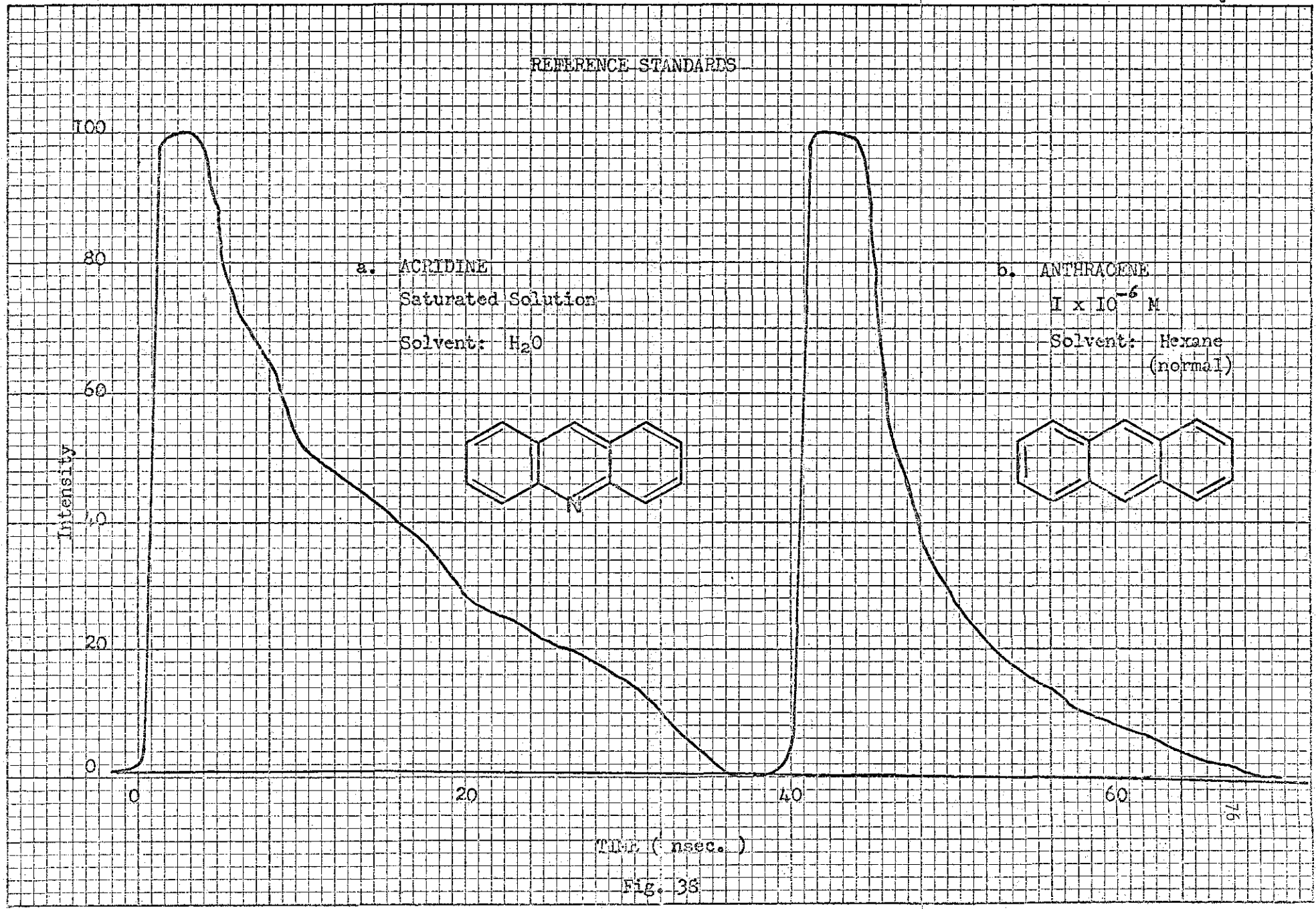

Fig. 38

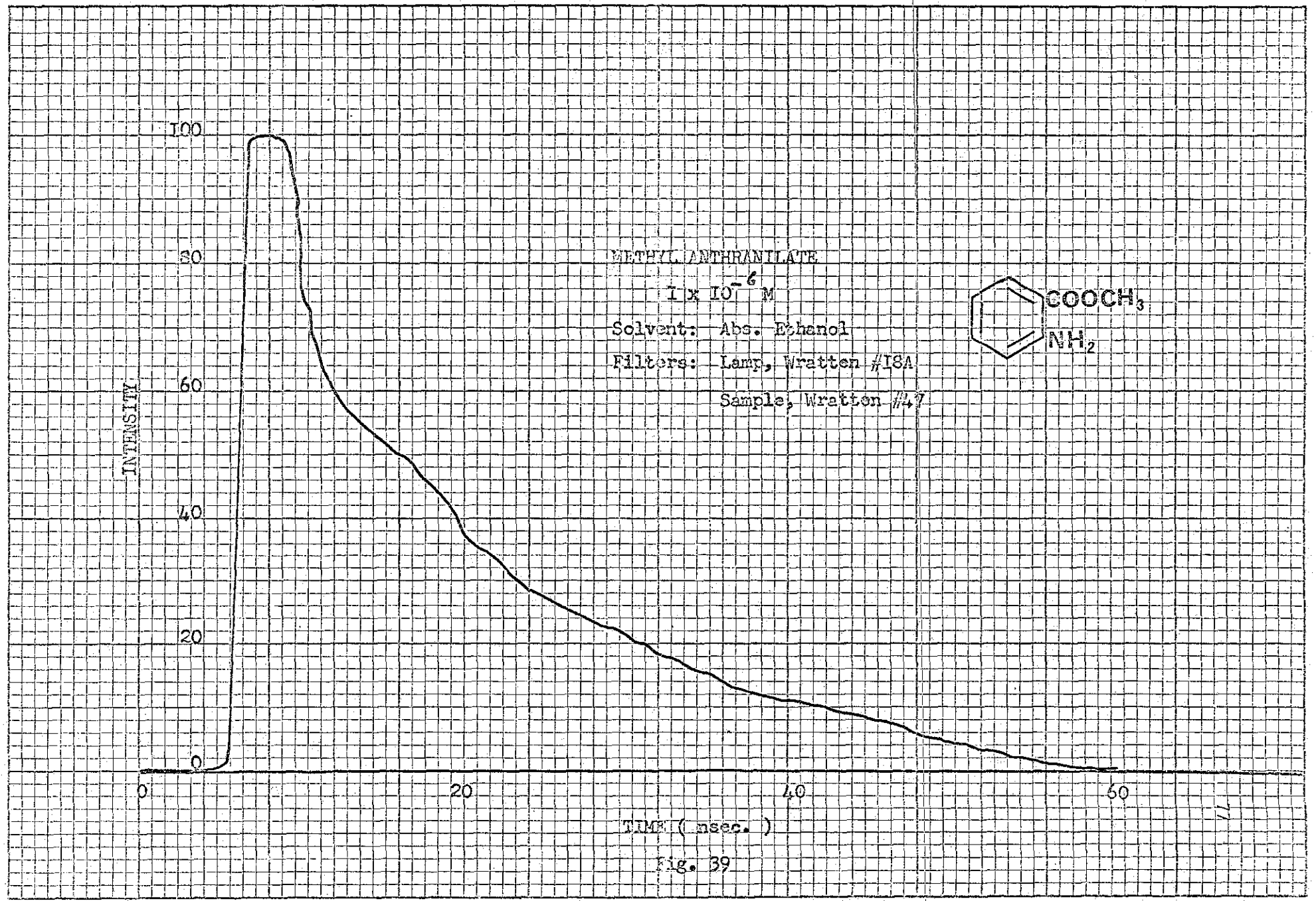
100
80
60
40
20
0
INTENSITY
0
20
40
60
TIME (msec.)
METHYL ANTHRANILATE
1 x 10⁻⁶ M
Solvent: Abs. Ethanol
Filters: Lamp, Wratten #18A
Sample, Wratten #47
COOCH3
NH2

Fig. 39

9, 10-DIPHENYLANTHRACENE

1×10^{-6} M

Solvent: Abs. Ethanol

Filters: Lamp, Wratten #18A

Sample, Wratten #2E

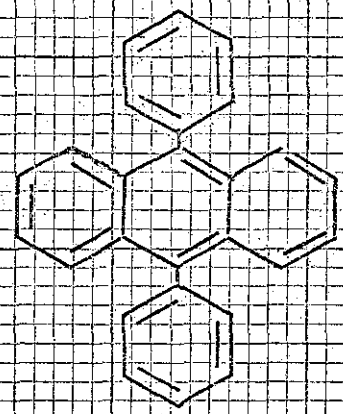

Fig. 40

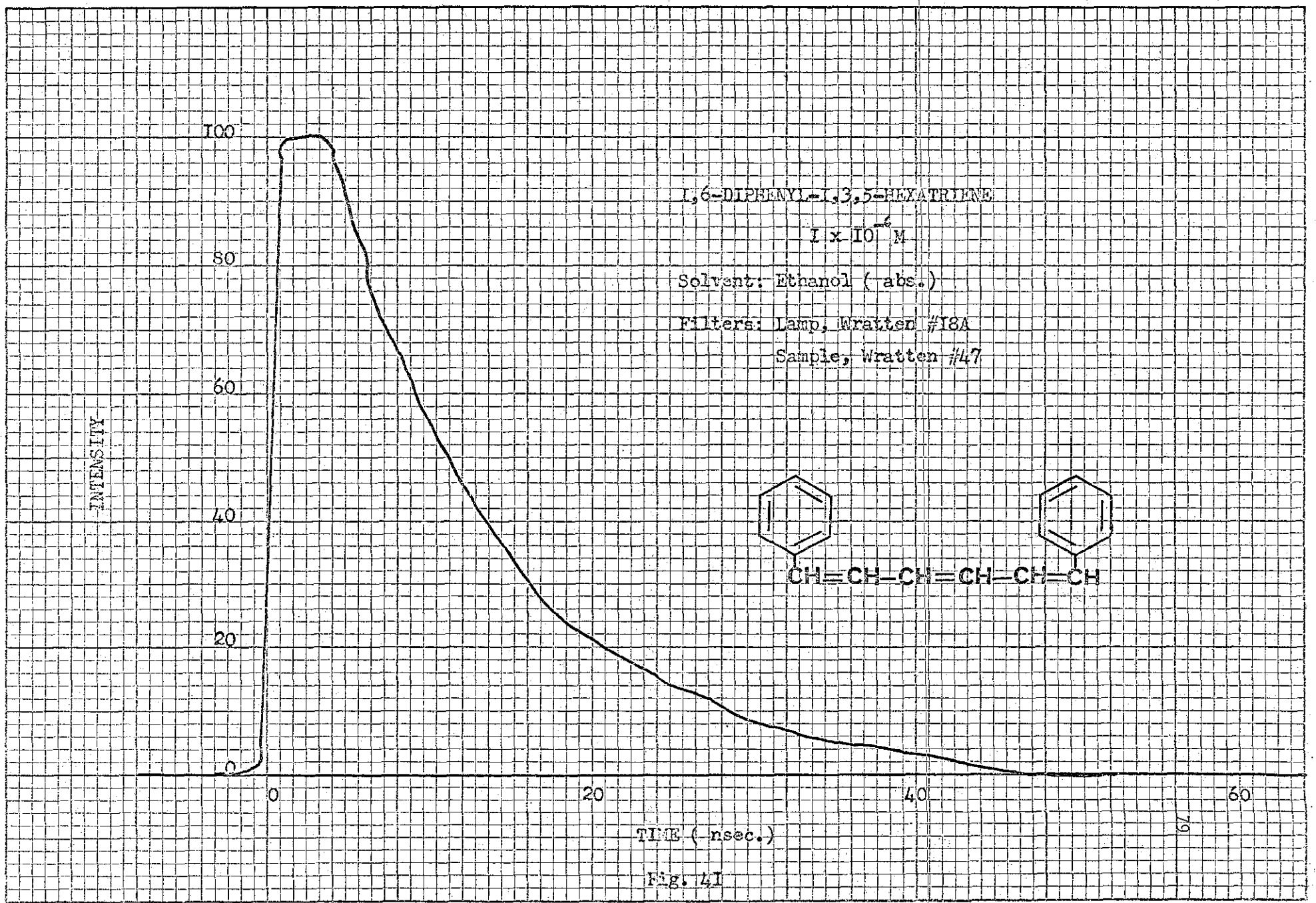
100
80
60
40
20
0
INTENSITY
0
20
40
60
TIME (nsec.)
1,6-DIPHENYL-1,3,5-HEXATRIENE
1 x 10⁻⁶ M
Solvent: Ethanol (abs.)
Filters: Lamp, Wratten #18A
Sample, Wratten #47
CH=CH-CH=CH-CH=CH

Fig. 41

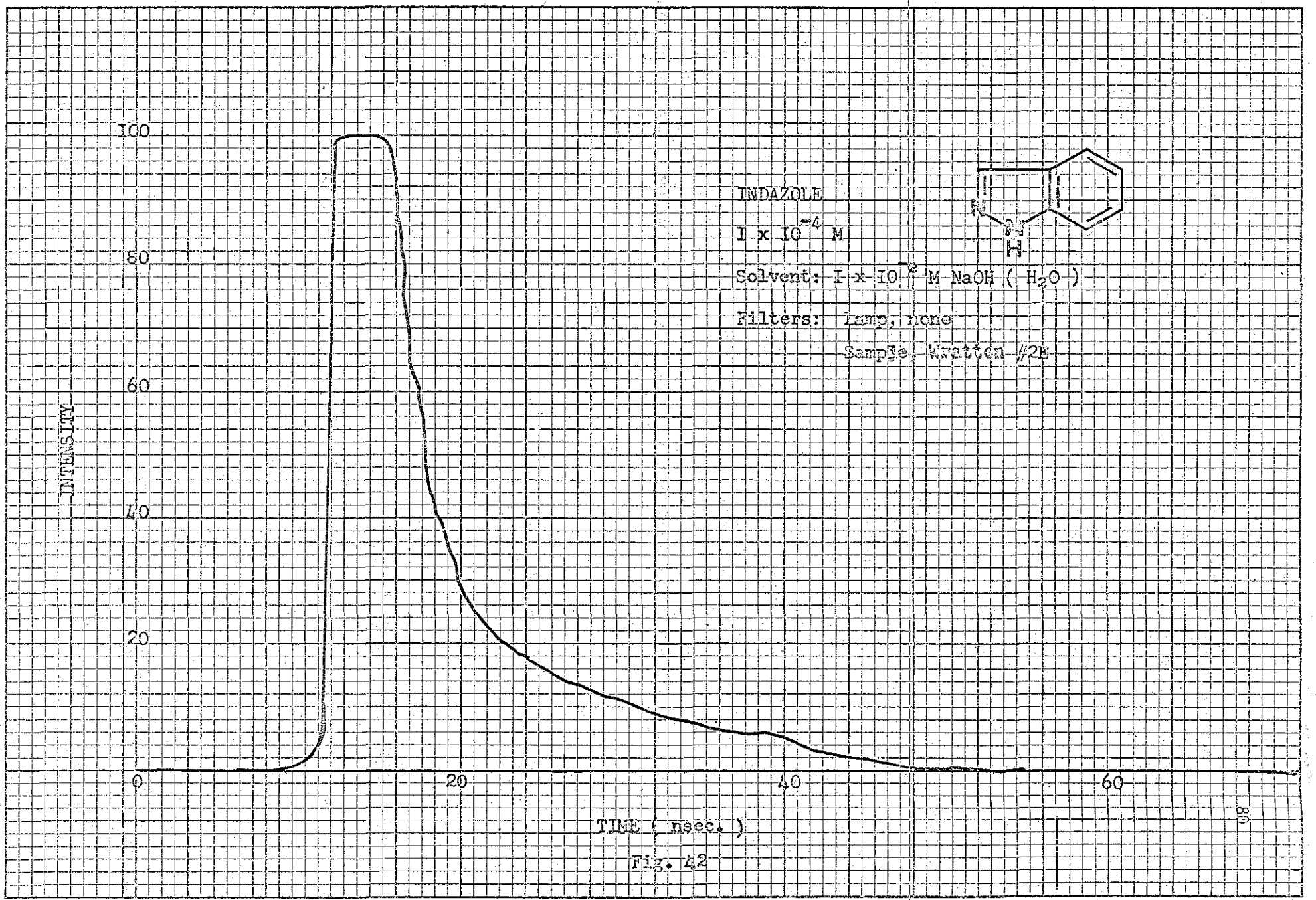
INDAZOLE
1×10^{-4} M
Solvent: 1×10^{-2} M NaOH (H_2O)
Filters: Lamp, none
Sample, Wratten #2b
INTENSITY
100
80
60
40
20
0
20
40
60
80
TIME (nsec.)

Fig. 42

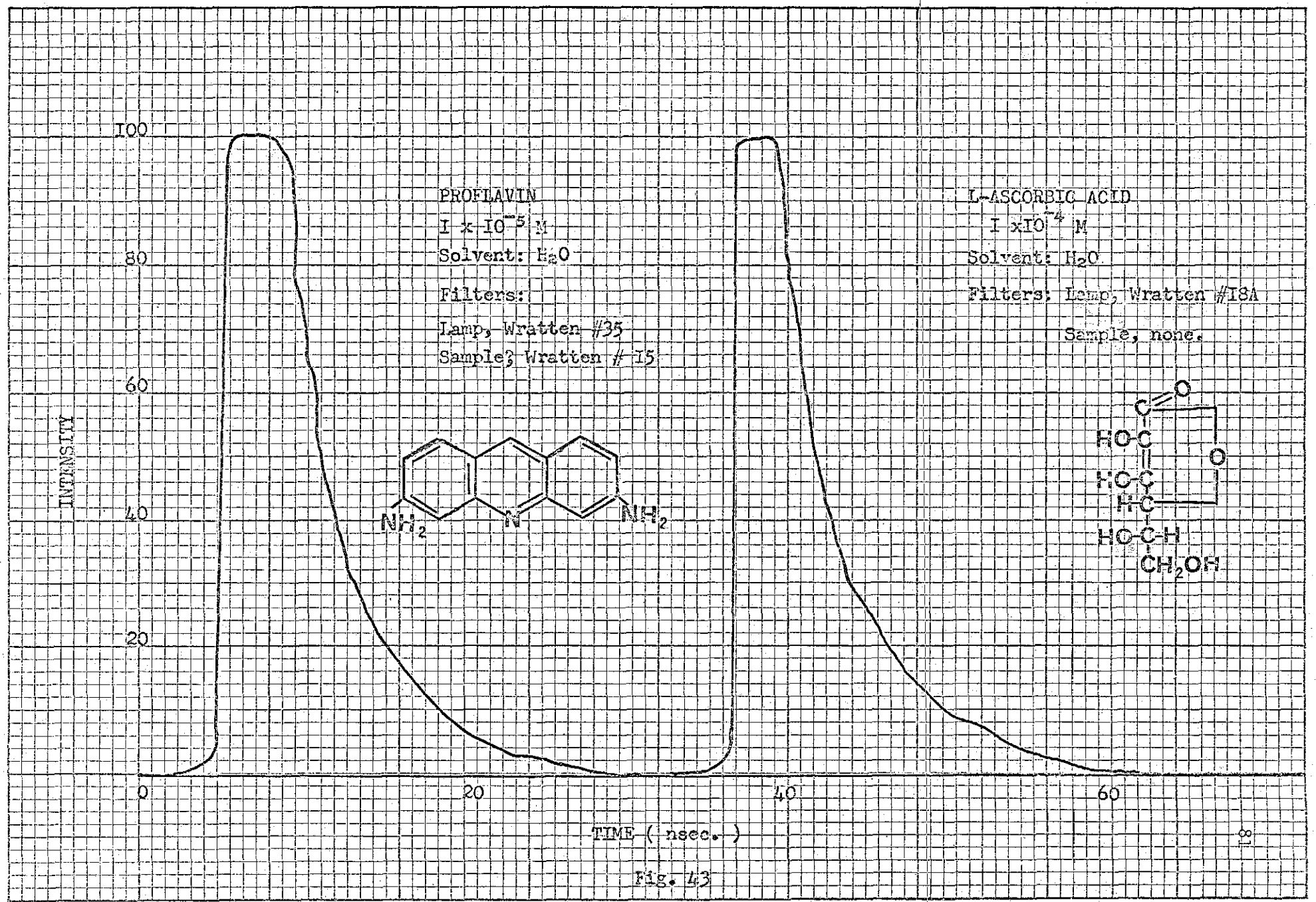
100
80
60
40
20
0
INTENSITY
PROFLAVIN
I x 10^{-5} M
Solvent: H_2O
Filters:
Lamp, Wratten #35
Sample; Wratten # 15
NH_2
N
NH_2
L-ASCORBIC ACID
I x10^{-4} M
Solvent: H_2O
Filters: Lamp, Wratten #18A
Sample, none.
O
C
HO-C
O
HC-C
HC-C
HO-C-H
CH_2OH
0
20
40
60
TIME (nsec.)

Fig. 43

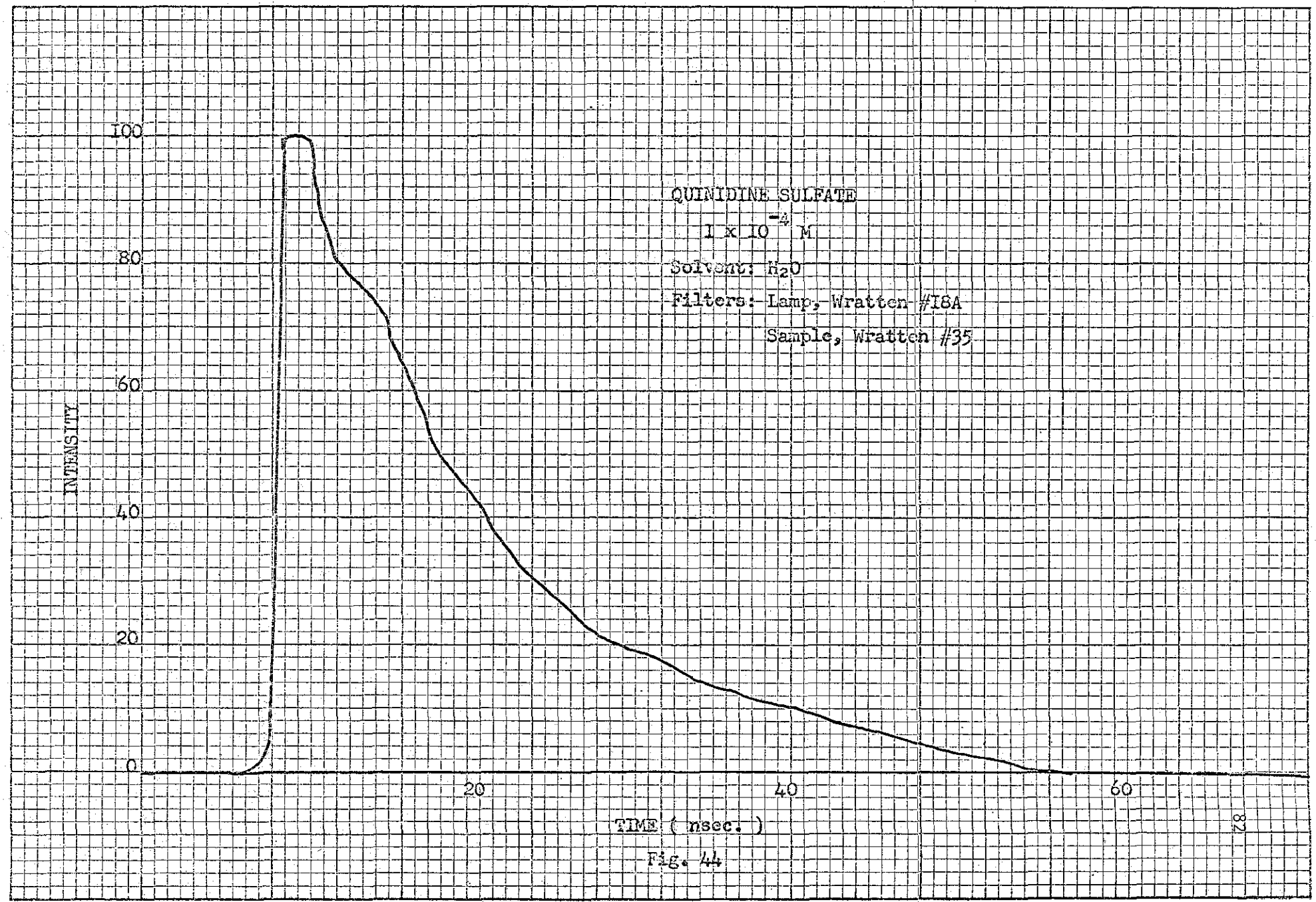
QUINIDINE SULFATE
1 x 10⁻⁴ M
Solvent: H₂O
Filters:- Lamp, Wratten #18A
Sample, Wratten #35
INTENSITY
100
80
60
40
20
0
20
40
60
TIME (nsec.)

Fig. 44

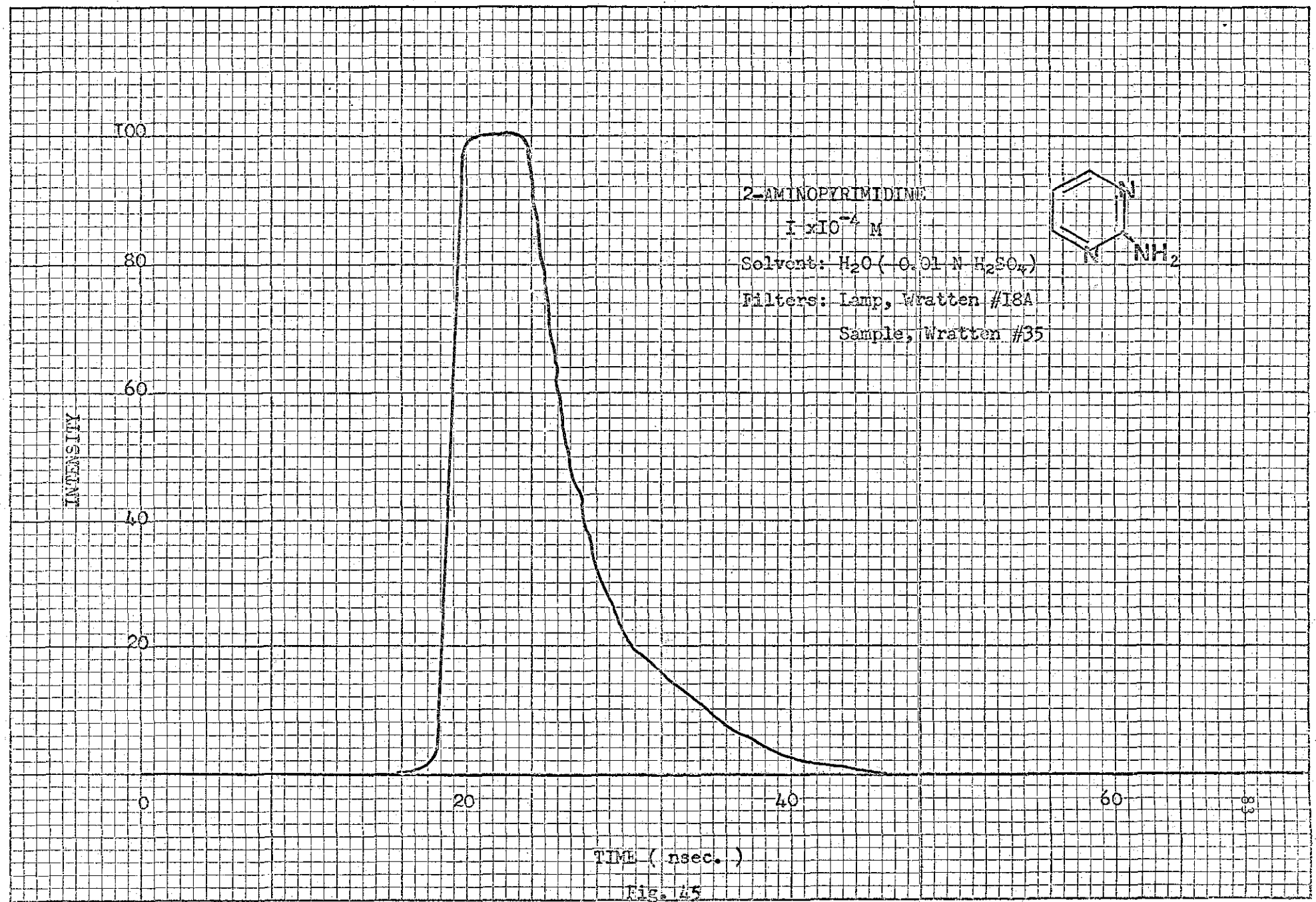
100
80
60
40
20
0
INTENSITY
20
40
60
TIME (nsec.)
2-AMINOPYRIMIDINE
1×10^{-4} M
Solvent: H_2O (0.01 N H_2SO_4)
Filters: Lamp, Wratten #18A
Sample, Wratten #35
N
N
NH_2

Fig. 45

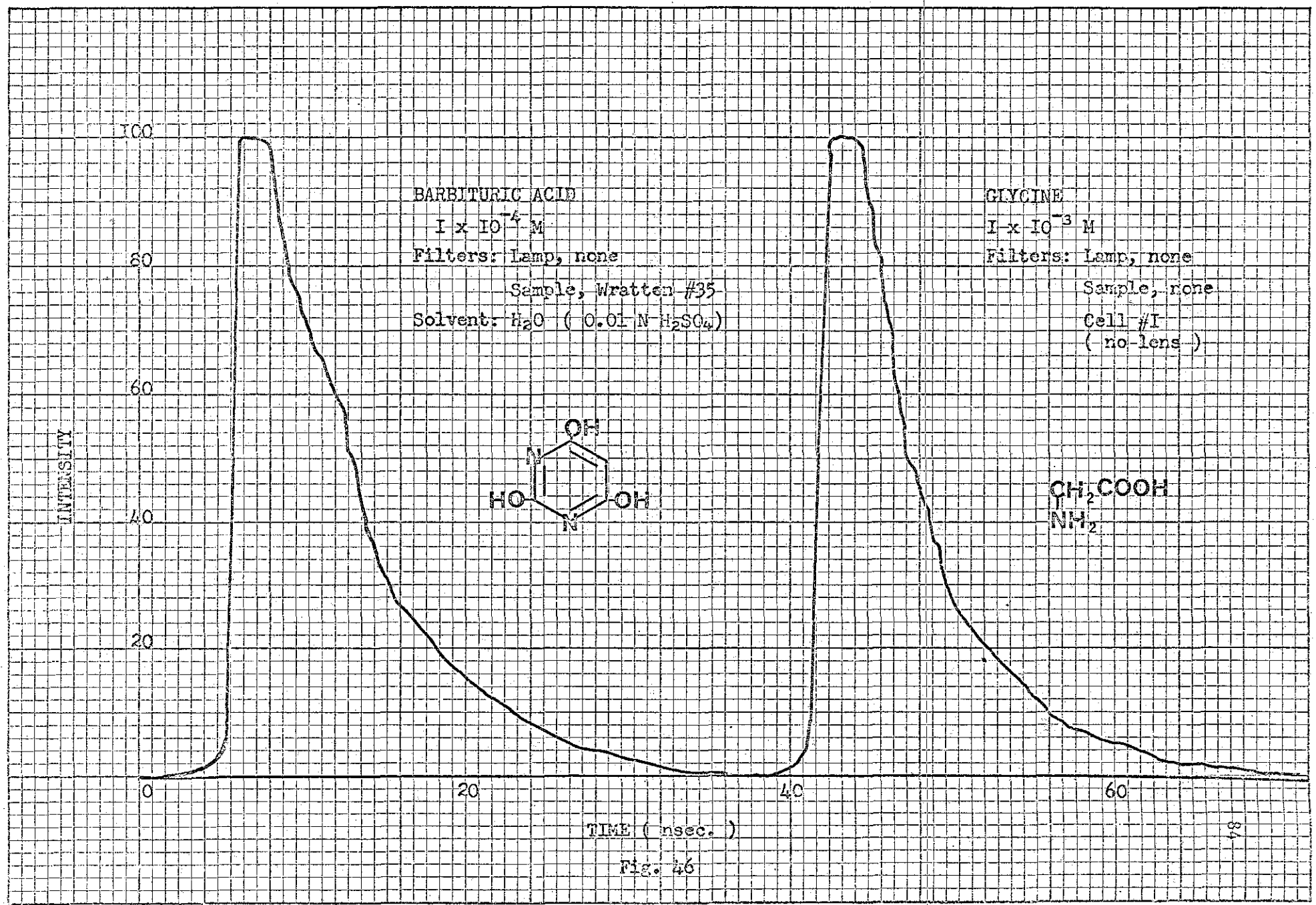
BARBITURIC ACID
I x 10^{-4} M
Filters: Lamp, none
Sample, Wratten #35
Solvent: H_2O (0.01 N H_2SO_4)
GLYCINE
I x 10^{-3} M
Filters: Lamp, none
Sample, none
Cell #1
(no-lens)
OH
N
HO
OH
N
CH_2COOH
NH_2
INTENSITY
100
80
60
40
20
0
20
40
60
TIME (msec.)

Fig. 46

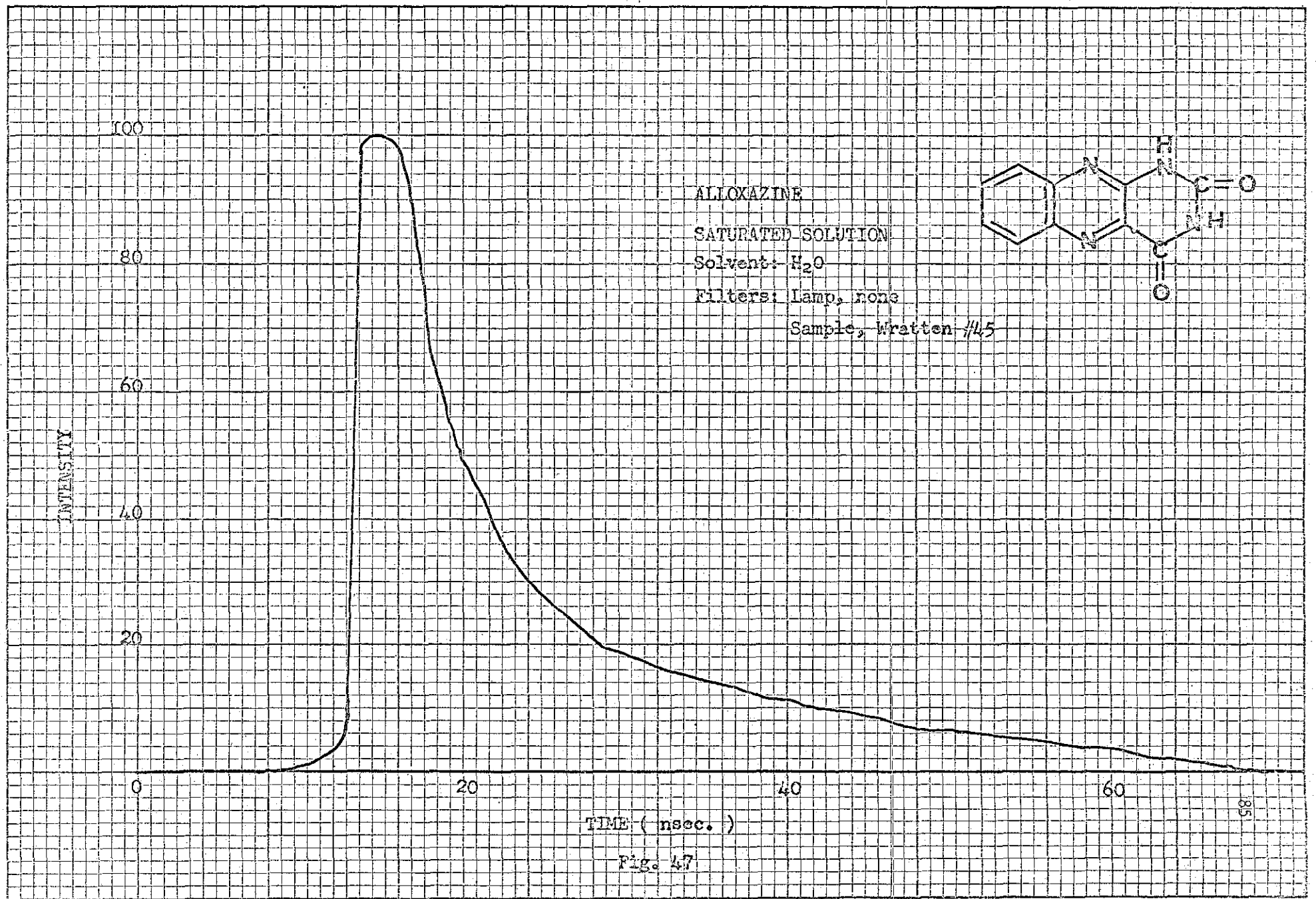
100
80
60
40
20
0
20
40
60
INTENSITY
TIME (nsec.)
ALLOXAZINE
SATURATED SOLUTION
Solvent: H_2O
Filters: Lamp, none
Sample, Wratten #45
H
N
C=O
C
H
N
C
O
85

Fig. 47

ALLOXAZINE

1×10^{-5} M

Solvent: 9M H_2SO_4 (H_2O l)

Filters: Lamp, none

Sample, Wratten #49

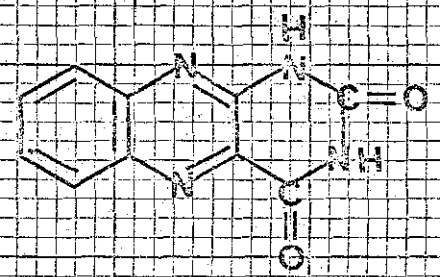

100

80

60

40

20

0

20

40

60

INTENSITY

TIME (nsec.)

Fig. 48

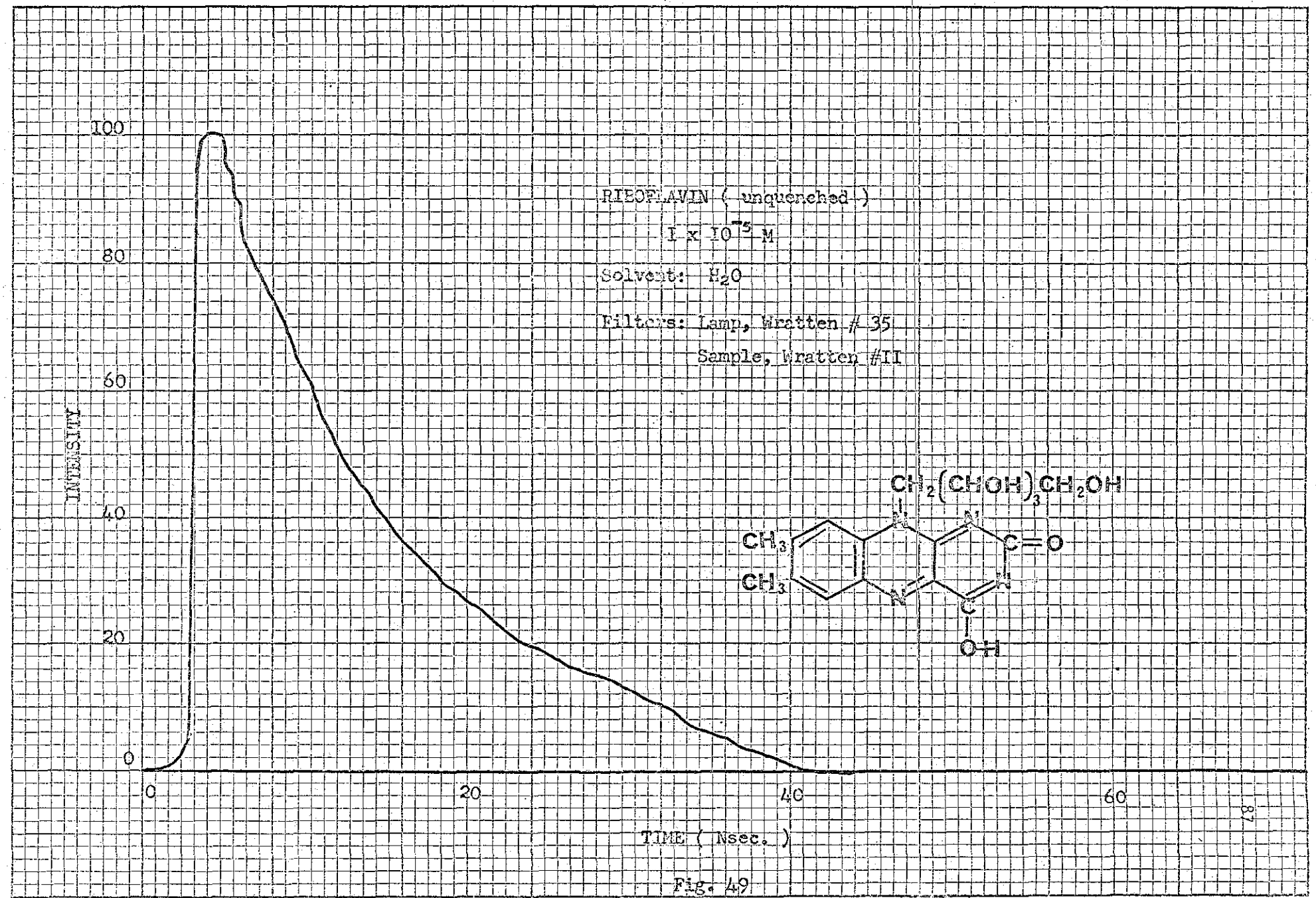
RIBOFLAVIN (unquenched)
1 x 10⁻⁵ M
Solvent: H2O
Filters: Lamp, Wratten # 35
Sample, Wratten #II
INTENSITY
100
80
60
40
20
0
0
20
40
60
TIME (Nsec.)
CH2(CHOH)3CH2OH
CH3
CH3
C=O
O-H

Fig. 49

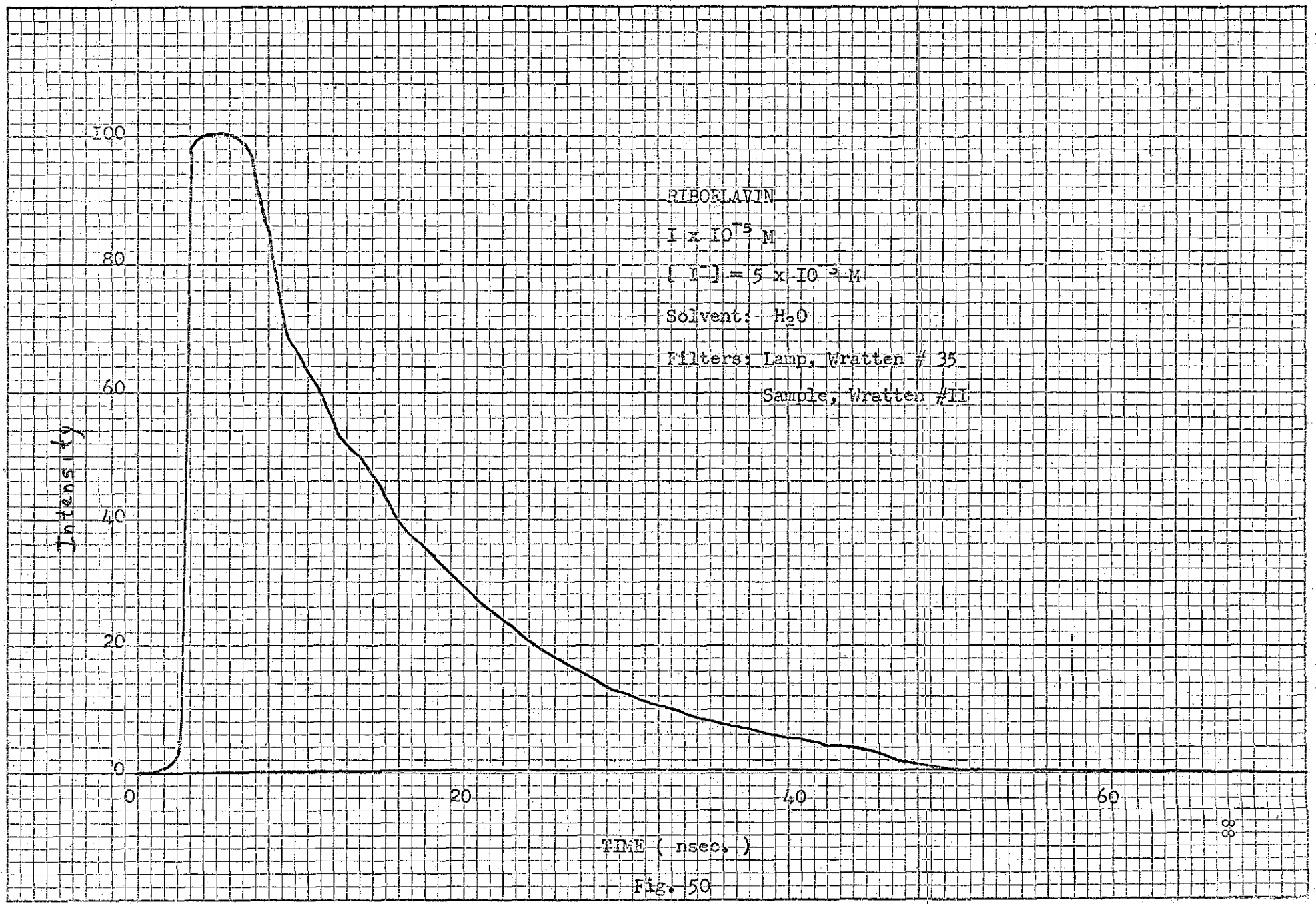
RIBOFLAVIN
1×10^{-5} M
$[I^-] = 5 \times 10^{-3}$ M
Solvent: H_2O
Filters: Lamp, Wratten # 35
Sample, Wratten #II
Intensity
100
80
60
40
20
0
0
20
40
60
TIME (nsec.)

Fig. 50

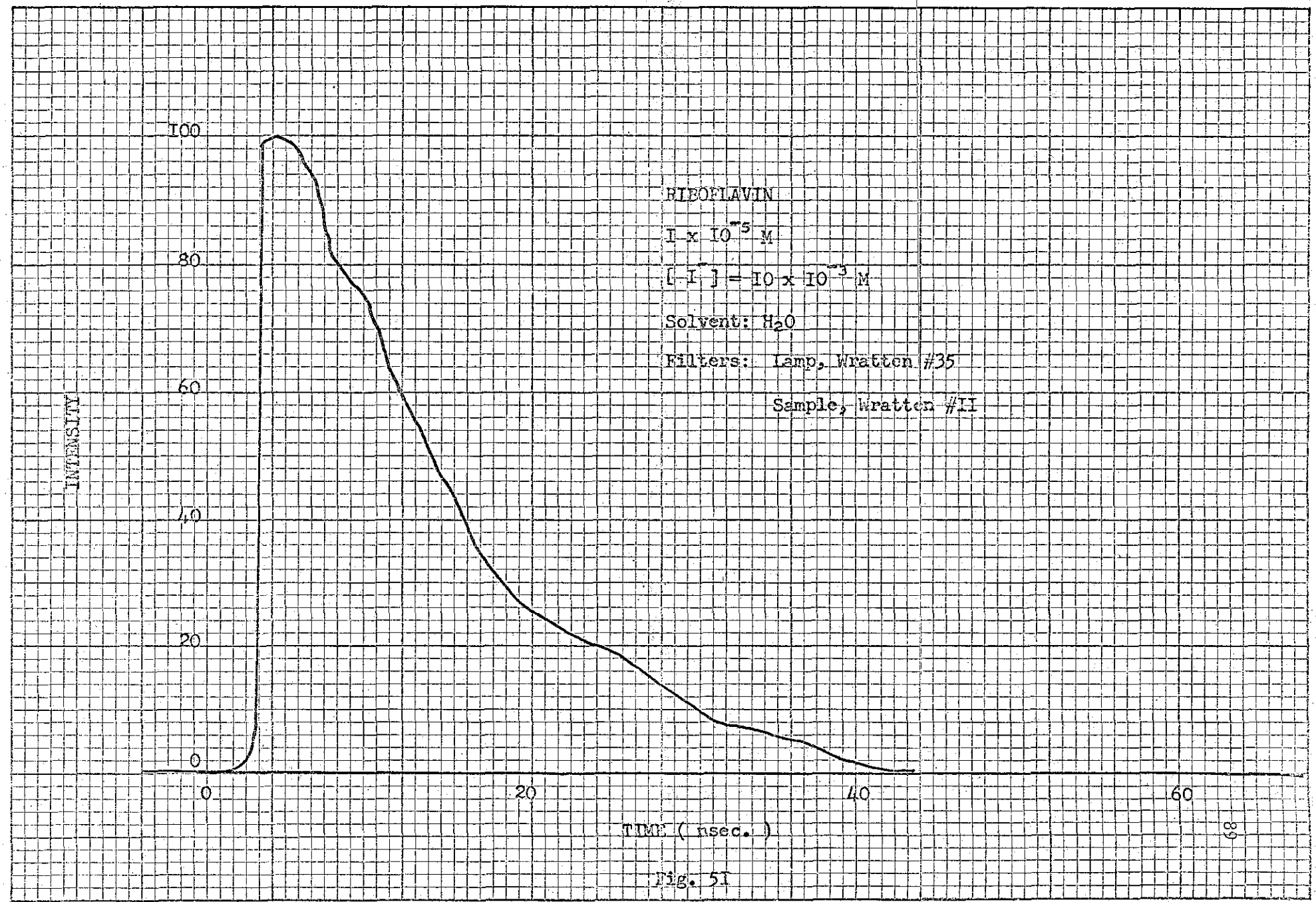
100
80
60
40
20
0
INTENSITY
0
20
40
60
TIME (nsec.)
RIBOFLAVIN
1×10^{-5} M
$[I^-] = 10 \times 10^{-3}$ M
Solvent: H_2O
Filters: Lamp, Wratten #35
Sample, Wratten #11

Fig. 51

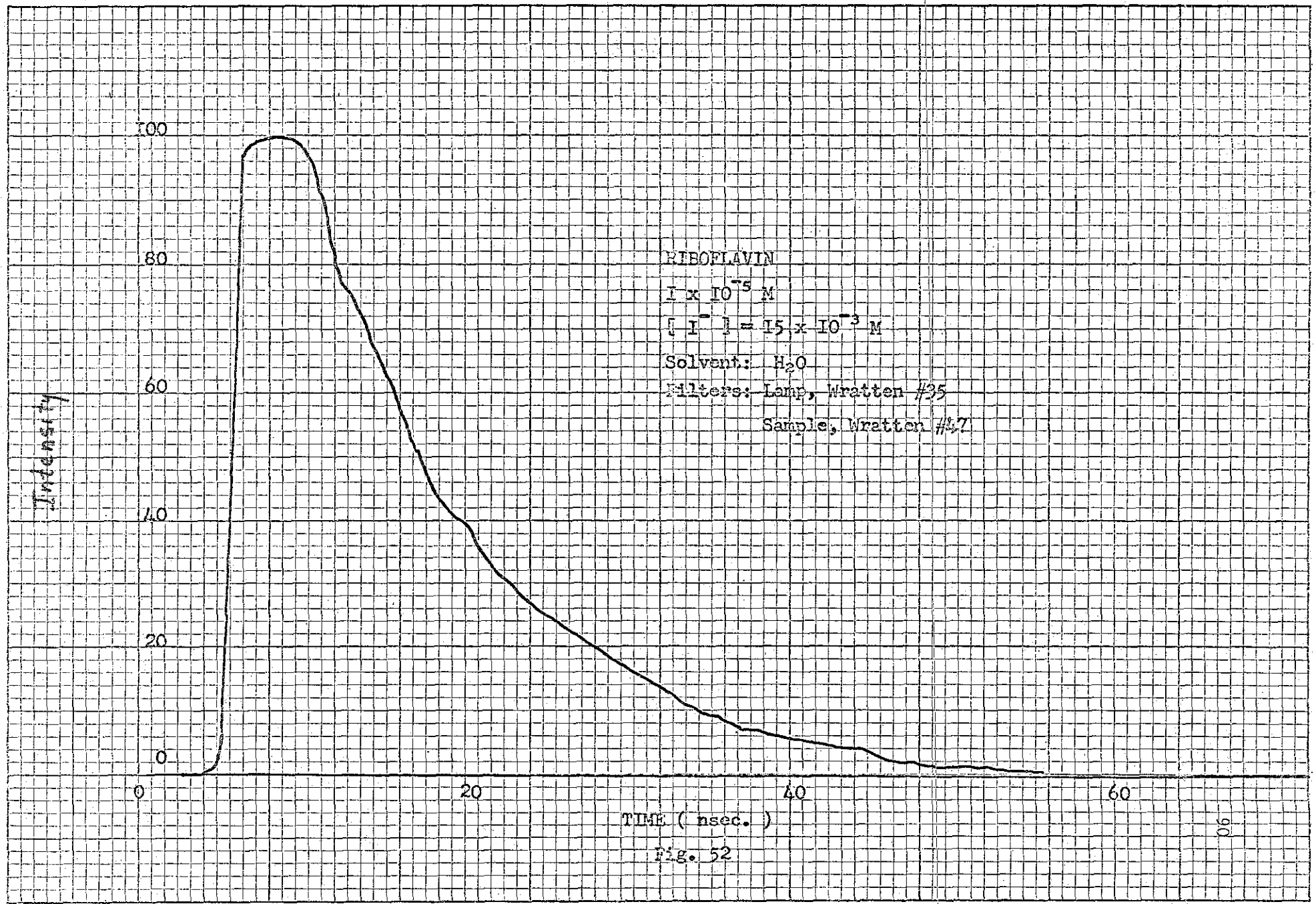
100
80
60
40
20
0
Intensity
0
20
40
60
TIME (nsec.)
RIBOFLAVIN
I x IO⁻⁵ M
[I⁻] = I5 x IO⁻³ M
Solvent: H₂O
Filters: Lamp, Wratten #35
Sample, Wratten #47

Fig. 52

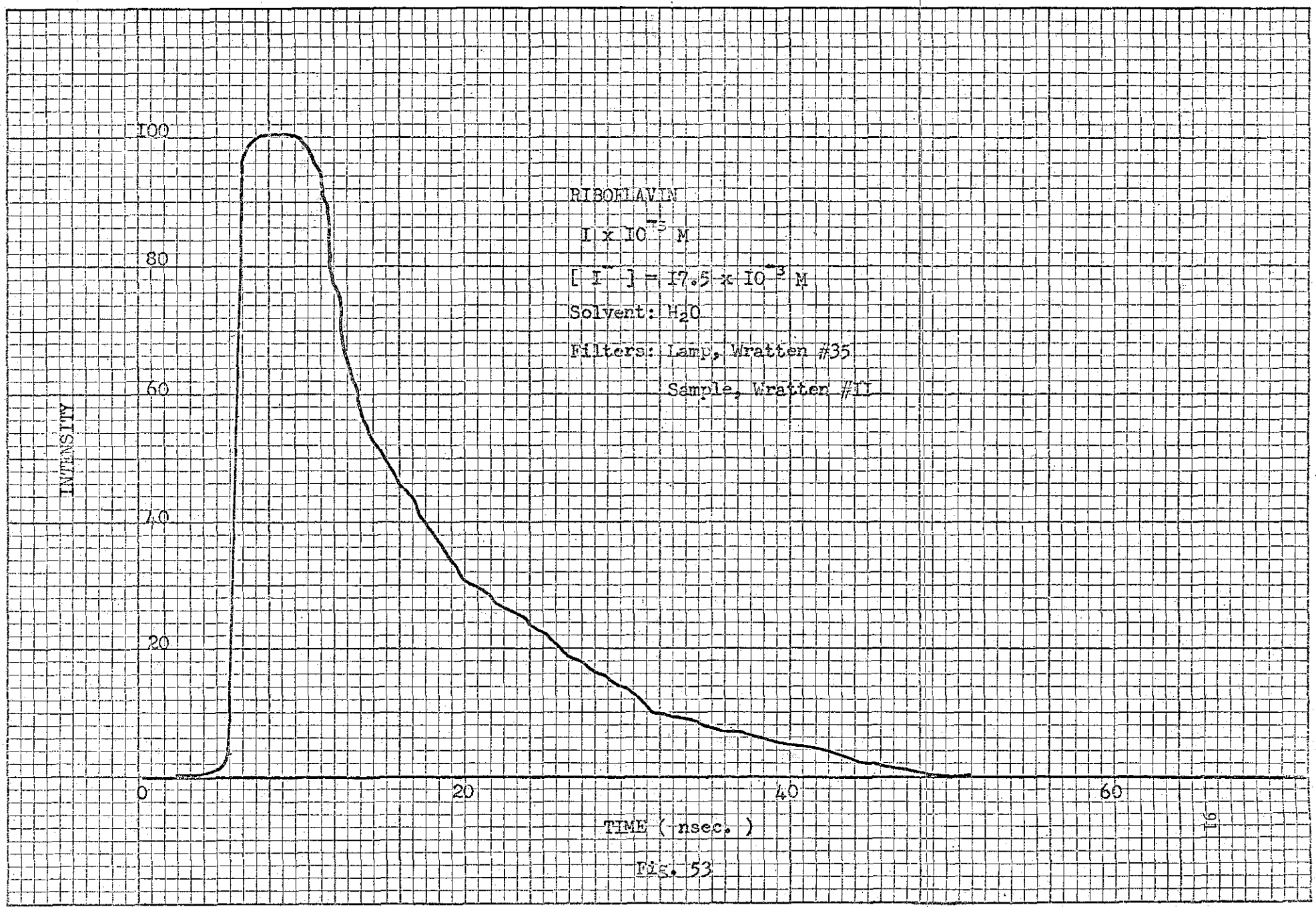
RIBOFLAVIN
1 x 10⁻⁵ M
[I⁻] = 17.5 x 10⁻³ M
Solvent: H2O
Filters: Lamp, Wratten #35
Sample, Wratten #47
INTENSITY
100
80
60
40
20
0
20
40
60
TIME (nsec.)

Fig. 53

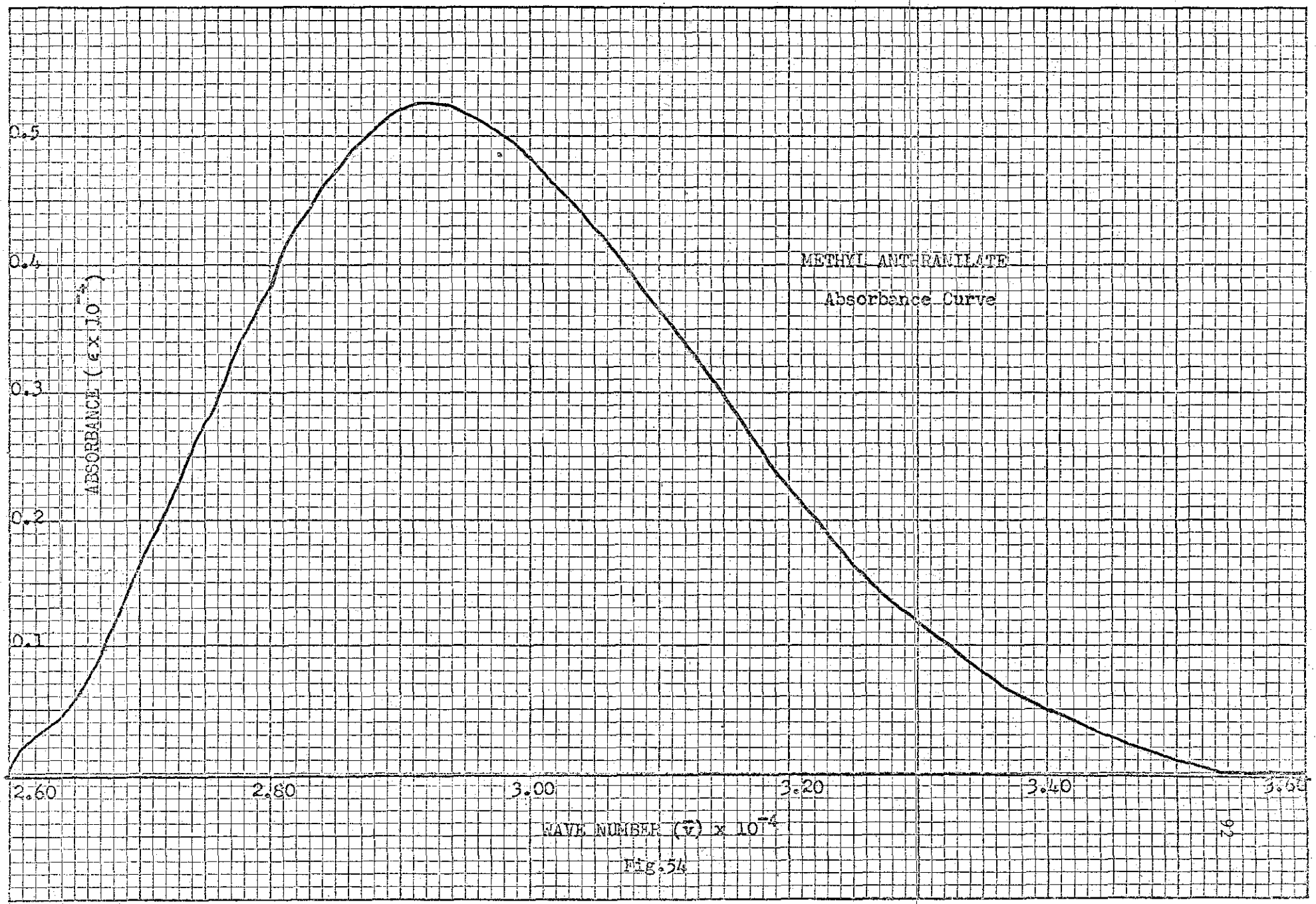
METHYL ANTHRANILATE
Absorbance Curve
ABSORBANCE ($\epsilon \times 10^{-4}$)
0.5
0.4
0.3
0.2
0.1
2.60
2.80
3.00
3.20
3.40
WAVE NUMBER ($\bar{\nu}$) x 10^{-4}

Fig.54

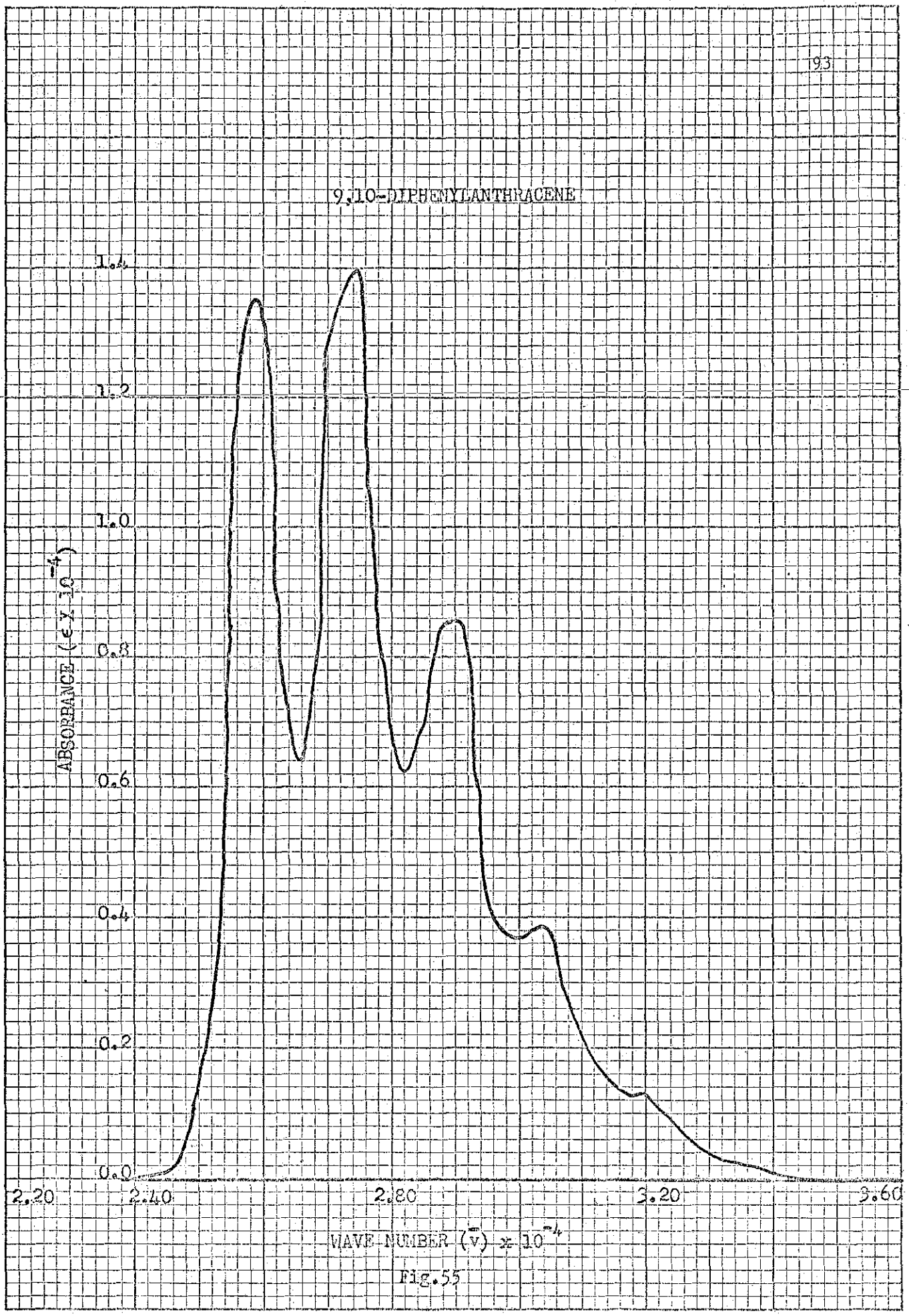
9,10-DIPHENYLANTHRACENE
1.4
1.2
1.0
0.8
0.6
0.4
0.2
0.0
ABSORBANCE (ε x 10⁻⁴)
2.20
2.40
2.80
3.20
3.60
WAVE NUMBER (ν̄) x 10⁻⁴

Fig.55

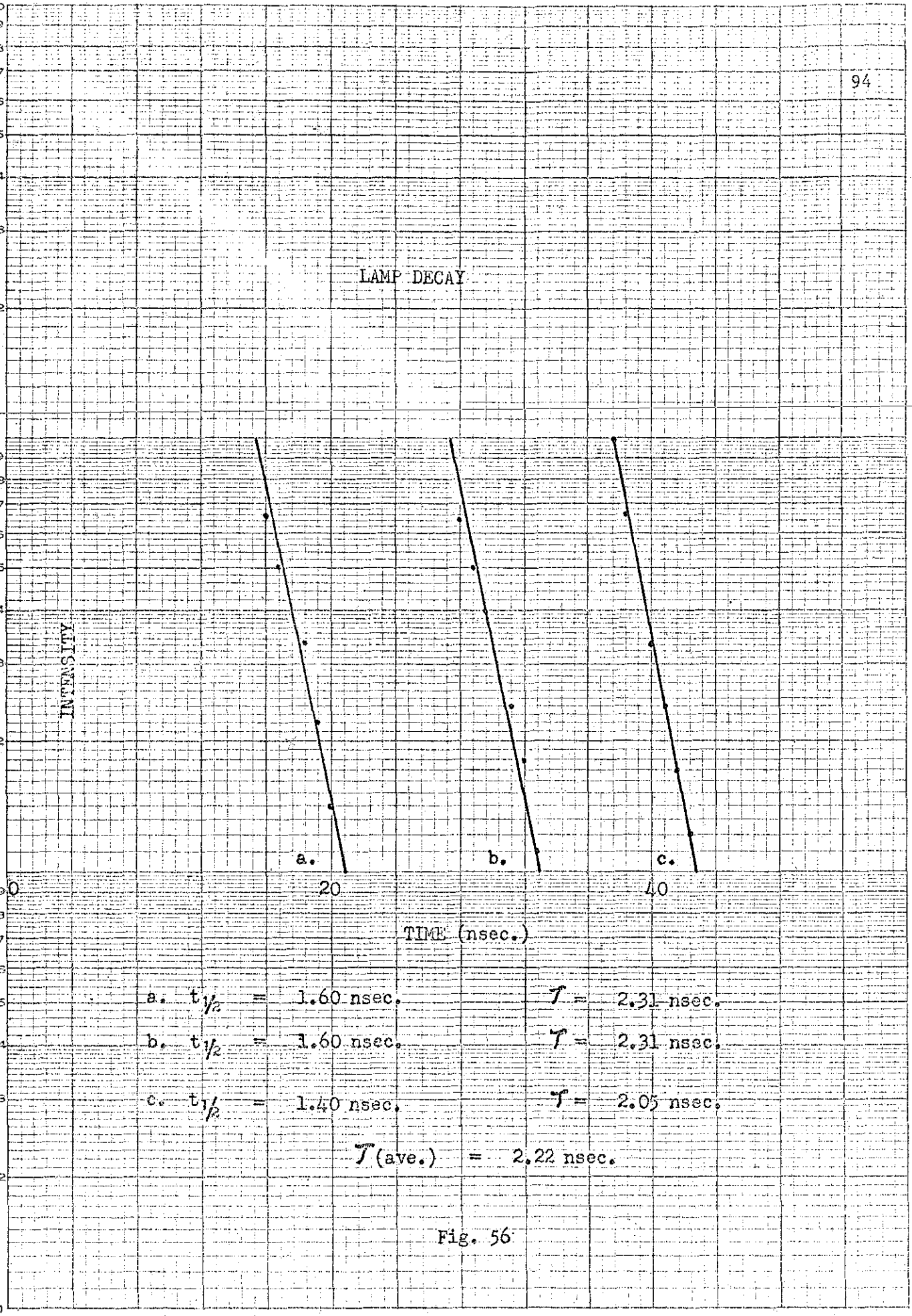

a. $t_{1/2}$ = 1.60 nsec. τ = 2.31 nsec.

b. $t_{1/2}$ = 1.60 nsec. τ = 2.31 nsec.

c. $t_{1/2}$ = 1.40 nsec. τ = 2.05 nsec.

τ (ave.) = 2.22 nsec.

Fig. 56

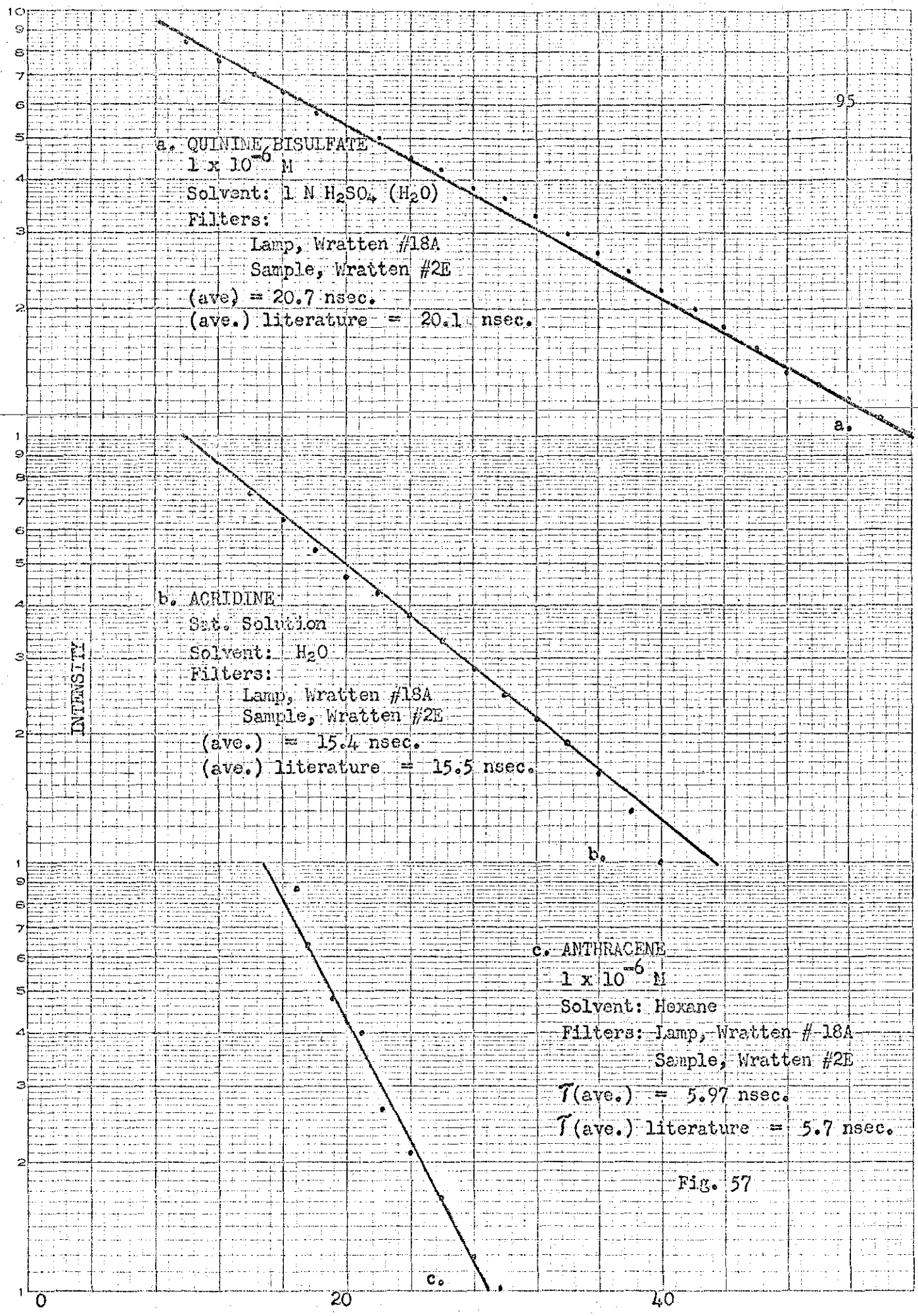
a. QUININE BISULFATE
1 x 10⁻⁶ M
Solvent: 1 N H₂SO₄ (H₂O)
Filters:
Lamp, Wratten #18A
Sample, Wratten #2E
(ave) = 20.7 nsec.
(ave.) literature = 20.1 nsec.
a.
b. ACRIDINE
Sat. Solution
Solvent: H₂O
Filters:
Lamp, Wratten #18A
Sample, Wratten #2E
(ave.) = 15.4 nsec.
(ave.) literature = 15.5 nsec.
b.
c. ANTHRACENE
1 x 10⁻⁶ M
Solvent: Hexane
Filters: Lamp, Wratten #-18A
Sample, Wratten #2E
τ(ave.) = 5.97 nsec.
τ(ave.) literature = 5.7 nsec.
c.
INTENSITY
TIME (nsec.)
0
20
40

Fig. 57

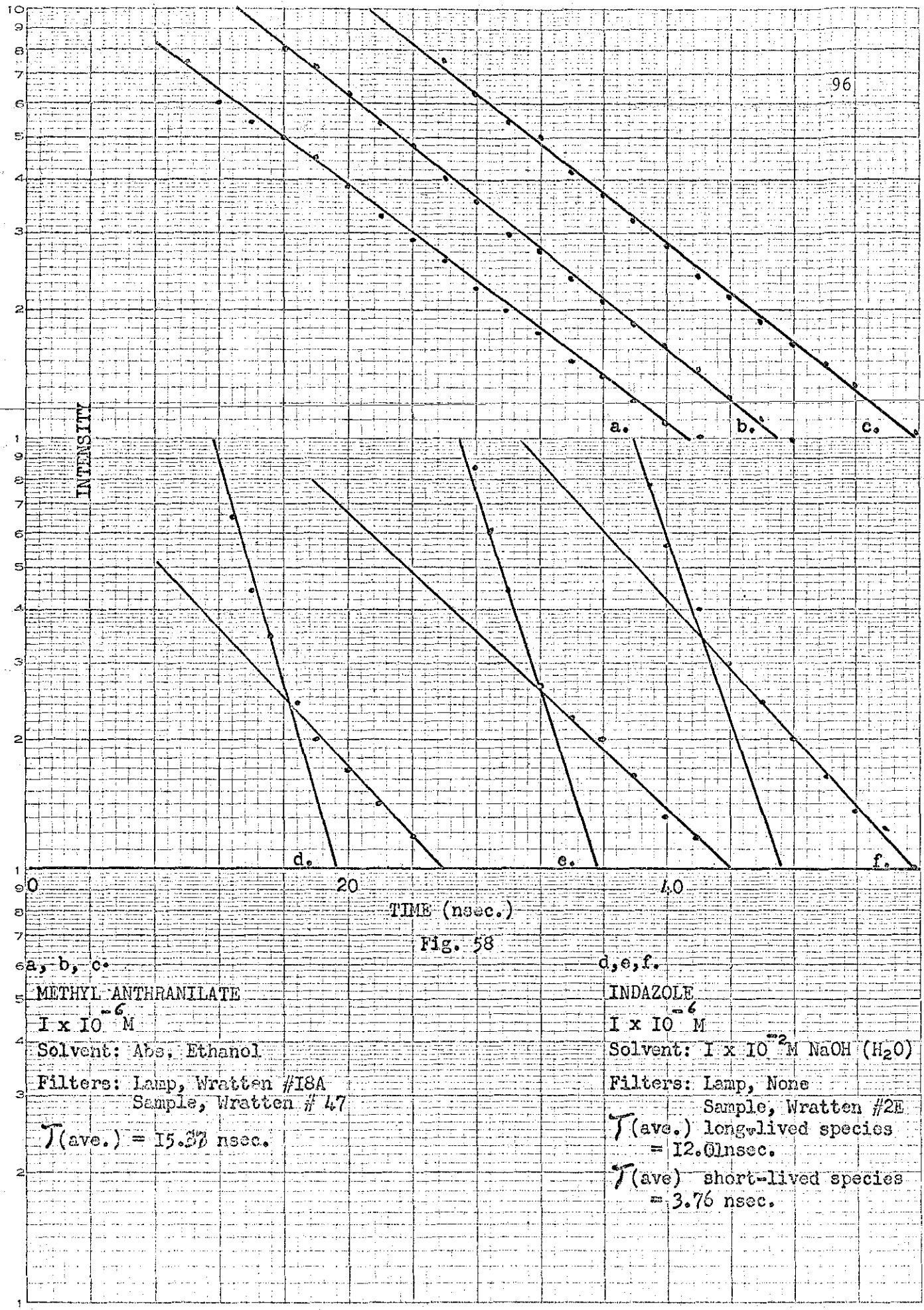

Fig. 58

a, b, c.

METHYL ANTHRANILATE

$I \times 10^{-6}$ M

Solvent: Abs. Ethanol

Filters: Lamp, Wratten #18A
Sample, Wratten # 47

τ (ave.) = 15.37 nsec.

d, e, f.

INDAZOLE

$I \times 10^{-6}$ M

Solvent: $I \times 10^{-2}$ M NaOH (H_2O)

Filters: Lamp, None
Sample, Wratten #2E

τ (ave.) long-lived species
= 12.01nsec.

τ (ave) short-lived species
= 3.76 nsec.

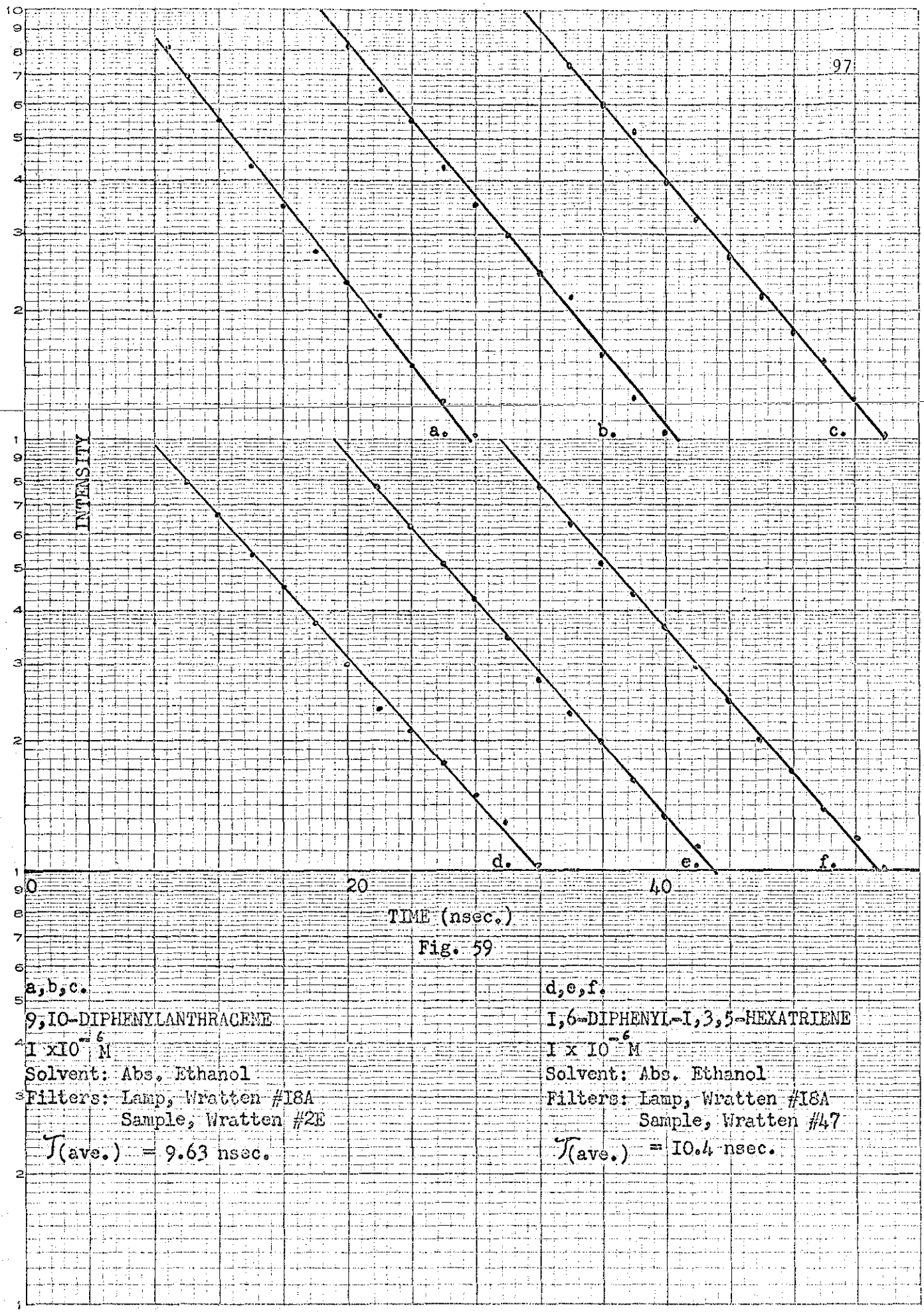

Fig. 59

a,b,c.
9,10-DIPHENYLANTHRACENE
1×10^{-6} M
Solvent: Abs. Ethanol
Filters: Lamp, Wratten #18A
Sample, Wratten #2E
τ(ave.) = 9.63 nsec.

d,e,f.
1,6-DIPHENYL-1,3,5-HEXATRIENE
1×10^{-6} M
Solvent: Abs. Ethanol
Filters: Lamp, Wratten #18A
Sample, Wratten #47
τ(ave.) = 10.4 nsec.

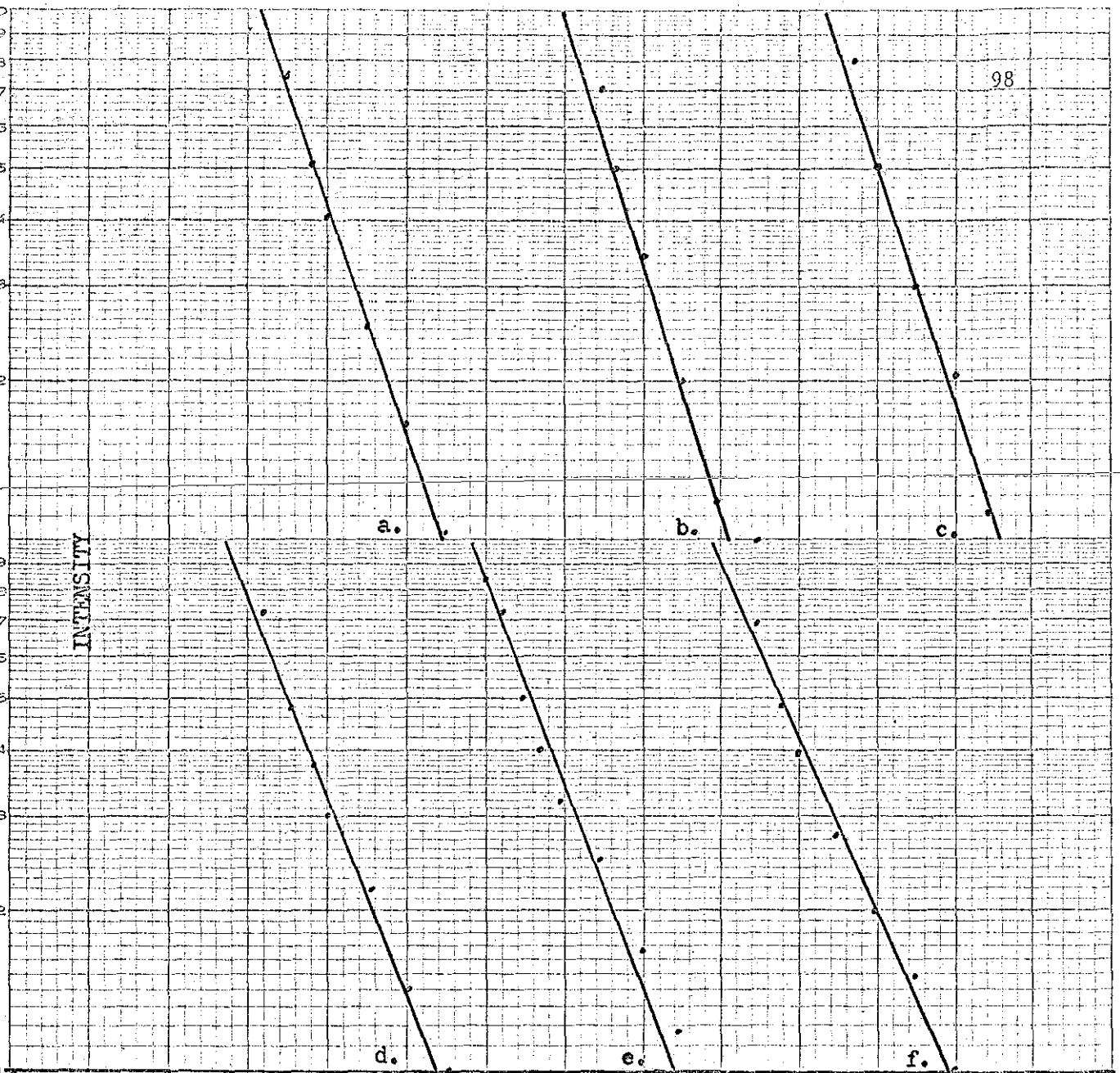

Fig. 60

a,b,c.
PROFLAVIN
$I \times 10^{-5}$ M
Solvent: H_2O
Filters: Lamp, Wratten #18A
Sample Wratten #35
$\tau_{(ave.)}$ = 4.08 nsec.

d,e,f.
L-ASCORBIC ACID
$I \times 10^{-4}$ M
Solvent: H_2O
Filters: Lamp, Wratten #18
Sample, NONE
$\tau_{(ave.)}$ = 4.61nsec.

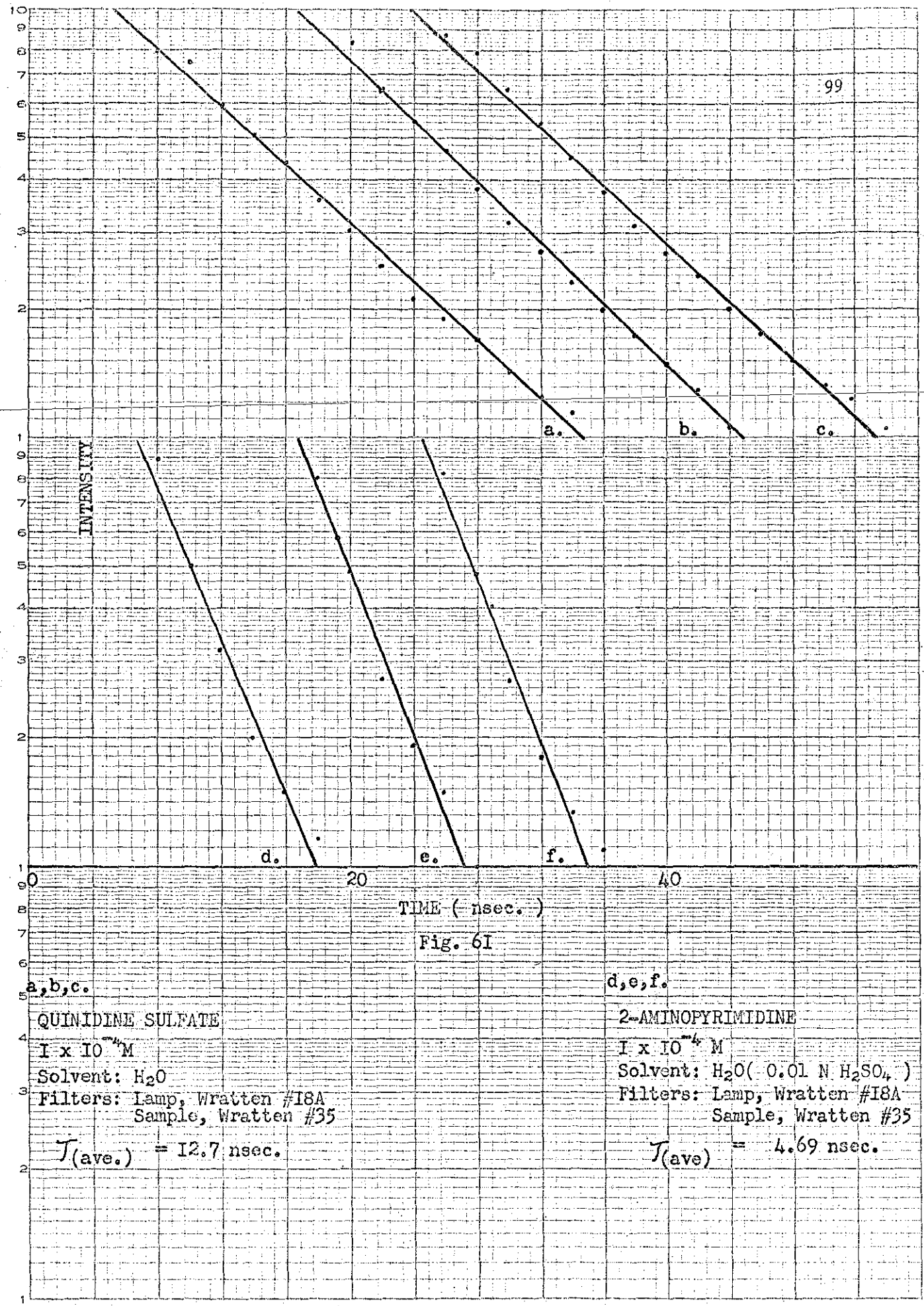

Fig. 6I

a,b,c.

QUINIDINE SULFATE

I x 10^{-4} M

Solvent: H_2O

Filters: Lamp, Wratten #18A
Sample, Wratten #35

$\tau_{(ave.)}$ = 12.7 nsec.

d,e,f.

2-AMINOPYRIMIDINE

I x 10^{-4} M

Solvent: H_2O(0.01 N H_2SO_4)

Filters: Lamp, Wratten #18A
Sample, Wratten #35

$\tau_{(ave)}$ = 4.69 nsec.

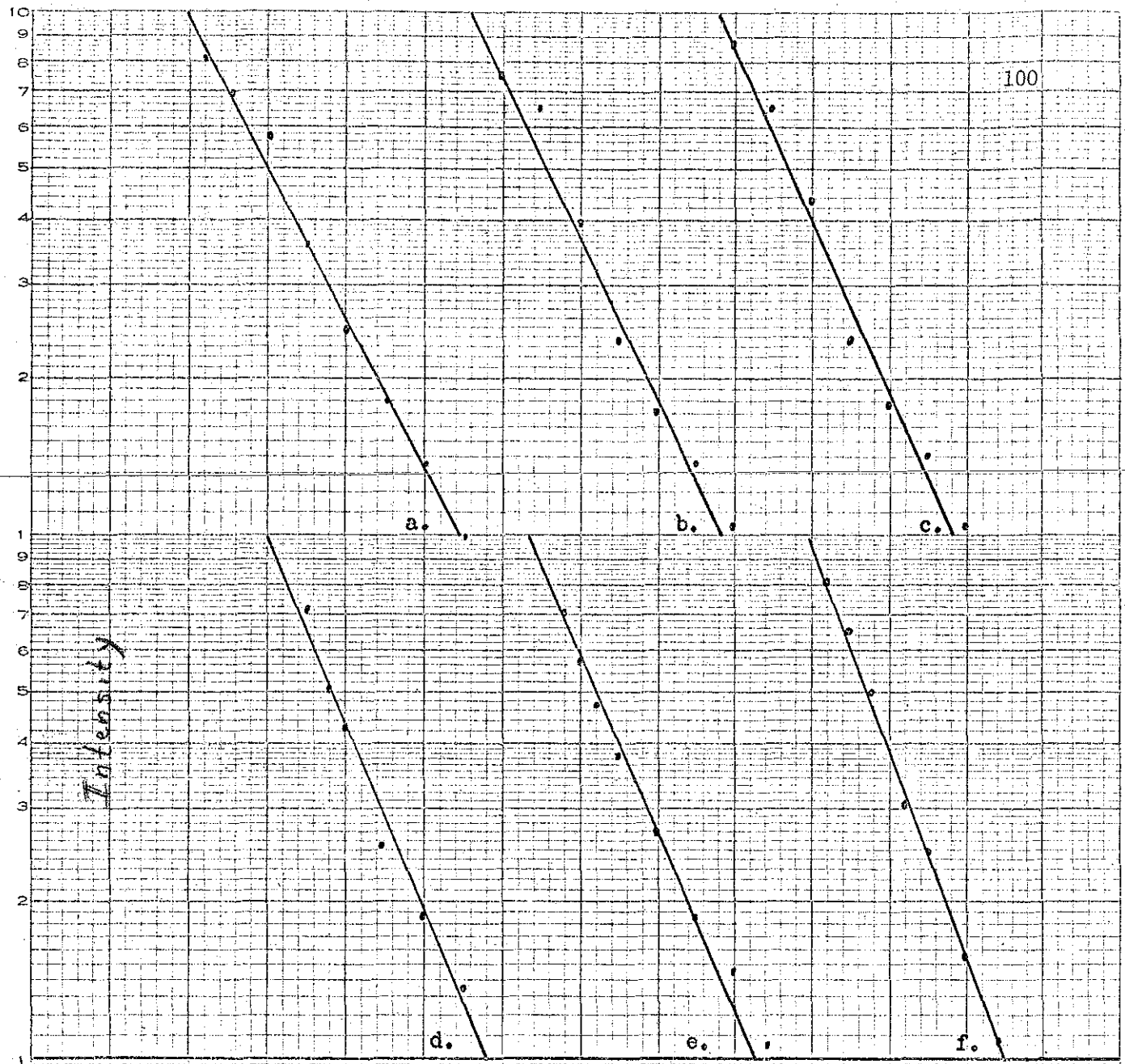

Fig. 62

a,b,c.
BARBITURIC ACID
$I \times IO^{-4}$ M
Solvent: .01 N H_2SO_4 (H_2O)
Filters: Lamp, none
Sample, Wratten #35
τ(ave.) = 5.8 nsec.

d,e,f.
GLYCINE
$I \times IO^{-3}$ M
Solvent: H_2O
Filters: none
(no lens)
τ(ave.) = 4.78nsec.

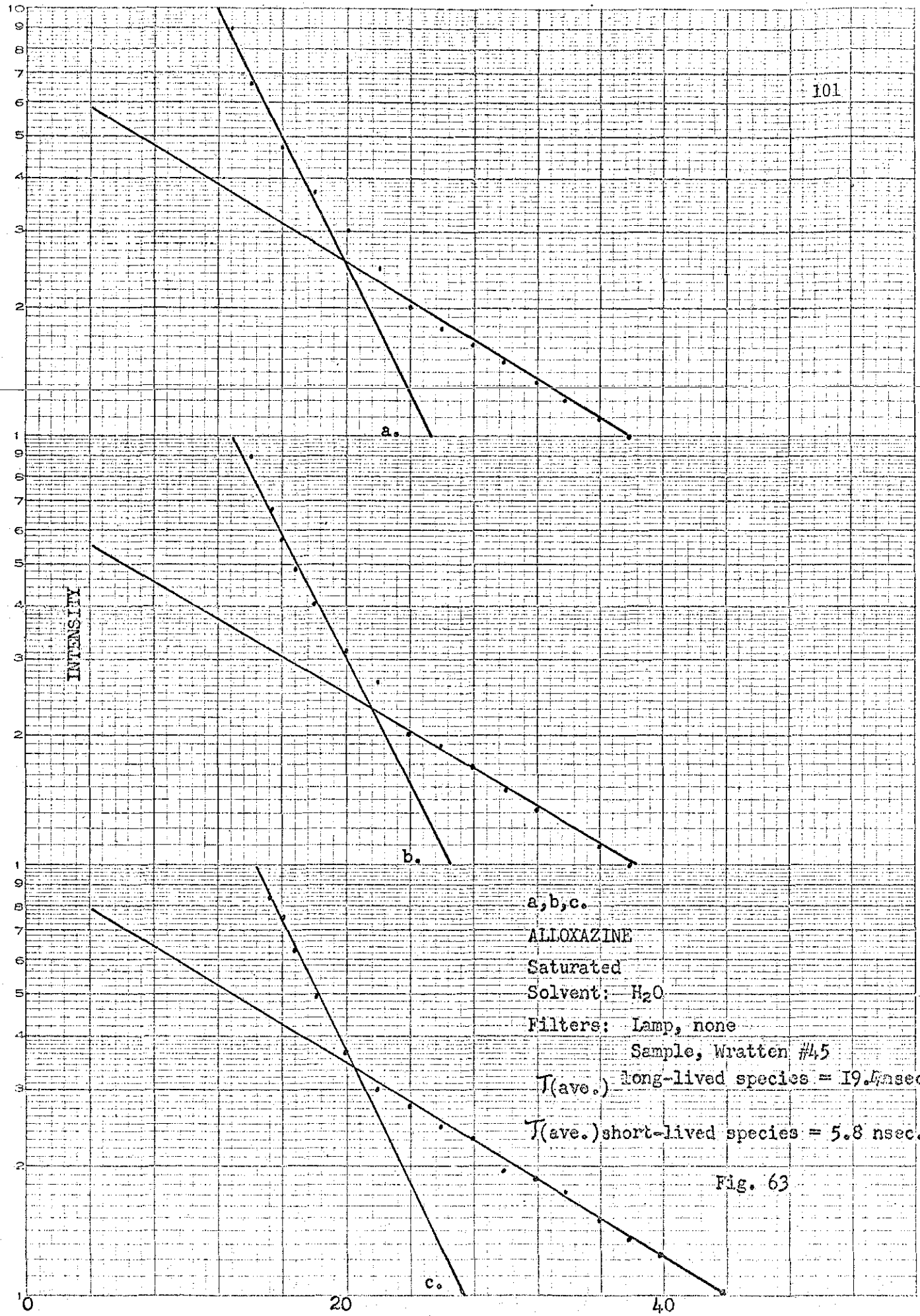

a,b,c.

ALLOXAZINE

Saturated

Solvent: H_2O

Filters: Lamp, none

Sample, Wratten #45

τ(ave.) long-lived species = 19.4 nsec

τ(ave.) short-lived species = 5.8 nsec.

Fig. 63

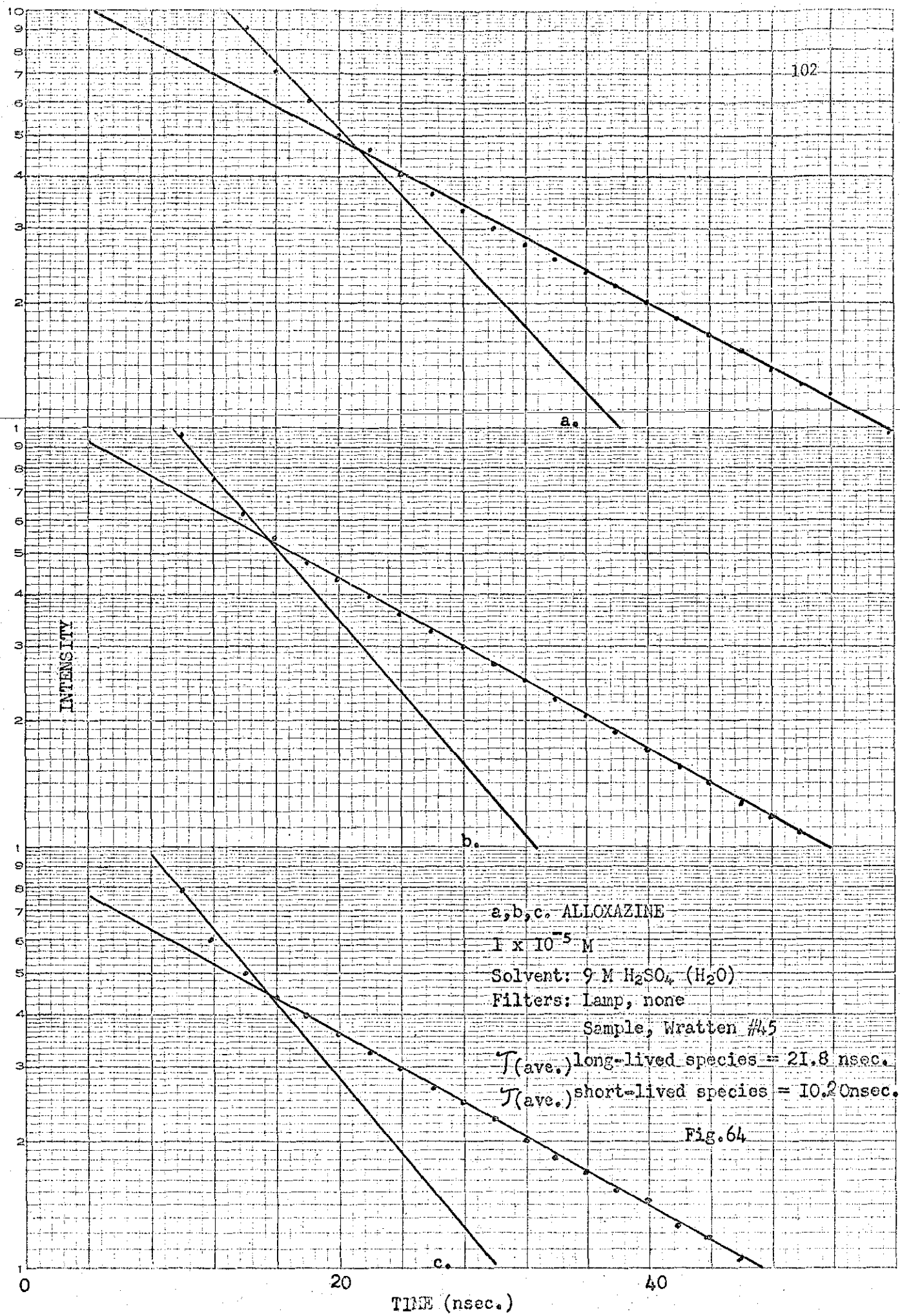

a,b,c. ALLOXAZINE

1×10^{-5} M

Solvent: 9 M H_2SO_4 (H_2O)

Filters: Lamp, none

Sample, Wratten #45

$\tau_{(ave.)}$ long-lived species = 21.8 nsec.

$\tau_{(ave.)}$ short-lived species = 10.2 nsec.

Fig.64

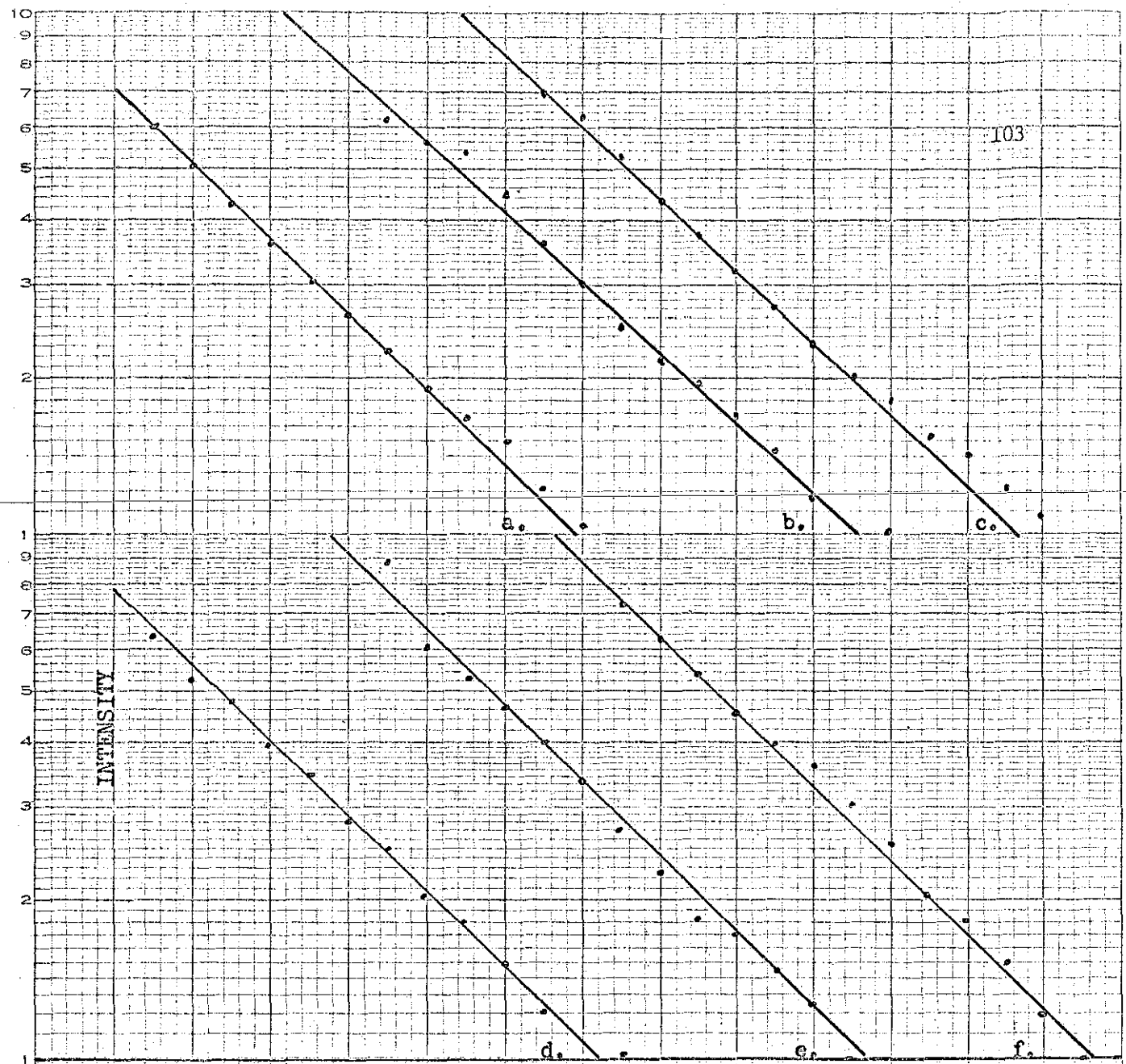

Fig. 65

a,b, c.

RIBOFLAVIN

I x 10^{-5} M

Solvent: H_2O

Filters: Lamp, Wratten #35

Sample, Wratten #II

$\tau_{(ave.)}$ = 12.8 nsec.

k_q = 7.82 x 10^7 sec^{-1}

d,e,f.

RIBOFLAVIN

I x 10^{-5} M

$[I^-]$ = 5 x 10^{-3}

Solvent: H_2O

Filters: Lamp, Wratten #35

Sample, Wratten #II

$\tau_{(ave.)}$ = 12.1 nsec.

k_q = 8.25 x 10^7 sec^{-1}

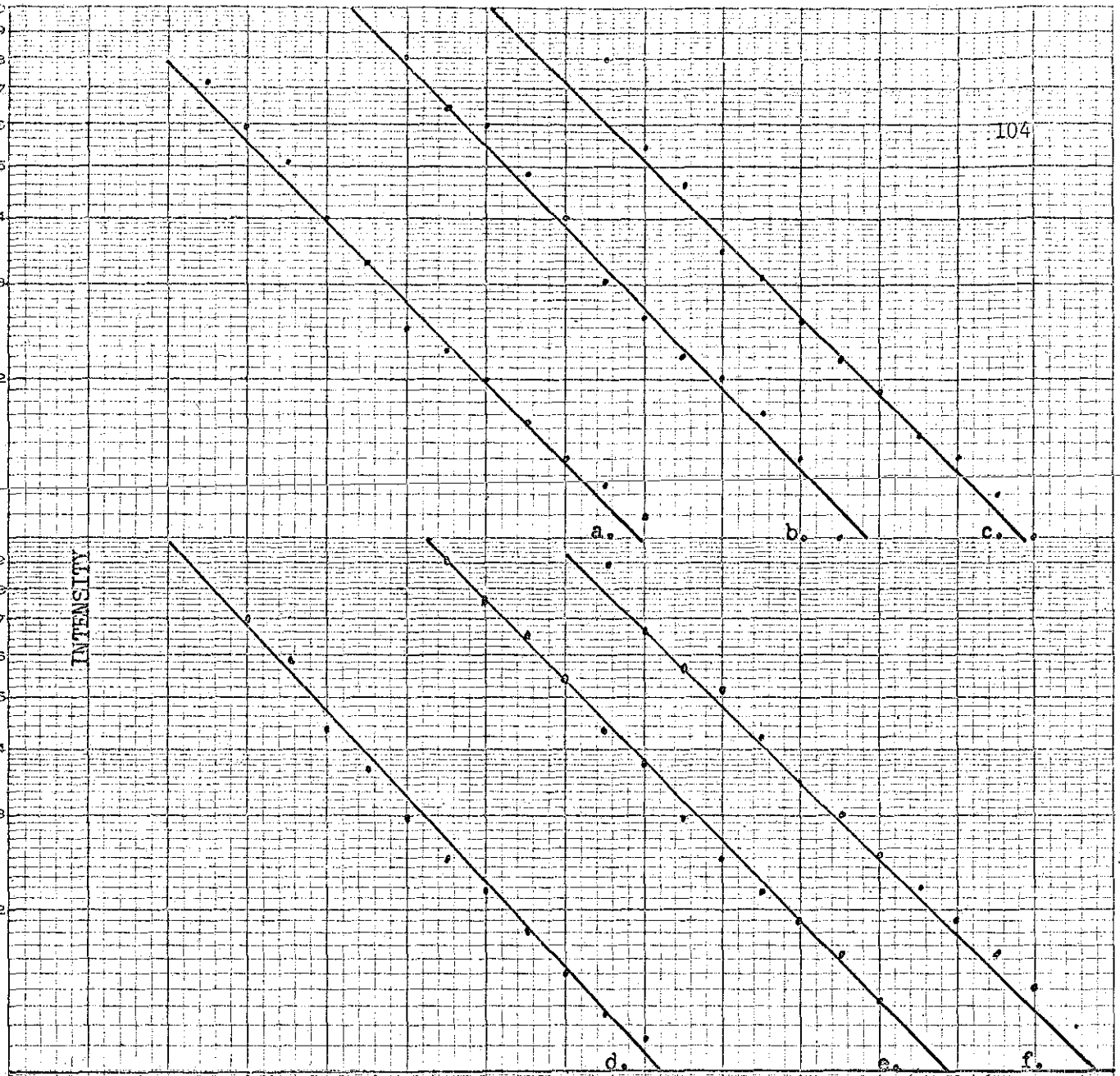

Fig. 66

a,b,c.
RIBOFLAVIN
$I \times 10^{-5}$ M
$[I^-] = 10 \times 10^{-3}$ M
Solvent: H_2O
Filters: Lamp, Wratten #35
Sample, Wratten #II
$\tau_{(ave.)} = 11.5$ nsec.
$k_q = 8.65 \times 10^7$ sec^{-1}

d,e,f.
RIBOFLAVIN
$I \times 10^{-5}$ M
$[I^-] = 15 \times 10^{-3}$ M
Solvent: H_2O
Filters: Lamp, Wratten #35
Sample, Wratten #II
$\tau_{(ave.)} = 11.07$ nsec.
$k_q = 9.05 \times 10^7$ sec^{-1}

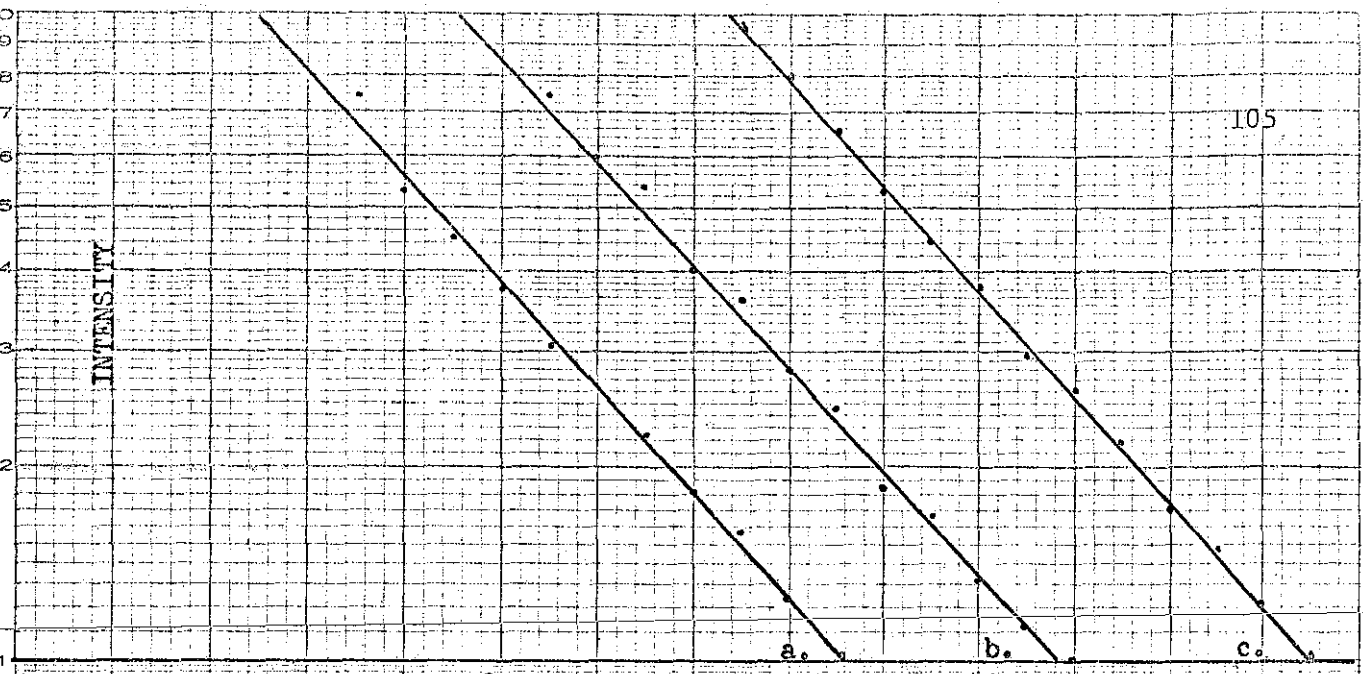

Fig. 67

RIBOFLAVIN

1×10^{-5} M

$[I^-] = 17.5 \times 10^{-3}$ M

Solvent: H_2O

Filters:

Lamp, Wratten #35

Sample, Wratten #II

$\tau_{(ave.)} = 10.62$ nsec.

$k_q = 9.42 \times 10^{7}$ sec^{-1}

CALCULATION OF LIFETIMES

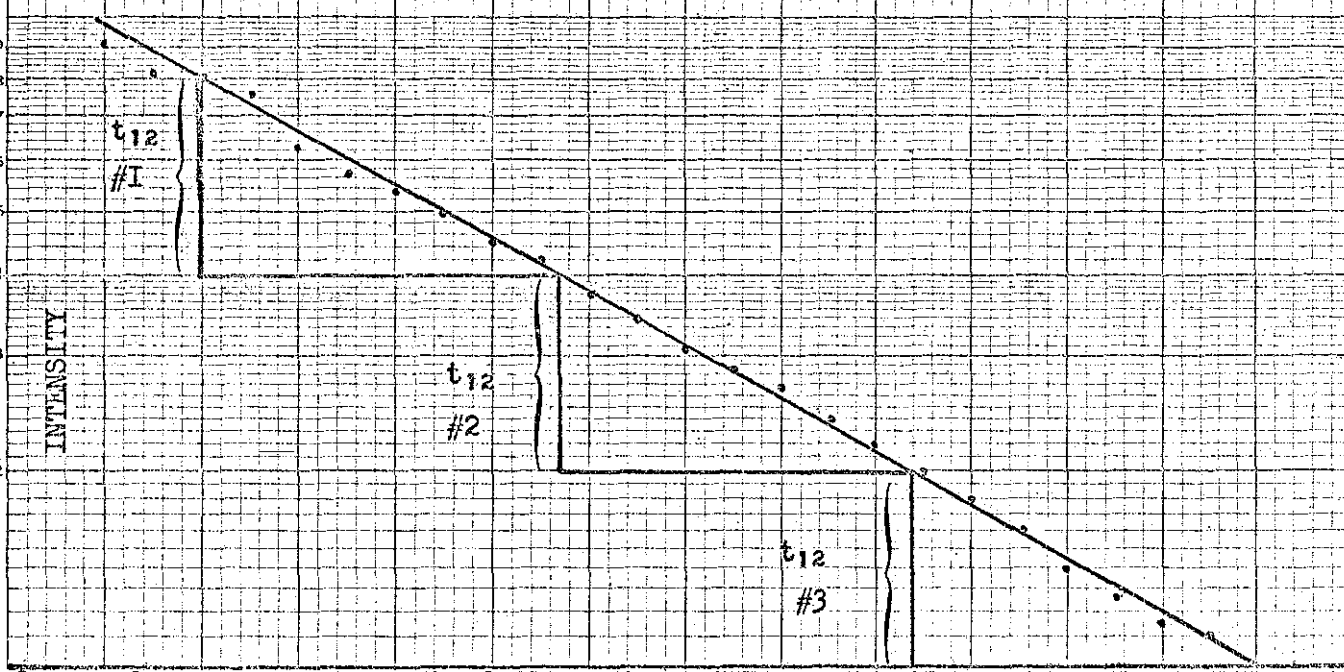

Fig. 68

#1

$t_{1/2}$ = 3.66 major divisions x 4 nsec. major division = 14.64 nsec.

#2

$t_{1/2}$ = 3.66 major divisions x 4 nsec. major division = 14.64 nsec.

#3

$t_{1/2}$ = 3.60 major divisions x 4 nsec. major division = 14.40 nsec.

$t_{1/2}$(ave.) = 14.56

$$\tau(\text{ave.}) = \frac{t_{1/2}}{0.693} = \frac{14.56}{0.693} \text{ nsec.} = 21.01 \text{ nsec.}$$

QUENCHING CONSTANT

FOR

RIBOFLAVIN

$$k_q = \frac{(-9.575 - 7.800)}{20 \times 10^{-3}} \times 10^7$$

$$k_q = 8.68 \times 10^8 \; ; \; \tau_o = \frac{1}{k_o}$$

$$\tau_o = \frac{1}{7.8 \times 10^7} = 1.26 \times 10^{-8}$$

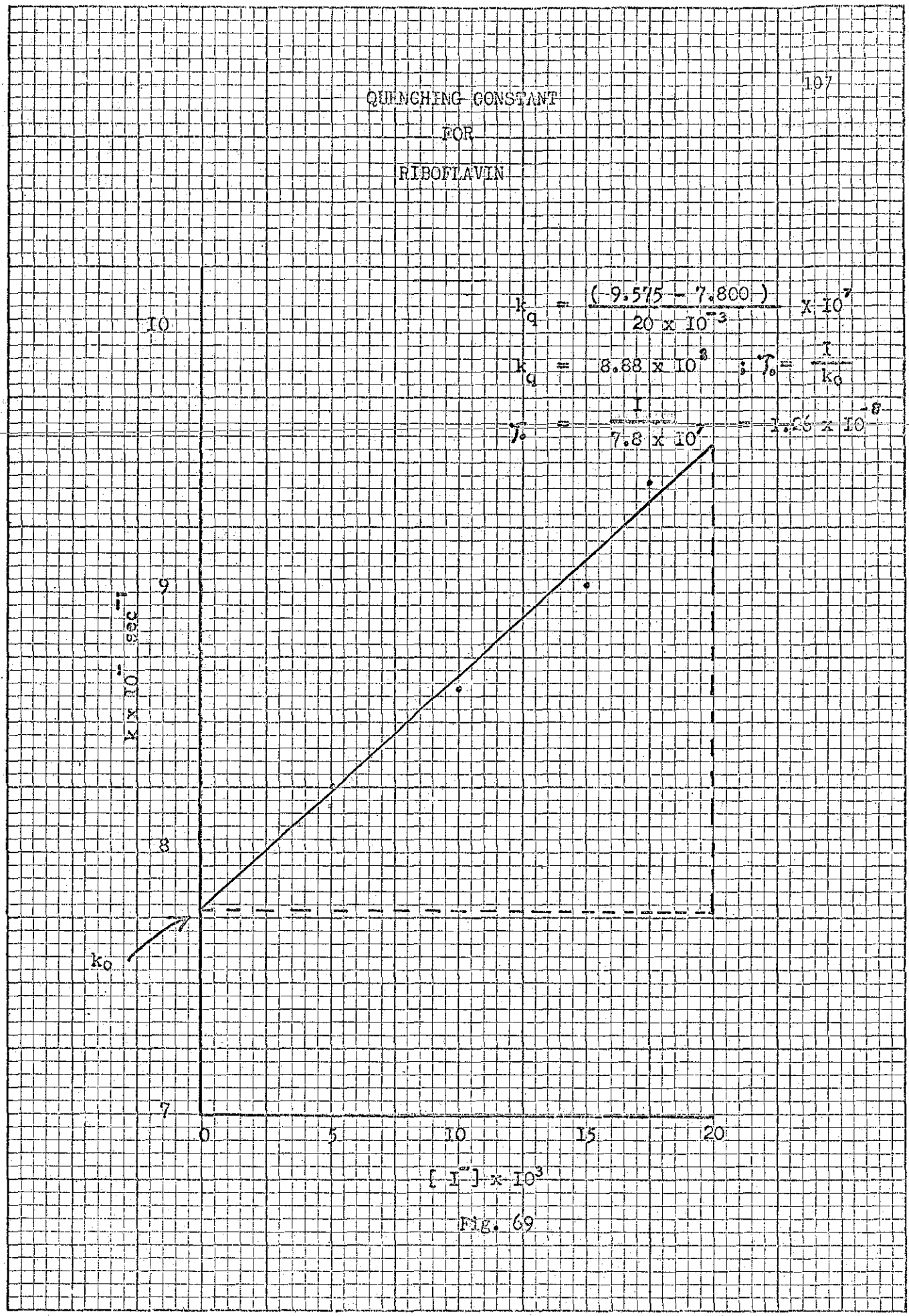

Fig. 69

10^7, the ^{7} was omitted.

Circuit for the Horizontal Time Base

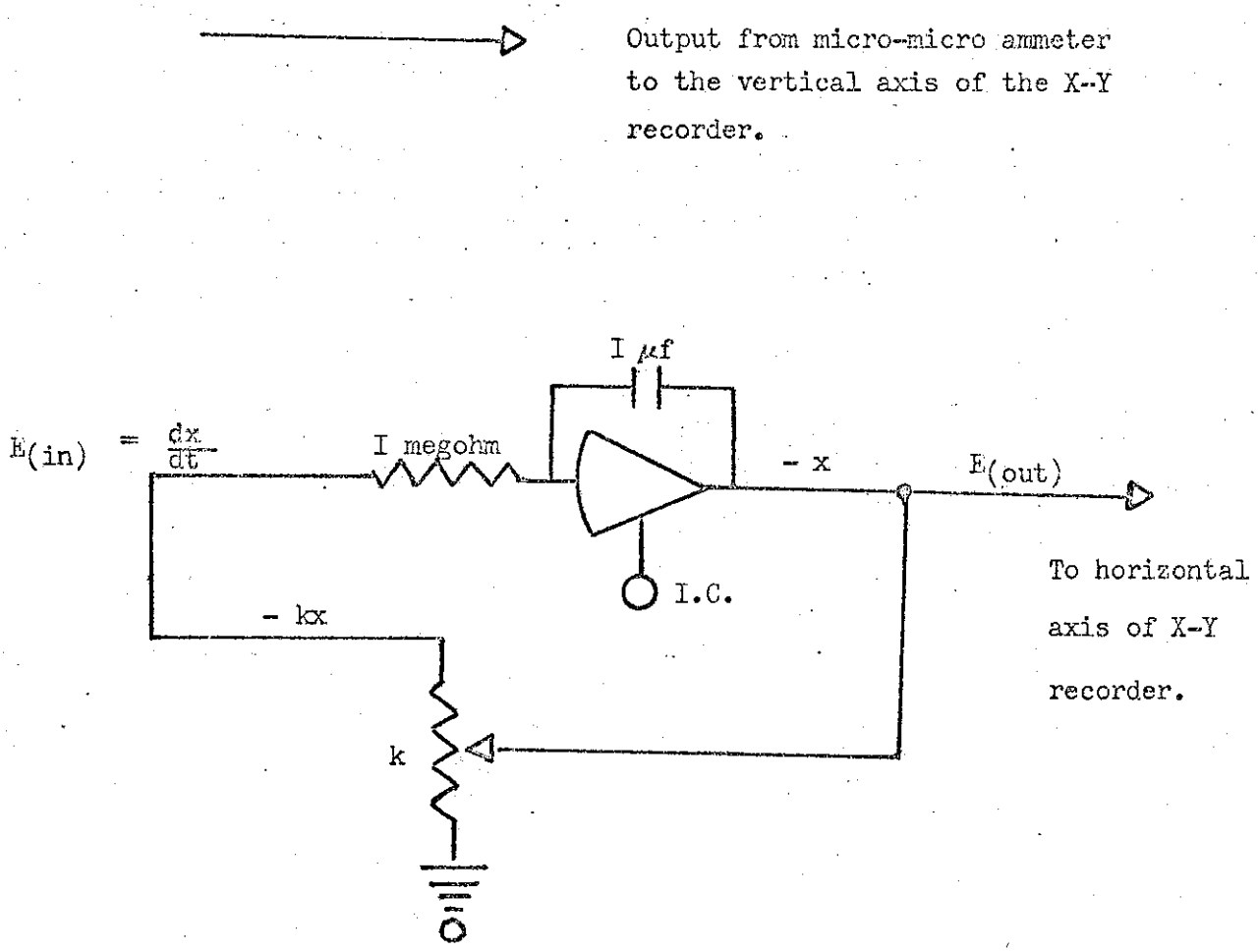

Fig. 70

BIBLIOGRAPHY

BIBLIOGRAPHY

1. T. Forster, Fluorenz Organischer Verbindungen, Vandenhoech and Ruprecht, Gottingen, (1957).

2. W. R. Ware and B. A. Baldwin, J. Chem. Phys. 40, 1703 (1964).

3. R. F. Chen, G. G. Vurek, N. Alexander, Science 156, #3777, 1967.

4. R. G. Bennett, Rev. Sci. Instr. 31, 1275, (1960).

5. R. W. Wood, Phil. Mag. 6, 427 (1905).

6. R. W. Wood, Proc. Roy. Soc., London, A99, 362 (1921).

7. H. Abraham and J. Lamoine, Compt. Rend. 129, 206 (1921).

8. P. F. Gottling, Phys. Rev., 22, 566 (1923).

9. E. Gariola, Z. Physik 35, 748 (1926).

10. L. A. Tummerman, J. Phys., Moscow, 4, 151 (1941).

11. E. A. Bailey and G. K. Rollefson, J. Chem. Phys. 21, 1315 (1953).

12. H. B. Phillips, R. K. Swank, Rev. Sci. Instr., 24, 611 (1953); R. F. Post, H. S. Shiren, Phys. Rev. 78, 80 (1950); R. Stringraber and B. Berlman, Rev. Sci. Instr., 34, 524 (1963).

13. N. J. Turro, Molecular Photochemistry, W. H. Benjamin, Inc., New York, 1966, 37 pp.; J. G. Calvert, N. J. Pitts, Jr., Photochemistry, J. Wiley and Sons, New York, 1966, pp. 96-107; E. J. Bowen, The Chemical Aspects of Light. Oxford at the Clarendon Press, 1946. pp. 125-31. g. M. Barrow, Molecular Spectroscopy, McGraw-Hill Book Company, New York, 1962. pp. 305-6.

14. C. Sandorfy, Electronic Spectra and Quantum Chemistry, Prentice-Hall, Inc., Englewood Cliffs, New Jersey, 1965. pp. 100-121.

15. J. H. Malmberg, Rev. Sci. Instr., 28, 1027 (1957).

16. C. F. Hendee, W. B. Brown, Phillips Tech. Rev. 19, 50 (1957); R. W. Engstrom, Rev. Sci. Instr., 18, 1587 (1947).

17. W. H. Melhuish, J. Phys. Chem., 65, 229 (1961).

18. O. Stern and M. Volmer, Physik. Z., 20, 183 (1919).

19. F. W. Lampe and R. M. Noyes, J. Am. Chem. Soc. 76, 2140 (1954); R. M. Noyes, J. Phys. Chem 65, 763 (1961); G. S. Hammond and J. R. Fox, J. Am. Chem. Soc., 86, 1918 (1964); P. Debye, Rans. Electrochem. Soc., R. M. Noyes, J. Am. Chem. Soc., 79, 1956.

20. W. Kauzmann, Quantum Chemistry. New York: Academic Press, Inc., 1957.

21. G. N. Lewis and M. Kasha, J. Chem. Soc., 67, 994 (1945); M. Kasha, Light and Life. Baltimore, Md.: ed. W. D. McElroy and B. Glass, John Hopkins Press, 1961. p. 31; M. Kasha, Disc. Faraday Soc., 9, 14 (1950); M. Kasha and S. P. McGlynn, Ann. Rev. Phys. Chem., 7, 403 (1956); J. W. Sidman, Chem. Rev. 58, 689 (1958).

22. C. Reid. Excited States in Chemistry and Biology. New York: Academic Press, 1957; Laidler, Keith. The Chemical Kinetics of Excited States. Oxford: Oxford at the Clarendon Press, 1955; pp. 46-50. Johnson, Eyring and Pollissar. The Kinetics of Molecular Biology. New York: J. Wiley and Sons, Inc., 1954. pp. 130-49.

23. S. J. Strickler and R. A. Berg, J. Chem Phys., 37, 814 (1962).